EXTRACTING SCENE FEATURE VECTORS THROUGH MODELING

VOLUME III

Joseph K. Berry
and
James A. Smith

Final Report
Earth Observations Division
NASA Johnson Spacecraft Center
NAS 9-14467

April, 1976

Department of Earth Resources
Colorado State University
Fort Collins, Colorado 80523

EXTRACTING SCENE FEATURE VECTORS THROUGH MODELING

VOLUME III

Joseph K. Berry
and
James A. Smith

Final Report
Earth Observations Division
NASA Johnson Spacecraft Center
NAS 9-14467

April, 1976

Department of Earth Resources
Colorado State University
Fort Collins, Colorado 80523

THE FINDINGS IN THIS REPORT ARE NOT TO BE CONSTRUED AS AN OFFICIAL NASA POSITION, UNLESS SO DESIGNATED BY OTHER AUTHORIZED DOCUMENTS.

THE FOLLOWING REPORT IS FROM A DISSERTATION SUBMITTED BY JOSEPH K. BERRY TO THE GRADUATE FACULTY OF COLORADO STATE UNIVERSITY IN PARTIAL FULFILLMENT OF THE REQUIREMENTS FOR THE DEGREE OF DOCTOR OF PHILOSOPHY.

FOREWORD

This is the third volume in a final report series describing work completed under Project NAS 9-14467. The overall objectives of the project are concerned with applying canopy reflectance modeling to signature extension tasks for wheat identification. This effort supports the LACIE program. Mr. T. Barnett is overall technical monitor of the project. Mr. M. McEwen is technical monitor for the Field Measurements Program.

Volume I presents the multiplicative and additive coefficient matrices for a linear sun-angle correction approach. These coefficient tables are calculated using either measured empirical canopy reflectance functions or model derived data. These values are then incorporated into an atmospheric radiation transfer model. The dependence of the coefficient matrices on crop stage, crop type, and canopy directional reflectance variations is reviewed. Finally, a method for inferring leaf area index, an intrinsic scene characteristic, from canopy reflectance is discussed.

Volume II presents the basic data and computer programs used in the study. A brief review of the radiometric and geometric data collection procedures is also given. In particular, two recent methods developed by the investigators for determining plant geometry are discussed. These include the Fourier diffraction and multiple view

angle approach. The data compilation consists of canopy reflectance Leaf-Area-Indices, and leaf slope distributions for four wheat crop development stages at Garden City, Kansas.

ABSTRACT OF THESIS

EXTRACTING SCENE FEATURE VECTORS THROUGH MODELING

The science of Remote Sensing has traditionally been involved with the identification of objects and materials, through variations in electromagnetic fields. More recent developments have extended this research into inferrences about target status or condition. The development of relationships used in estimating scene status has been primarily based on empirical study. This report represents a different approach, in that it utilizes computer modeling in the development of a data base expressing the relationships under investigation.

The specific area of research is the remote estimation of leaf area index of winter wheat at Finney County, Kansas. The procedure developed consists of three activities: 1) field measurements; 2) model simulations; and 3) response classifications. The first activity is designed to identify model input parameters and develop a model evaluation data set. A stochastic plant canopy reflectance model is employed to simulate reflectance in the LANDSAT bands as a function of leaf area index for two phenological stages. An atmospheric model is used to translate these surface reflectances into simulated satellite radiance. A divergence classifier determines the relative similarity between model derived spectral responses and those of areas with unknown leaf area index. The unknown areas are assigned the index associated with the closest model response.

This research demonstrated that the SRVC canopy reflectance model is appropriate for wheat scenes and that broad categories of leaf area index can be inferred from the procedure developed in this study. The evaluation data set was insufficient for testing the procedure's accuracy in predicting specific indices.

Other significant contributions of the study include the development and refinement of two field techniques for assessing leaf angle distribution, and the presentation of an empirical data set containing environmental factors, intrinsic scene parameters and canopy reflectance for a single area throughout two phenological stages.

ACKNOWLEDGEMENTS

The research effort described in this report was supported by the National Aeronautical and Space Agency, Johnson Space Center, under Contract Number NAS 9-14467. The field data were collected under the supervision of the Large Area Crop Inventory Experiment and involved the cooperation of several agencies and academic institutions. Of particular assistance was Dr. R. Harlan of Texas A & M University.

Participating personnel included Dr. J. A. Smith, Associate Professor of the Earth Resources Department and Principal Investigator; F. Heimes, Graduate Research Assistant; and C. Conrad, staff. This report is an extension of the original work of natural grassland canopy reflectance modeling done at Colorado State University by Dr. R. Oliver, currently of the IBM Corporation, Clear Lake City, Texas.

TABLE OF CONTENTS

LIST OF TABLES

LIST OF ILLUSTRATIONS

1.0 INTRODUCTION

An enduring characteristic of man is his earnest efforts to domesticate his environment. This process of modifying wildland conditions in order to benefit mankind is predicated on his ability to survey the earth's surface; in order to learn about its resources and thus manage them better. Questions as to how this information can be derived and the mechanisms necessary to extract it have fostered the establishment of the field of remote sensing.

Remote sensing is the science of acquiring information about material objects from a distance. This process involves two principal activities: 1) the procurement of physical measurements; and 2) the translation of these data into useful information about objects. In remote sensing, physical information may be transmitted to the observer either through force fields or electromagnetic fields; in particular, through the spectral, spatial, and temporal variations of these fields. Therefore, in order to derive useful information from these field variations, one must be able to

- measure the variations and
- relate these measurements to those of known objects or materials.

Of the two types of fields, electromagnetic fields provide the greatest contemporary use. In particular, the visible and near infrared portions of the electromagnetic spectrum dominate the science of remote sensing. The remainder of this paper is confined to fields

of this type, and procedures for translating these data into information about the status of the target.

Previous development of the methodologies for relating physical measurements to information, have been principally based on empirical studies. These investigations correlate measured changes in one variable, or set of variables, to the induced changes in another set of variables. This study represents a different approach, in that it utilizes computer modeling in the development of a data base of the relationships under investigation.

1.1 Statement of the Problem

The principle hypothesis of this study is:

- Plant canopy reflectance and atmospheric modeling can be used to infer intrinsic scene geometry variables from spectral measurements.

In dealing with this principle hypothesis two sub-hypotheses can be identified:

- Wheat canopy reflectance can be predicted by computer modeling both as a function of low and high plant densities and as a function of sun angle.
- Low wheat density and high wheat density categories can be inferred from model data sets.

The principle hypothesis stipulates that a procedure can be developed which utilizes modeling in relating composite scene spectral measurements to the geometric make-up of the scene. The variables used to identify intrinsic scene geometry are: 1) leaf area index (LAI), which is a measure of plant density; 2) leaf angle distribution (LAD), which is a measure of plant orientation; and

3) spatial dispersion, which is a measure of foliage clumping. This study specifically involves relating wheat plant density (i.e., LAI) to spectral measurements.

The two sub-hypotheses identify specific aspects involved in the development of the classification procedure. The first sub-hypothesis deals with the validity of applying a canopy reflectance model to wheat. The second addresses the limits which can be tested for inferring scene geometry through computer modeling.

The development of these hypotheses is an outgrowth of several previous investigations undertaken at Colorado State University. These studies can be divided into two broad categories: 1) canopy reflectance modeling; and 2) biomass mapping from spectral measurements. The first category is represented by R. Oliver, J. Smith and the author's work in developing a stochastic canopy reflectance model for natural grassland (Smith and Oliver, 1972, 1974). The study specifically addressed the development of a computer model which could account for bi-directional effects of reflectance from a Blue Gramma canopy type. This orientation resulted in a primary concern for sun angle effects and canopy reflectance.

The second category is represented by J. Tucker's, R. Pearson's, L. Miller's and G. Johnson's studies into the inferrence of plant biomass from remote sensing data (Tucker, 1973; Pearson and Miller, 1972, 1973; Johnson, 1975). Their studies again dealt with natural grassland canopy types. Tucker was primarily concerned with surface measurements, Pearson and Miller with aircraft data, and Johnson dealt with satellite data.

The justification for merging the thrusts of these basic studies is the difficulty in obtaining and controlling empirical data relating canopy spectral variations and biomass. The modeling efforts have the potential of deriving data sets which effectively control the scene variables and provide a framework for field measurement activities.

The vehicle for this study was a NASA sponsored project principally concerned with the application of the canopy reflectance model in developing a wheat signature extension algorithm for sun angle. This was an applied project which was an extension of Colorado State University's earlier efforts in sun angle reflectance variations. Oliver's earlier work had resulted in a canopy reflectance model which indicated the potential for simulating sun angle dependence. The NASA effort was designed to (1) apply the model to wheat and (2) develop a formal approach for sun angle correction algorithms.

However, it was felt that the field measurement program could permit an initial evaluation of the capability of a modeling approach to infer intrinsic scene parameters (e.g., LAI). If the results warranted further study, this initial investigation could serve as a guide for a more applied, in-depth experiment.

1.2 Approach

Figure 1 depicts a schematic of the approach used in this study. It consists of three primary activities: 1) field measurements; 2) model simulations; and 3) leaf area index classification. The field measurements program was designed to determine the values of

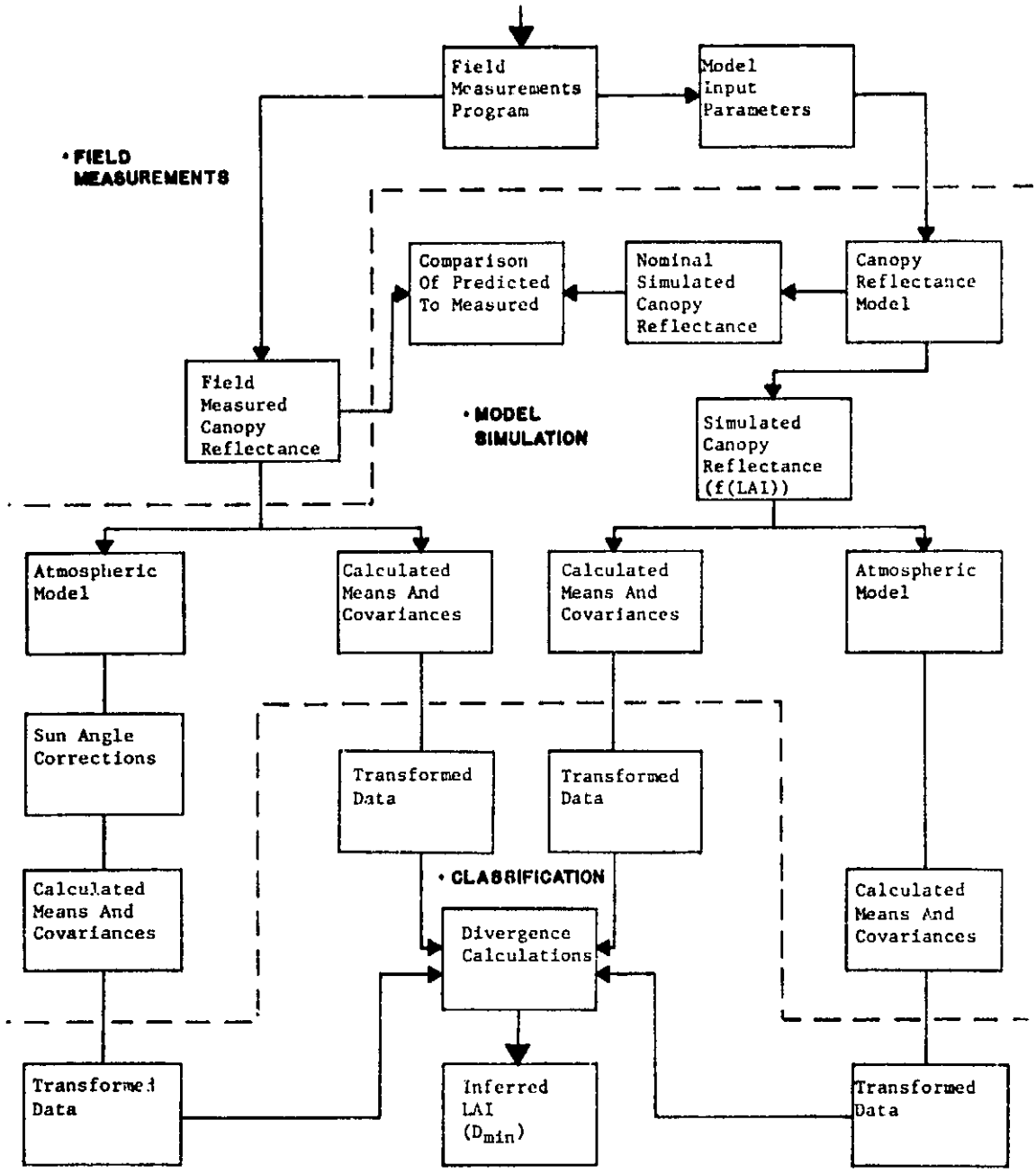

FIGURE 1. THESIS APPROACH. The approach of the thesis consists of the general activities of Field Measurements, Model Simulation and Classification.

the input parameters for the canopy reflectance model and to measure canopy reflectance for subsequent model calibration and evaluation.

The model simulation activities resulted in a data base incorporating spectral measurements as a function of leaf area index. The basic reflectance data was derived by executing the canopy reflectance model with a nominal input data set, with systematically varying LAI. In addition, an evaluation of the model's performance was made. An atmospheric model was employed to translate both the field and model derived canopy reflectances into simulated satellite radiance. Sun angle corrections were made to the empirical data in order to make it compatible with the sun angle used in the canopy reflectance model.

The final activity consisted of the actual classification of leaf area index from spectral measurements. This process involved the mathematical comparison of the spectral signature of an area in which LAI was to be determined, to each of the modeled signatures. The leaf area index of the area was inferred to be the same as that of the "closest" model derived signature. Several data transformations were employed in order to investigate alternative classification procedures.

1.3 Thesis Organization

The origanization of this paper follows the principle activities outlined above. The following section identifies other research which is related to this study. Sections 3.0 through 5.0 are concerned with the field measurements program. These sections contain considerable discussion of the procedures used in assessing the leaf

angle distribution of a plant canopy. They are particularly significant as they describe and evaluate two new techniques developed during this study.

Section 6.0 is concerned with the model simulation effort. A brief discussion is devoted to the concepts of the two models, and the results are presented and interpreted. Section 7.0 discusses the classification algorithm, and Section 8.0 reports the results of the classification for leaf area index. The final section summarizes the conclusions which can be drawn from the study, and identifies areas of future research.

2.0 BACKGROUND

The activities involved in this study can be grouped into two broad categories: ground truth collection and extensive area mapping. The first category deals with the necessity to calibrate the canopy reflectance model with accurate estimates of leaf area index (LAI) and leaf angle distribution (LAD). Existing field techniques were inappropriate in this application as they were either too tedious or yielded only approximate estimates. The second category is the association between target status and remote sensing data. The bulk of previous research in this area has been empirically based, and has resulted in mixed success.

2.1 Field Procedures for Estimating LAI and LAD

The more traditional approach to assessing LAI and LAD of an individual plot is by direct measurement (Suits, 1972; Vanderbilt, 1975; Oliver and Smith, 1973). The procedure involves first clipping all of the plants within a small area, then recording their geometric parameters. The principal measurements include plant height, number of leaves, length and width of each leaf, and the series of angles from the horizontal used to approximate the leaf's curvature. From these measurements the plant surface area in the plot can be readily determined, which, in turn, can be directly translated into leaf area index. The leaf angle distribution for the plot is estimated by calculating the normalized frequency of

occurrance of each leaf inclination angle, weighted by the length of the leaf segment forming the angle. The geometric parameters of an entire field are developed by averaging a representative number of plot statistics.

The direct measurement method is potentially the most accurate. However, it has two serious drawbacks. First, it is extremely tedious and time consuming, which tends to minimize the number of plants used in developing plot statistics. The second short-coming, which is not bounded by experimentor fortitude, is ingrained in the non-*in situ* procedure of measurement. The physical removal of the plants can greatly affect the estimate of LAD. Wilting and loss of true stem orientation are obvious problems. LAI assessment is particularly confounded by the necessary determination of discrete plot boundries. The principal advantage of the technique is its conceptual and mechanical simplicity.

Variations of the direct measurement method include ocular estimate extension and the application of a surface area meter. The ocular or visual method of estimation requires the visual observation of several training plots by a technician (Pechanec and Pickford, 1937). The LAI of these sacrifice plots are then measured in order to refine the observer's estimations. After an adequate training period, the trained observer's estimations can be used to augment the direct measurements. This extension, however, suffers from human variations among estimators, is limited in spatial and temporal extent of the application, and does not directly characterize the vegetation.

Another extensively used technique for determining canopy geometry is the point quadrat method (Goodall, 1952; Wilson, 1973; Knight, 1970). This method involves the calculation of LAI and LAD by determining the average number of pin contacts with the plant canopy for a slender, sharp-pointed rod oriented at a fixed angle with reference to the ground surface. The average number of contacts for several pin-angles are then substituted into derived linear equations relating LAI and the leaf inclination angle to the frequency of contact. The primary advantage of the point quadrat technique is its in situ nature, which minimizes plot disturbance. The major disadvantages are the substantial amount of time involved in characterizing each sample plot and sensitivity of the derived equations to genetic, environmental and phenological changes. A more detailed discussion of the technique is presented in Section 5.0.

Two other field methods of LAI determination warrant brief consideration. They are direct measurement by a capacitance meter (Fletcher and Robinson, 1956) and dry weight of plant material estimation (Harlan, 1976). Both procedures are driven by changes in biomass, which can be converted to LAI estimates through a double-sampling method described by Wilson (1963).

Capacitance meters measure the mass of the vegetation between two or more metallic probes of a specially designed capacitor which are inserted into the plant canopy. The meter utilizes the significant differences between the dielectric constant of air ($\varepsilon \sim 1$), and that of water ($\varepsilon \sim .80$). As the density of plant material increases, leaf water present in the vegetation increases, which yields higher

capacitance readings. These readings must be calibrated for varying species composition and environmental conditions. The primary advantages of this method include simplicity of use and *in situ* measurement. The primary disadvantage is the induced experimental error caused by the variations in soil water in the near-surface soil layers.

The dry weight procedure attempts to develop a regression relationship between plant surface area and dry weight. Like the capacitance method, this technique is sensitive to changes in composition and conditions, and therefore requires frequent calibration.

2.2 Spectral Methods for Estimating Biomass

Spectro-optical methods for assessing vegetation biomass have been studied by several investigators. The research activities can be divided into two related camps. Those which concentrate on ground level canopy spectral reflectance (Pearson and Miller, 1973; Tucker, 1973), and those based on elevated platform scene radiance (Maxwell, 1975; Johnson, 1975; Miller and Pearson, 1971). These empirical studies involve the development of predicting equations through the joint consideration of spectral response and biomass of individual study plots.

A fundamental assumption is that the electromagnetic energy striking a plant canopy is, in part, spectrally modified by the biomass present in the scene. It is further assumed that this unique coding can be decoupled from random signal noise, and is sufficient information for biomass classification. This contention is closely related to the hypothesis under study in this report. The salient

difference between the previous investigations and this one is in their methodologies. The earlier studies utilized empirical methods to develop predictive relationships, whereas this study employs model derived data to capture the information. Another important difference is the type of target under study. Whereas earlier studies dealt with natural grasslands, this study concentrates on a monoculture.

The results of the ground based investigations have been successful in relating spectral reflectance of natural grasslands to estimates of biomass. Classification of biomass from elevated platforms (aircraft and satellite) has been relatively less successful (Maxwell 1975; Johnson 1975). A major reason for this is the inability of the researchers to effectively control the composition of their study plots. As the altitude of the sensor increases, the area within the field of view also increases, which tends to increase the heterogeneity of the natural scene. The result is that the differences in responses that are presumed to be driven by variations in biomass alone. may be, in part, a function of species composition and canopy status.

Another contributing factor to the increased difficulty of using elevated platforms is the enlarged bandwidth of the sensors. As the altitude is increased, atmospheric effects tend to rapidly attenuate and degrade the signal. In order to maintain a strong signal the spectral bandwidth is increased, thereby increasing the total energy reaching the sensor. This design has the affect of averaging the spectral signature, and conceals some of the potential narrowband information.

3.0 DATA COLLECTION AND REDUCTION

3.1 General Description

The field measurements activity presented in this report was supported by the National Aeronautical and Space Agency (NASA), in connection with its Large Area Crop Inventory Experiment (LACIE). The entire field measurement program is ongoing and involves several research institutions. Among the principle groups participating in the data acquisition reported in this study were Colorado State University, Texas A & M University, Purdue University, the Environmental Research Institute of Michigan, Earth Observations Division of NASA, and the U.S.D.A. Crop Reporting Service. The program's activities were divided between an extensive empirical investigation of the field spectral signatures for wheat and several related crops, and the measurement of intrinsic wheat scene reflectance variables.

Two study sites were selected; one in Finney County, Kansas, which typifies a winter wheat region, and a second in Williams county, North Dakota, which is representative of spring wheat. The necessity for two sites is based on the dramatic differences in appearance between the two groups of wheat, as governed by fundamental differences in crop development patterns and structure. In addition to this genetic stratification, periodic measurements were made to correspond to the major phenological stages in the crop's development.

Only a portion of this vast data set is utilized in this report. The data is from the Finney County site during the March 20 and April 23 recording periods, which correspond to the tillering and heading stages of winter wheat. Appendix A presents these data. Figures 2 and 3 are descriptive photographs of these periods. The striking differences between the total amount of plant cover in each should be readily apparent. Less obvious is the change in the leaf angle distribution toward a more erect canopy in April. Other subtle changes in the intrinsic parameters include a drying out of the soil (lighter color) and a slight decline in over-all leaf vigor (incipient chorolysis) in the transition from the tillering to heading stages.

3.2 Field Measurement Procedures

The field measurement procedures used in this report can be subdivided into radiometric and geometric methods depending on whether they are involved with the estimate of optical or geometric intrinsic variables. The former group includes measurements of canopy and soil reflectance, global and sky irradiance, and individual leaf transmission. The geometric procedures include an estimate of leaf area index (LAI) and leaf angle distribution (LAD). The format for discussing the data collection process adheres to the actual sequencing of activities used in the field.

All of the modeling directed data was collected from a single field. As the method for assessing plant surface area was destructive, a new series of plots had to be established for each reporting period. Plot selection involved the establishment of three 2' by 2'

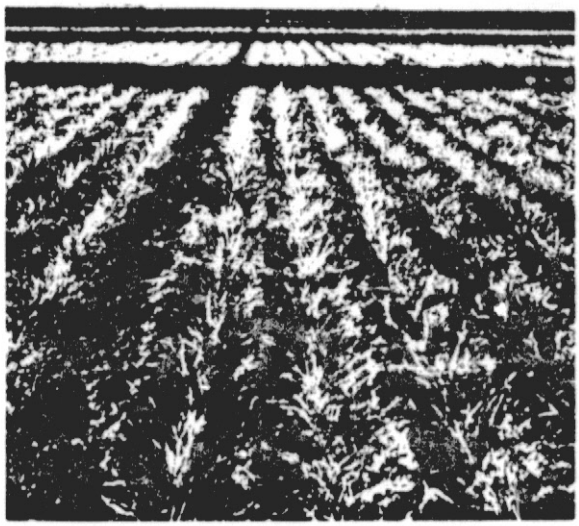

FIGURE 2. MARCH FIELD MEASUREMENT SITE. Relatively low plant density typlified the March field measurements. A pronounced "rowing" effect between bare soil and vegetation was present.

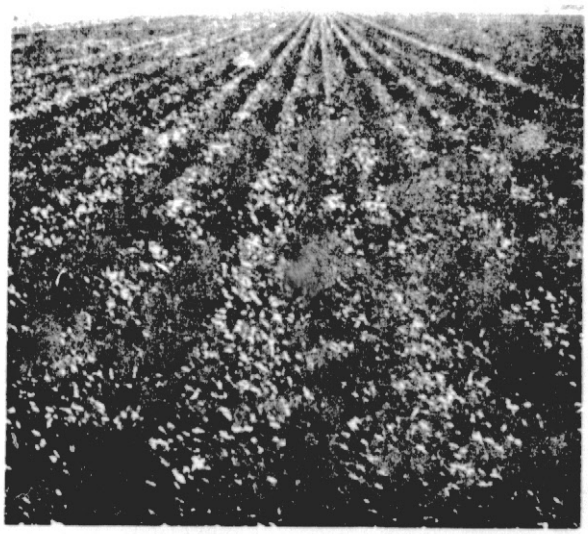

FIGURE 3. APRIL FIELD MEASUREMENT SITE. A substantial increase in plant density, compared to the March period, was present during the April field measurements.

plots throughout the field, which were chosen to typify the expected variance in the field. A rigorous statistically based sampling design was not used because of the minimal number of plots involved. It was felt that an experienced agronomist could more effectively mentally assess the field and position the plots. A 2' by 2' configuration was chosen for two reasons: 1) it allowed for the consideration of two adjacent rows (drill spacing was approximately 10"); and 2) it entirely bounded the field of view of the radiometer used to record canopy reflectance. The objective of this design and positioning was to identify plots which could be intensively described.

3.2.1 Radiometric Measurements

Following the establishment of the sample plots, canopy reflectance measurements were made for the remainder of the day, or until cloud cover became excessive. The determination as to whether atmospheric conditions were acceptable was primarily subjective, however, if repeated measurements of global irradiance fluctuated by more than 15%, it was a clear indication that radiometric measurements should cease.

All of the radiometric data were collected using a LANDSAT radiometer commercially available through EXOTECH, INC. (Figure 4). This instrument is a portable, battery powered radiometer which uses interference filters to measure the signal in the discrete wavelength bands of .5-.6, .6-.7, .7-.8, and .8-1.1μm wavelength. The first two bands are sensitive to the green and red portion of visible light respectively, whereas the latter two bands record

responses at the slightly longer wavelengths in the reflective infrared region of the electromagnetic spectrum. These bands correspond to those aboard the LANDSAT-B satellite currently in orbit. The only modification installed on the factory unit was to convert the normal analog readout to a digital display in order to simplify manual recording.

The operating procedure for determining canopy reflectance involved taking a set of readings for each wavelength band from a barium sulfate coated standard, then from the wheat canopy itself. The highly reflective and diffusing standard affords a measure of the total irradiance impinging on the scene, while the canopy measure identifies the portion of that energy which is reflected from a target. The instrument's design employs a silicon cell detector positioned behind an interference filter and focusing optics. The ratio of the energy coming off the canopy to the total irradiance (outgoing/incoming) is defined as the reflectance of the scene for the given conditions.

During a single "set-up" over one of the plots, four canopy reflectance "observations" would be collected. These included two instrument positionings centered over a row, and two centered between rows. This multiple sampling was required as there is a separate aperture for each detector, which results in each having a slightly different portion of the canopy in its field of view. By averaging the four readings most of the variance due to crop rowing could be eliminated. A complete set of canopy reflectance measurements for a recording period was accomplished by rotating between the three plots, with a typical day consisting of twelve "set-ups" (Figure 5).

Also included at each set-up was a measure of the relative proportions of direct solar and diffuse sky irradiance. The procedure entailed obtaining readings of a fully exposed reflectance standard and then shading the standard. The unshaded measurement represents total global irradiance, while the shaded reading estimates the diffuse sky component. The difference between the two identifies the direct solar contribution. Periodically during the radiometric measurement period, the reflectance for bare soil in the immediate vicinity would be obtained in a manner similar to canopy reflectance determination.

The final radiometric variable to be measured in the field was the actual spectral transmission of several individual leaves. An attempt was made to sample healthy green leaves, chlorotic (yellowing), and dead material whenever convenient. A special attachment to the LANDSAT radiometer was designed and constructed at Purdue University which enabled the direct measurement of leaf transmission (Figure 6). The device consists of a short cylinder (barrel), a sphere, and two interlocking flat disks with small slots cut in them. The sphere is internally coated with barium sulfate reflectance paint and contains a blocking baffel to prevent the passage of direct solar radiation, thereby, insuring only diffuse radiation at the detector. The entire apparatus fits over a single sensor port and must be shifted for measurements in each of the four bands.

The sequence of operational steps begins with the alignment of the unit toward the sun through the use of a pinhole type sight on the side of the barrel assembly. Once in alignment, an unobstructed aperture reading is taken. The leaf is then inserted between the

two disks, so as to completely obscure the slots, and securely locked in place. A second reading is made which represents the proportion of light transmitted through the leaf. The ratio of the second reading to the first determines the faction of the total incident energy in a band which is transmitted through the leaf.

Constituent transmission measurements could not be made for the March and April periods under study in this report. An estimate of this measure was made by using the green leaf transmission obtained during the May field session. The large proportion of green leaves noted during the LAI measurements of both periods tends to support this data substitution. Also inherent in this procedure is the assumption that healthy green leaves at one crop development stage exhibit similar optical properties as those in another stage. The close agreement between model prediction and field measurement indicates that this was a reasonable assumption for the plots used in this study.

Individual green leaf reflectance was approximated by setting these values equal to the measured transmission values. This relationship of constituent transmission and reflectance for healthy green leaves being nearly equal, holds for most plant types. A study by Gausman (1971) shows a similar relationship in the wheat plants they studied. A problem in the application of this assumption was encountered for constituent measurements in band 7 (.9 - 1.1μm). The average transmission value was calculated as 54.6%. In order to conserve mathematical integrity, both transmission and reflectance values were set at 49.5%. A special attachment for the

LANDSAT radiometer which directly measures constituent reflectance is currently being designed, and should be in use during the 1976 field season.

3.2.2 Geometric Measurements

Field measurement of plant surface area in each plot involved a tedious procedure in which the one-sided surface area of all the living plant material in the 2' by 2' plot was determined. The ratio of the total one-sided surface area of all photosynthetically active leaves to a unit area of ground defines leaf area index. This measure can be easily conceptualized by imagining a tall rectangular box being dropped edge-wise over the canopy, without any disturbance. The total one-sided surface area of all living plant material (stalks or leaves) encased in the imaginary box, divided by the surface area of the bottom edge of the box defines leaf area index as used in this report.

The first step in determining LAI was to remove all standing material within each plot. An assumption was made that equal amounts of plant material extended into, as out of, the plot. This simplified the extraction task by limiting consideration to only those plants whose bases were within the plot boundary. The bagged material was transported to an appropriate facility for surface area measurement.

A portable Lamda Surface Area Meter (Lamda Instrument Corporation) was utilized for direct measurement of leaf surface area. The instrument consists of a rechargeable power supply, digital readout, and detector head (Figure 7). The detector head contains a six inch long bank of photo cells and a matching bank of light sources. As a leaf is passed between the sources and detectors, the leaf will interdict

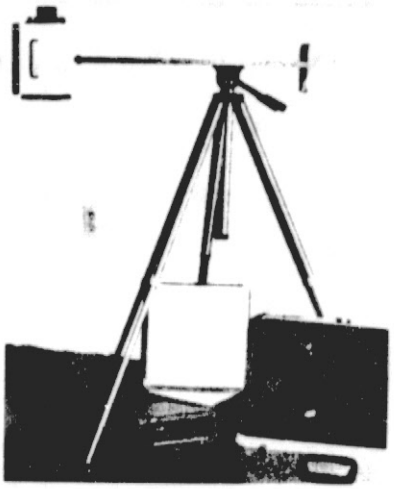

FIGURE 4. LANDSAT RADIOMETER. The field radiometer used in this study is sensitive to four broad wavelength bands in the visible and near infrared portions of the electromegnetic spectrum.

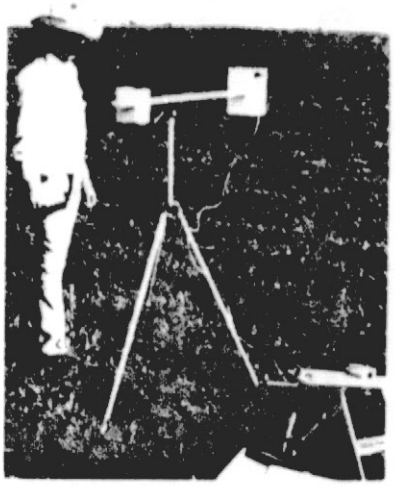

FIGURE 5. FIELD MEASUREMENTS OF CANOPY REFLECTANCE. Alternating radiance readings from the wheat canopy and a barium sulfate coated reference determined canopy reflectance.

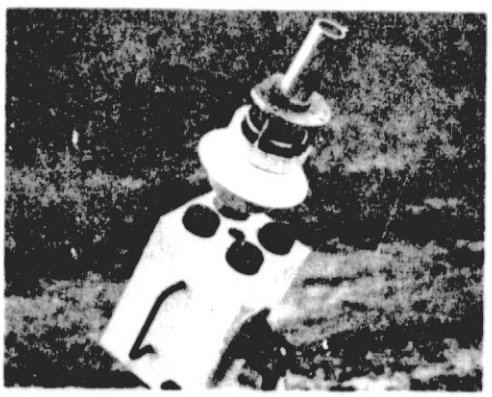

FIGURE 6. LEAF TRANSMISSION ATTACHMENT. A special attachment to the LANDSAT field radiometer was constructed to determine individual leaf transmission.

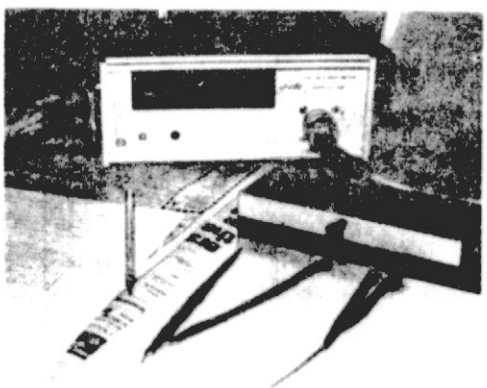

FIGURE 7. SURFACE AREA METER. The surface area of plant material was determined by passing the material in an acetate carrier through the photo sensitive detector of the instrument.

some of the light paths, thereby indicating the total width of all plant material in the instrument at a point in time. The total surface area is the summation of all the areas of the rectangular segments formed by the instrument's descrete sampling, as the material is pulled through the detector head.

The procedure first involves separating all of the plant material in each field plot into live and dead components. The surface area of all the living material was then measured using the surface area meter. The ratio of the total leaf surface area to the surface area of the field plot identified the leaf area index of the plot.

In most cases, the determination of LAI consumed an entire day for each plot. The field measurement techniques for estimating leaf angle distribution proved much more expeditious. Two techniques were employed. The Fredholm method is based on a series of off-angle photographs of the wheat canopy (Figure 8). This method could only be used during the March 20th period, as it requires a relatively low plant density. The actual field procedure consists of taking color slides at 0, 10, 20, 30, 40 and 50 degrees off-normal; both with and perpendicular to the direction of crop rows.

The Fourier technique requires several horizontal field photographs of a thin portion of the plant canopy, silhouetted against a white backdrop (Figure 9). Ten inch squares were drawn on the backdrop to facilitate procedures involved in data reduction. A complete set of photographs for a plot consisted of three photos taken perpendicular to the field's rows and three aligned with the direction of rowing. Fourier diffraction analysis, as explained later, was then applied to the images.

FIGURE 8. FREDHOLM FIELD TECHNIQUE. The field procedure for the Fredholm method consists of a series of multiple view angle photographs of the plant canopy.

FIGURE 9. FOURIER FIELD TECHNIQUE. The Fourier field procedure consists of orthogonal pairs of silhouetted photographs.

3.3 Field Data Reduction

A computer program was developed which analyzes the field radiometric measurements and calculates the simple canopy reflectance, soil reflectance, direct to total irradiance ratio, and constituent transmission. This information was combined with the derived leaf area indices for each plot and inferred constituent reflectance to yield a data base stratified by field plot and phenological stage. The determination of leaf angle distribution, however, required substantial additional data reduction. The remainder of this section discusses the procedures involved in this process, whereas the following sections describe the theoretical framework and evaluation of the techniques employed.

The technique for assessing leaf angle distribution which utilizes multiple off-angle photographs of the plant canopy was recently developed by R. Oliver and J. Smith (1974). This procedure solves a Fredholm integral to estimate LAD, and has been termed the "Fredholm technique."

In general terms the Fredholm algorithm capitalizes on the readily observable phenomenon of increasing apparent plant density with increasing view angles. This response is primarily due to the diminishing probability of foliage gap (seeing through the canopy to the soil) with views nearer to the horizon. When looking straight down the scene is marbled with patches of bare soil and dead material. As the line of sight becomes more glancing, more of the live plant material dominates the scene. The surface area of the standing material projected in the direction of the camera, increases as view angle increases. The rate and pattern of this increase in projected surface

area serves as information for the Fredholm integral estimation of a canopy's leaf angle distribution.

The data reduction procedure involved with this technique requires the determination of percent foliage cover in each off-angle photo. This was accomplished by overlaying a transparent dot grid on each print and recording the proportion of dots which did not intersect a foliage element. The probability of gap in each of the photographs serves as input to a computer algorithm which estimates the distribution of angles in the plant canopy.

It should be apparent that the Fredholm technique is inappropriate for dense canopies. At the extreme, the canopy can become so dense as to prohibit any foliage gaps, even when viewed from the vertical.

A radically different procedure had to be developed for assessing LAD at crop development stages with relatively high plant densities. Fundamental to its methodology is the optical generation of a Fourier diffraction pattern, which resulted in its being termed the "Fourier technique".

This method consists of two fundamental steps. The first step involves the determination of the distribution of angles formed by the foliage elements in a pair of orthogonal projections of a plant canopy. The two distributions are established by sampling the angular bias of the diffraction patterns generated from the orthogonal projections. These diffraction patterns can be conceptualized as a statistical summary of all the orientations and arrangements in the original scene. The second major step involves the mathematical

convolution of the two planner distributions of angles into an estimate of the canopy's 3-space leaf angle distribution.

The operational steps involved in the Fourier technique's data reduction begins with the generation of diffraction patterns for each of the silhoutted photographs (Figure 10). This is accomplished by placing the 35mm negative of the scene into the diffractometer as shown in Figures 11 and 12. The resulting diffraction pattern is photographed (Figure 13). Experimentation proved that high contrast black and white film was best for all the photography involved with this technique.

The angular bias of the 35mm negative of the diffraction pattern is then sampled with a photo cell densitometer (Figure 14). A wedge blocking filter is attached to the detector which limits its field of view to a pie shaped wedge emanating from the center of the diffraction pattern. As the wedge filter is rotated, the intensity of light passing through the negative is recorded for the successive "pie slices". The measured distribution of angles in the diffraction pattern acts as input to a computer program (program PROP, described in Appendix C) which calculates the distribution of leaf angles in the original scene (Figure 15).

The final step involves the execution of another computer program (program CONVOL, described in Appendix C) which uses the distribution of leaf angles in two orthogonal projections in estimating the 3-space angle distribution of the canopy.

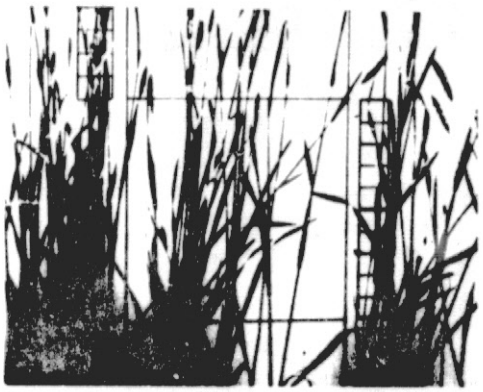

FIGURE 10. FOURIER FIELD PHOTOGRAPH. The "input" in the generation of an optical diffraction pattern is a 35mm high contrast negative of silhouetted plants.

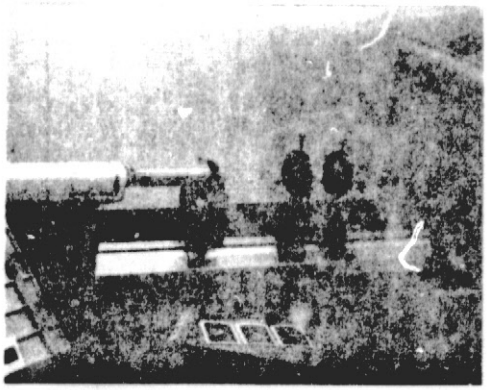

FIGURE 11. LASER DIFFRACTOMETER. The optical diffraction pattern of the "input" is displayed on the screen at the end of the optical bench.

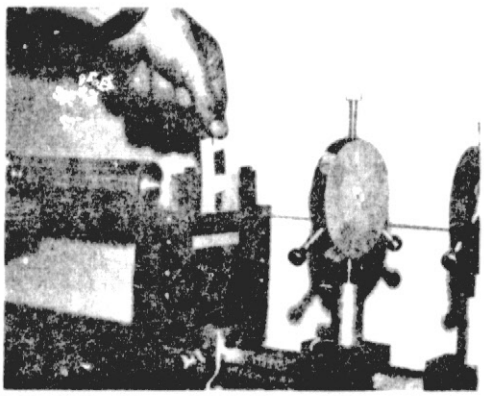

FIGURE 12. INPUT PLACEMENT IN DIFFRACTOMETER. The field negative is positioned between the LASER and the first lens.

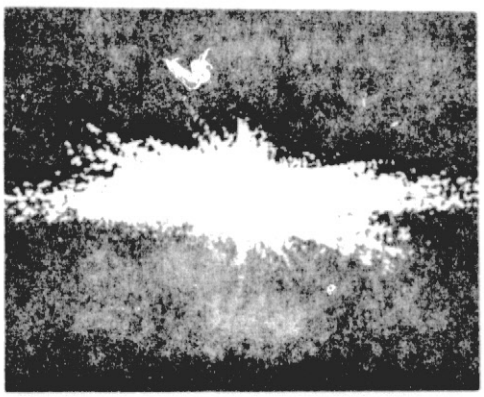

FIGURE 13. WHEAT DIFFRACTION PATTERN. A diffraction pattern can be conceptualized as a statistical summary of all the orientations and spacings in the "input".

FIGURE 14. DIFFRACTION PATTERN SAMPLING. A photo sensitive probe with a wedge filter is rotated around the diffraction pattern, while discrete readings are made.

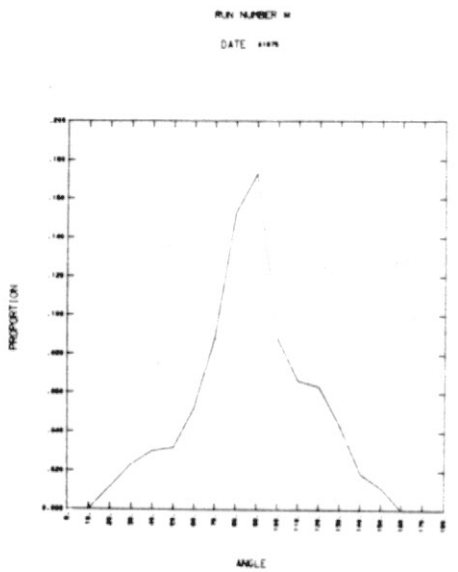

FIGURE 15. WHEAT DISTRIBUTION OF ANGLES. A computer program analyzes the diffraction pattern sampling data to infer the distribution of angles in the "input".

4.0 THEORETICAL FRAMEWORK OF LAD FIELD TECHNIQUES

The development of field techniques for assessing the leaf angle distribution of a plant canopy is a major effort of this study. The methods used by previous investigators yield incomplete data or are time consuming. This section is designed to familiarize the reader with the two new procedures employed. Considerable emphasis is given to the Fourier technique, as it was developed during this study. Minimal attention is directed toward the theoretical foundation of the Fredholm technique, as it is aptly discussed in the report by Oliver and Smith (1974). A sensitivity analysis of the technique, however, is presented in order to identify its more important aspects.

4.1 The Fredholm Technique

The Fredholm technique utilizes the rate and pattern of the increase in projected surface area noted at multiple view angles of a plant canopy, to infer the leaf angle distribution of the canopy. A relatively erect canopy will exhibit a slow progression of increasing plant projected surface area as the view angle is increased towards the horizon. An inflection point in the trend is usually observed. An opposite trend and pattern is noted for a flat canopy.

The proportion of gap, $P_0(\theta_r)$, as a function of view angle is dependent on the mean canopy projection in the direction of view, averaged over all foliage elements. Several explicit expressions of this functional dependence are given in the literature (Nilson, 1971). For example:

$$P_0(\theta_r) = e^{-LAI\ g(\theta_r)\ \sec\ \theta_r} \qquad (1)$$

where $g(\theta_r)$ is the mean canopy projection in the direction θ_r; and LAI is the leaf area index. Given a measured $P_0(\theta)$, we can then invert the expression to derive $g(\theta_r)$.

This mean canopy projection in direction $g(\theta_r)$ can then be related to the leaf slope distribution $f(\theta_a)$ via a Fredholm integral equation of the first king (Oliver and Smith, 1974); $g(\theta_r) = \int_0^{\pi/2} K(\theta,\theta_a)\ f(\theta)d\theta$, where the kernel $K(\theta,\theta_a)$ takes a different form depending on whether $\theta_a \leq \frac{\pi}{a} - \theta_r$ or $\theta_a > \frac{\pi}{a} - \theta_r$. A numerical solution to this equation, given a measured $P_0(\theta_r)$, has been implemented in FORTRAN, and is presented in the article by Oliver and Smith.

4.1.1 Sensitivity Analysis of the Fredholm Technique

The sensitivity analysis procedure developed for understanding the Fredholm technique is unique, as it studies the effects of changes in an input vector on an output vector. Classical sensitivity analysis involves incremental perturbations to a single variable of a complex model, while noting the induced changes in the model's prediction. This relationship is usually expressed in graphical form as a percent change in the output verses the percent change in the input (all other input variables are set at nominal values).

In the case under study, a methodology had to be derived which allows for control over the incremental changes in the input vector, and enables a description of the output vector changes. Figure 16 is a general flow chart of the procedure used. The probability of foliage gap in multiple view angle photos (P(GAP)) forms a nineteen element input vector to the Fredholm algorithm. The first element

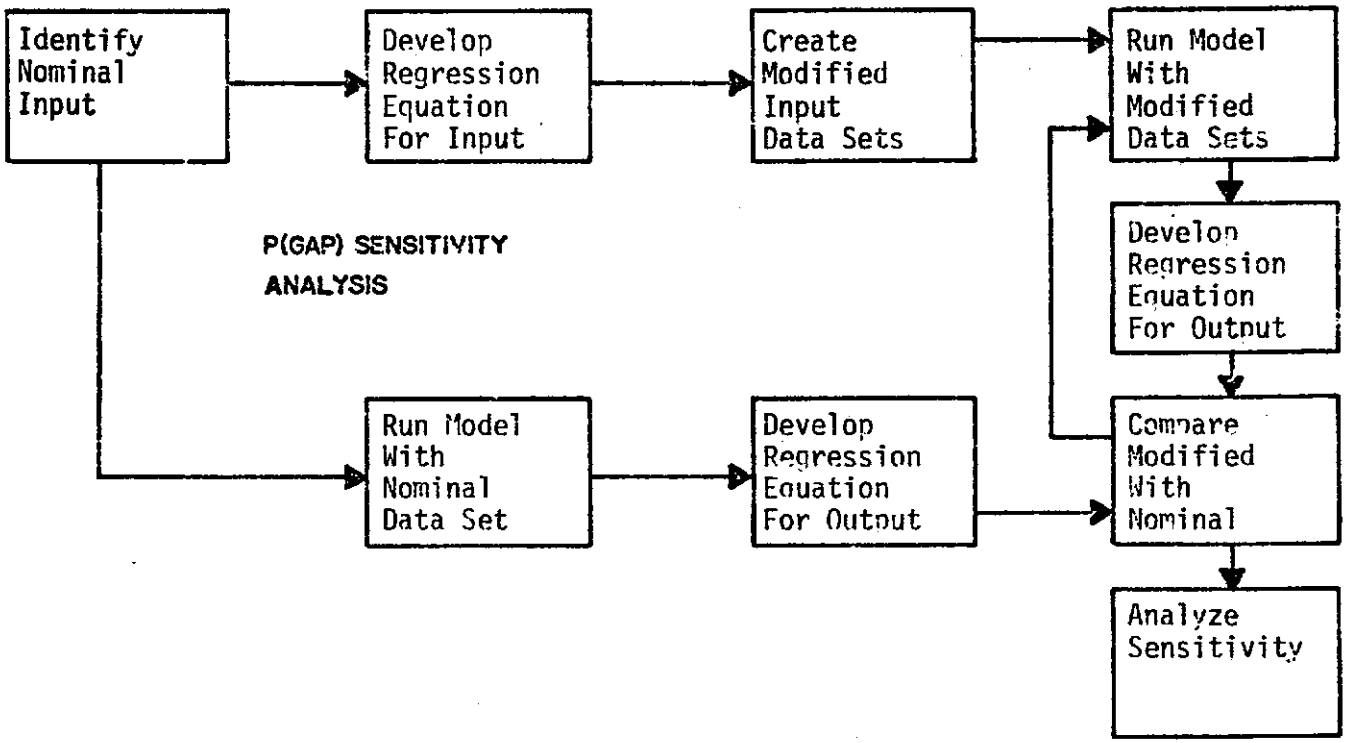

FIGURE 16. APPROACH TO FREDHOLM SENSITIVITY ANALYSIS. Regression equations for both the input and output vectors constituted the basis of the approach.

identifies the probability of gap from a vertical view, with the remaining elements defining off-angle views to the horizontal in increments of five degrees. Actual physical changes in canopy leaf angle distributions (LAD) are characterized in unique changes in the P(GAP) vector. The sensitivity analysis of the Fredholm technique investigates the responsiveness of the algorithm to controlled changes in this input vector.

The procedure begins with the fitting of a nominal input vector with a prediction equation (Figure 17). A perturbated data set is constructed by inducing scaler, rotational and translational shifts through uniform changes in each parameter of the prediction equation (Figure 18). The model is then run with each of the artificial input vectors, and the output noted.

The analysis of the output involves a procedure similar to that of generating the perturbed data sets. The model is executed with a nominal input vector, and a prediction equation is fit to its output. A gross analysis of the model's sensitivity is obtained by plotting the average percent deviation from the nominal output associated with the percent change in the input vector. Figure 19 shows this result for the three types of modifications. Note that the Fredholm technique is most sensitive to translational shifts in the P(GAP) vector, and nearly insensitive to scaler shifts.

Before this analysis can be meaningful, physical factors must be identified with each form of input modification. An upward scaler shift in the P(GAP) vector implies that the probability of seeing soil in all of the multiple angle views is increased. This effect could most likely arise by an overall decrease in plant density,

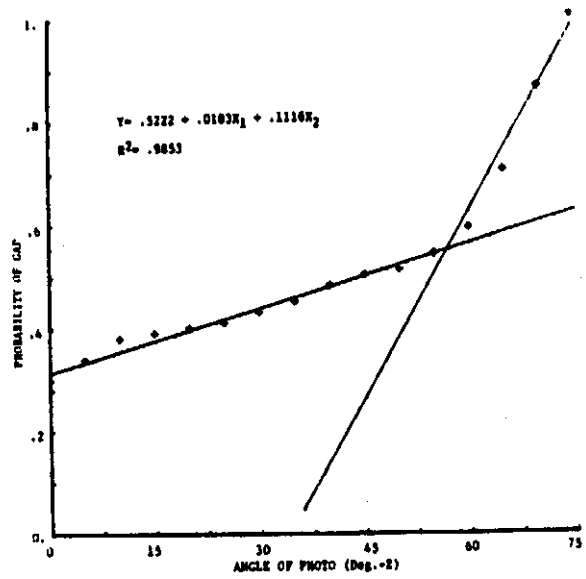

FIGURE 17. REGRESSION FIT OF INPUT VECTOR.

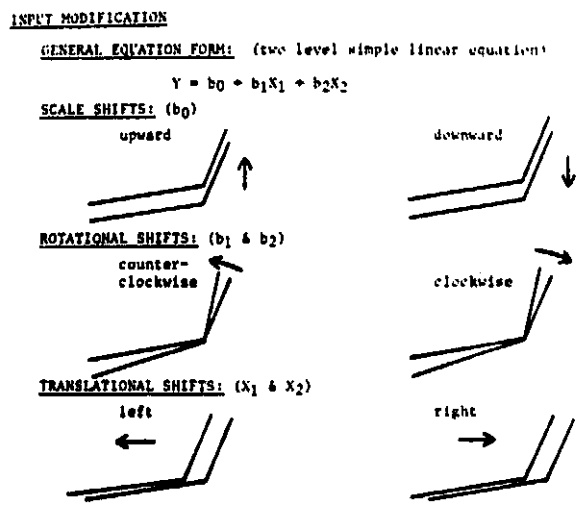

FIGURE 18. INPUT VECTOR MODIFICATIONS.

as measured by the leaf area index. Clockwise rotation of the input vector results in an increase in the probability of soil at the more vertical view angles, with a simultaneous decrease at the more horizontal views. This effect is most likely the result of the canopy's LAD becoming more vertically biased. Translational shifts represent relative plant dispersion and spacing which are driven by complex interactions of both LAI and LAD. It can be generalized, therefore, that the Fredholm technique is most sensitive to changes in canopy dispersion and LAD, and relatively insensitive to LAI, until plant cover becomes extremely dense.

Figures 20 through 22 show the type and magnitude of the induced effect on the model's output. The "a" and "b" curves identify scaler and rotational shifts in the output vector (LAD), respectively. In general, it can be stated that all three types of input vector modifications (scale, rotation, and translation), manifest themselves primarily in "a" factor shifts of the predicted LAD vector. As this vector is renormalized in the actual Fredholm algorithm, a purely scaler shift in LAD is not possible. However, an increase in the "a" factor does indicate a bias towards smaller inclination angles and a flattening of the slope of the LAD vector.

The "b" parameter best describes the relative form of the leaf angle distribution. A large positive "b" indicates a steep slope, which in turn, implies an erect canopy. In reviewing Figures 20 through 22, it is apparent that translational and rotational shifts dominate the determination of the slope of the output vector. Specifically, counter-clockwise rotation of the P(GAP) vector results

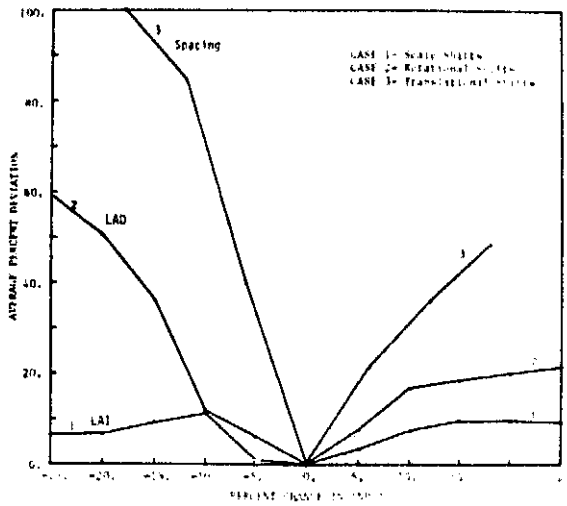

FIGURE 19. AVERAGE SENSITIVITY. Translational shifts in the P(GAP) input vector had the greatest effect on the LAD output vector.

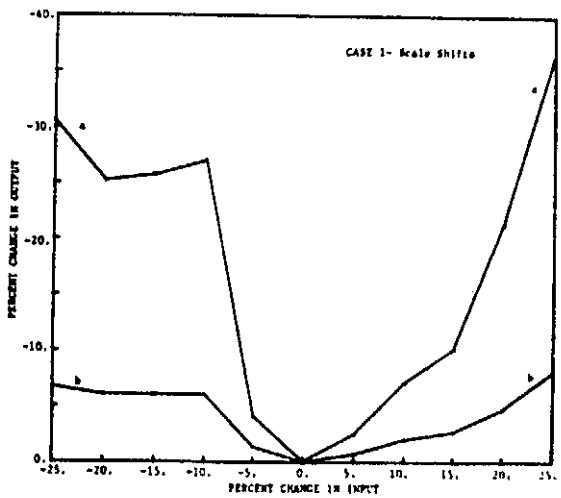

FIGURE 20. SENSITIVITY TO SCALER SHIFTS.

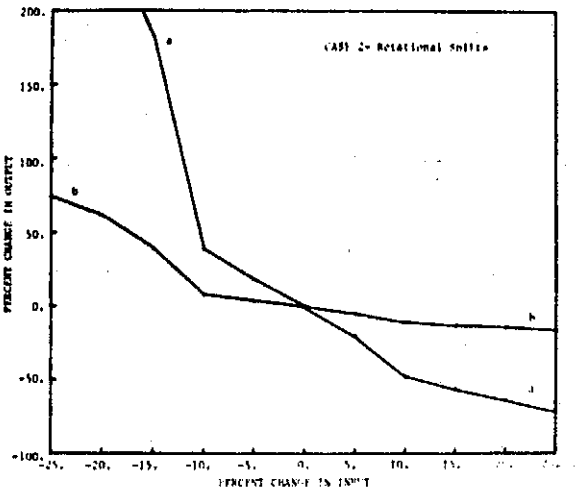

FIGURE 21. SENSITIVITY TO ROTATIONAL SHIFTS.

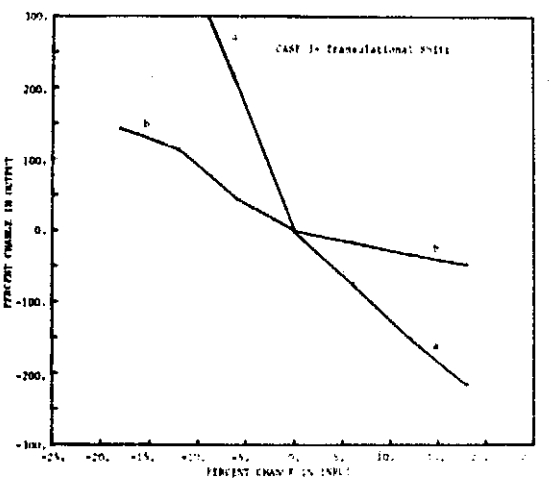

FIGURE 22. SENSITIVITY TO TRANSLATIONAL SHIFTS.

in an increase in the "b" parameter. The movement of the inflection point to the lower view angles generates a similar response.

In summary, the Fredholm model's prediction of leaf angle distribution is most responsive to rotational and translational shifts in the P(GAP) input vector. Clockwise rotation of the P(GAP) vector is principally the result of a flattening of the foliage's inclination angles, and results in the LAD's bias towards the smaller angles. Movement of the P(GAP) vector's characteristic inflection point to the left implies a complex condition (dependent on both LAI and LAD), where the projected surfaces of the foliage elements tend to become rapidly obscured at smaller view angles. This condition denotes LAD's bias towards the larger inclination angles.

4.2 The Fourier Technique

The Fourier technique involves the mathematical convolution of the distributions of angles for two or more orthogonal horizontal projections of a plant canopy to infer the three-space leaf angle distribution. In discussing this method, the physical process generating diffraction patterns is first presented, followed by discussions on the mechanics of sampling the patterns and the theoretical basis of convoluting the orthogonal distributions of angles.

4.2.1 Fundamentals of Optical Diffraction Patterns

Diffraction patterns result from the diffraction of light rays and their subsequent unique interference patterns. Diffraction refers to the bending of waves around an obstacle. Interference is an effect that occurs when two waves of equal frequency are superimposed. If, at the point of meeting, two waves are in phase (vibrating in

unison, and the crest of one coinciding with the crest of another), they combine to form a new wave of the same frequency and a larger amplitude equal to the sum of the amplitudes of the original waves (Figure 23). This effect is termed constructive interference.

If two waves meet out of phase (crest of one coinciding with a trough of the other), the result is a wave whose amplitude is the difference of the original amplitudes. The counterpart process is termed destructive interference. If the original waves have equal amplitudes and meet out of phase, they can be conceptualized as completely destroying each other; leaving no wave at all. Purely destructive interference, therefore, produces a dark spot, while constructive interference produces a bright spot. Partial constructive or destructive interference results whenever the waves have an intermediate phase relationship.

The process generating diffraction patterns involves optical diffraction and interference (Dobrin, 1968; Goodman, 1968). The diffraction of light as it passes edges, uniquely changes the phasing of light waves, thereby altering the interference relationships forming the diffraction pattern. As the relationships of the edges change, a corresponding change is induced in the interference pattern. Figure 24 schematically shows this fundamental process.

Stable diffraction patterns can only be generated if the phasing of the light rays forming them are not constantly changing. This stable condition is termed coherent. Most light is non-coherent, as the radiation from different atoms, acting as light sources, are constantly changing their relative phase relationships. An ordinary light source radiates light of mixed wavelengths in an out-of-step

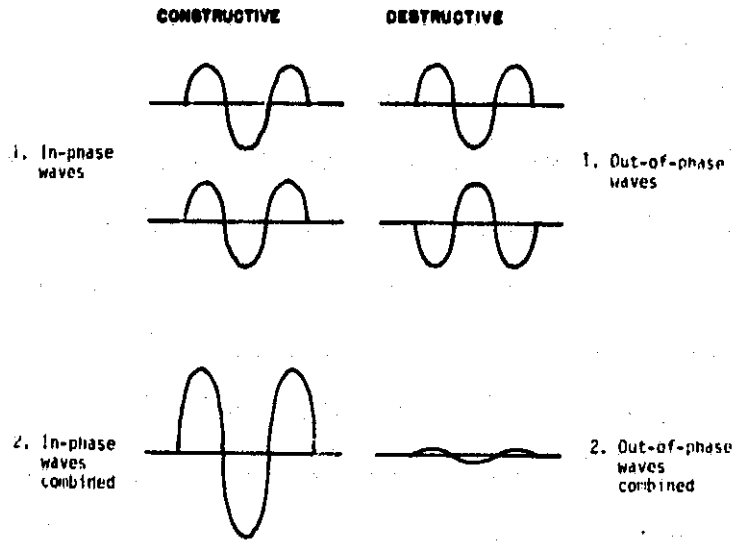

FIGURE 23. CONSTRUCTIVE/DESTRUCTIVE INTERFERENCE. Interference describes the interaction between two waves when they met.

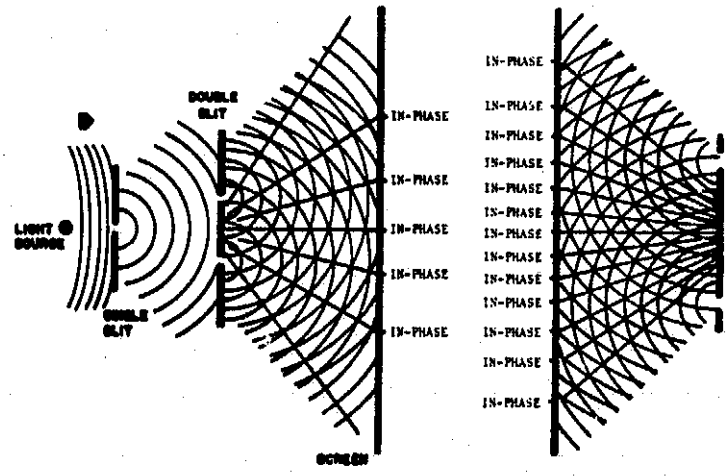

FIGURE 24. GENERATION OF DIFFRACTION PATTERNS. The display of the unique interference pattern on a screen is termed a diffraction pattern. Note the difference in diffraction pattern spacing and slit spacing between the two schematics.

(non-coherent) and random manner. In contrast, LASERs emit monochromatic, coherent light waves. The single slit in Figure 24 is required as it converts a normal light source into a nearly coherent source. In current applications, a LASER is used as the light source in diffraction analysis, because of its coherent properties and strong illuminance.

Figure 25 shows the process of generating diffraction patterns with the aid of a lens. This configuration allows for the concentration of the energy in the diffraction pattern, and results in much stronger and more discernable patterns.

Figure 26 outlines the fundamental relationships between the input image and the diffraction patterns which can be analyzed for spatial information (Pincus, 1969; Pincus and Dobrin, 1966). The types of information that can be uncovered include:

1. Orientation of elements
2. Spacing of elements
3. Location of elements

Element direction information is contained in the orientation of the diffraction "dots", which are perpendicular to the linear elements producing the dots. The spacing intelligence is inferred by the spacing of the dots, with the distance between the dots varying inversely with the true spatial frequency in the input. The techniques used in determining element location involve the related field of Holography and operate on the retention of the true phasing of two wave fronts. The work reported in this paper capitalizes on the ability to infer element orientation from diffraction patterns.

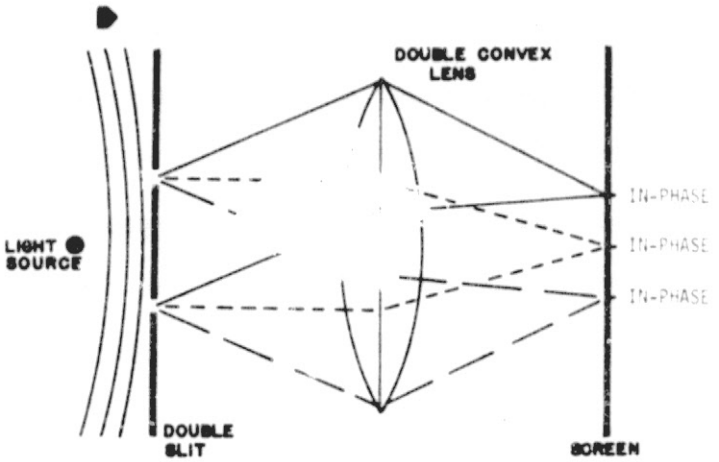

FIGURE 25. LENS CONTROLLED DIFFRACTION PATTERNS. The introduction of a lens between the "input" and screen increases the intensity of the diffraction pattern.

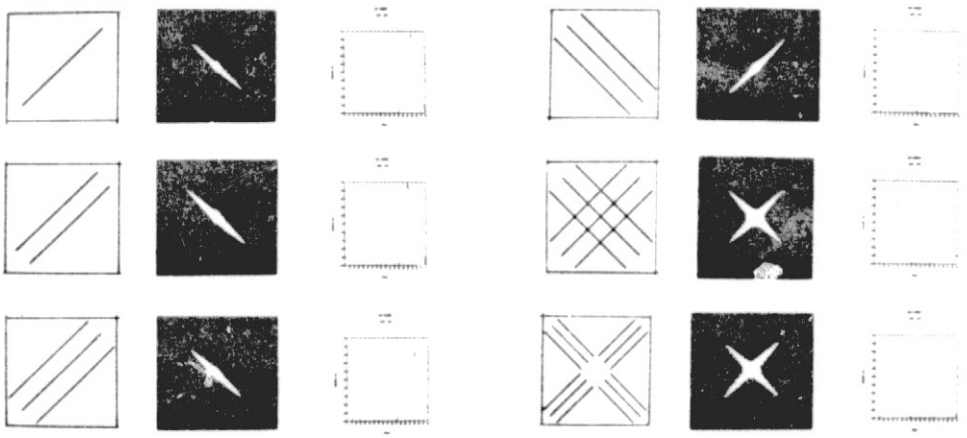

FIGURE 26. DIRECTIONAL INFORMATION IN DIFFRACTION PATTERNS. The orientation of the diffraction pattern is perpendicular to the linear segments in the "input".

In addition to the principle effects driving the orientation, spacing and location information, secondary effects are induced through multiple order considerations, interactions between elements, and irregular element spacing and orientation. The simultaneous interaction of both the primary and secondary factors results in clouds of points rather than descrete dots. These clouds can be thought of as a statistical summary of all the spatial information contained in a complex scene.

4.2.2 Sampling and Interpreting Orientation

Figure 27 shows the components of a simple optical diffractometer used to generate diffraction patterns. The LASER acts as a monochromatic, coherent light source which illuminates a reduced transparency (input) of a field scene (in this study the scene consisted of a horizontal picture of silhouetted wheat). The input functions as a diffraction grating with unknown spatial properties and bends the waves in a unique way. The altered light rays are passed through an objective lens which focuses the diffraction pattern onto a plano-convex lens. This final lens enlarges the pattern and displays it onto a rear projection screen. The diffraction pattern can then be photographed and retained for later analysis.

Sampling the diffraction pattern for spacing and orientation information about the original scene involves recording the portion of the pattern in appropriate segments. Spacing intelligence, as earlier noted, is contained in the distance between diffraction dots and the origin of the pattern. By placing consecutively larger circular bands around the origin and measuring the relative amounts of

the pattern contained in each, an estimate of the distribution of spacings can be obtained (Figure 28). Similar to ring sampling for spacing bias, is wedge sampling, which involves rotating a "pie slice" shaped filter about the origin. A distribution of angles in the input is inferred by the relative proportions of the diffraction pattern contained in each slice. Simultaneous sampling with a ring and wedge filters results in an estimation of the proportion of lines with a particular spacing that are oriented in a specific direction.

Figure 29 shows the wedge sampling procedure used in this study. The high contrast negative of the diffraction pattern is placed on a light table and covered with a small circular frame. A filter designed to fit into the frame, was constructed from a disk with a three degree slice removed. The relative intensity of light passing through the diffraction pattern segment defined by the wedge filter, is measured by a digital photometer. As the filter and attached detector are advanced equal distances (corresponding to equal degree rotations), discrete readings of the proportion of angles are recorded.

The tonal mapping of the diffraction pattern by the photographic negative is reversed. Therefore, a high reading by the photometer indicates a minimal portion of the pattern, while a low reading identifies the presence of a large portion. Program PROP (Appendix C) analyzes this information and develops the distribution of angles contained in the input scene.

In the application of spatial analysis to determining the leaf angle distribution of an entire canopy, it is necessary to convolute

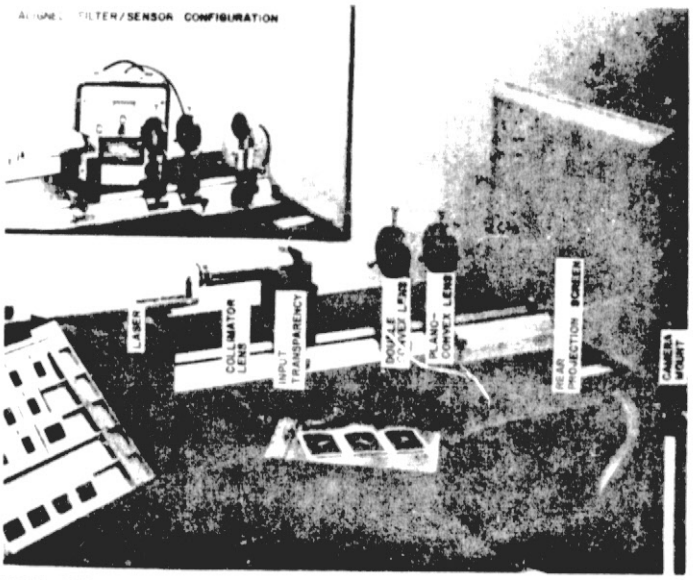

FIGURE 27. DIFFRACTOMETER COMPONENTS. The components of a laser diffractometer consists of a coherent, monochromatic light source, "input", focusing optics, and display screen.

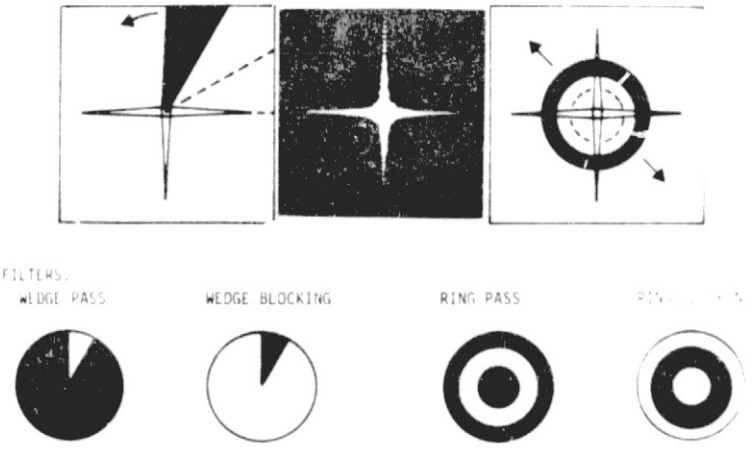

FIGURE 28. SAMPLING FILTERS. Ring and wedge filters are used to sample spacing and orientation of the diffraction patterns, respectively.

the two orthogonal probability distributions inferred from the diffraction patterns. Program CONVOL (Appendix C) is used to execute this process. The theoretical foundation of CONVOL's algorithm is presented below.

Given: distribution of angles in XZ view
distribution of angles in YZ view

Find : distribution of angles in XYZ space

Step 1 develop a matrix identifying the three-space angles associated with all pairwise combinations of descrete angles (e.g., 5 degree intervals between 0-90 degrees) which are possible in the orthogonal views.

Subproblem: (refer to Figure 30)
Derive a mapping function from θ in orthogonal views to θ in three-space.

Given: a line in three-space with θ_{XZ} and θ_{YZ}
assume lowest point is at origin (X=Y=Z=0)

Solution: $Z_2 = a + bX_2$

$= 0 + \tan \theta_{XZ} X_2$

and if we chose $X_2 = 1.$

$Z_2 = 0 + \tan \theta_{XZ}(1)$

$= \tan \theta_{XZ}$

in plane YZ,

$Z_2 = a + bY_2$

FIGURE 29. SAMPLING DEVICE. The components of the sampling device used in this study consist of a 3 degree wedge pass filter, a photo sensitive detector, and a digital readout.

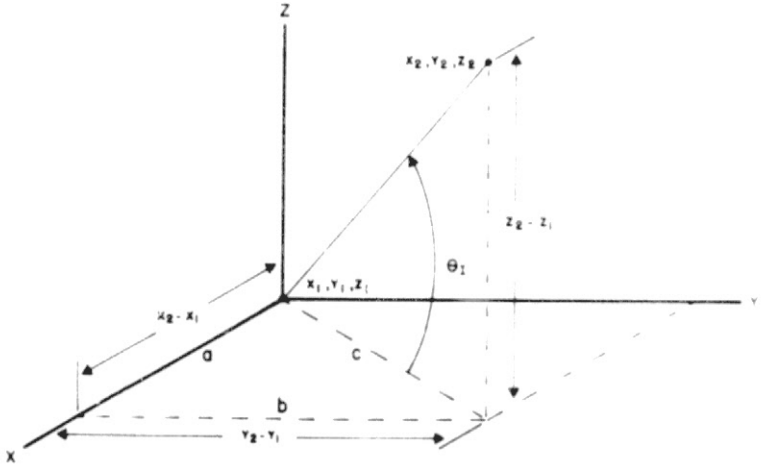

FIGURE 30. LINE IN 3-SPACE.

substituting,

$$\tan \theta_{XZ} = (0 + \tan \theta_{YZ})Y_2$$

$$Y_2 = \tan \theta_{XZ}/\tan \theta_{YZ}$$

therefore, two points on the line are known in three-space;

$$X_1 = Y_1 = Z_1 = 0$$

$$X_2 = 1;\ Y_2 = \tan \theta_{XZ}/\tan \theta_{YZ};\ Z_2 = \tan \theta_{XZ}$$

using the Pathagorean therom,

$$c = \sqrt{a^2 + b^2}$$

$$= \sqrt{(X_2-X_1)^2 + (Y_2-Y_1)^2}$$

$$= \sqrt{(1-0)^2 + \left(\frac{\tan \theta_{XZ}}{\tan \theta_{YZ}} - 0\right)^2}$$

$$= \sqrt{1 + \left(\frac{\tan \theta_{XZ}}{\tan \theta_{YZ}}\right)^2}$$

using the tangent relationship (opposite over adjacent) and substituting,

$$\tan \theta_Z = (Z_2-Z_1)/c$$

$$= (\tan \theta_{XZ} - 0)/c$$

$$= \tan \theta_{XZ}/c$$

or,

$$\theta_I = \tan^{-1} \left(\tan \theta_{XZ} \Big/ \sqrt{1 + \left(\frac{\tan \theta_{XZ}}{\tan \theta_{YZ}}\right)^2}\right) \quad (2)$$

This equation can be used to reduce any pair of orthogonal angles describing a line in three-space to the three-space inclination angle of the line, as required in step 1. It is used by program THETA (Appendix C) in developing the data matrix used by program CONVOL.

Step 2 The probability of any θ_{XZ}, θ_{YZ} pair is the joint probability of θ_{XZ} and θ_{YZ}.

$$P(\theta_{XZ}, \theta_{YZ}) = P(\theta_{XZ}) * P(\theta_{YZ})$$

The diffraction analysis of the orthogonal field photos yields the distribution of angles in the XZ and YZ planes.

Step 3 A unique θ_I may occur by several planer combinations, therefore,

$$P(\theta_I) = \sum_i (P(\theta_{ZXi}) * P(\theta_{YZi})) \qquad (3)$$

where $\sum_i$ indicates summing of all of the joing probabilities of all the pairwise combinations forming θ_I.

4.2.3 Qualitative Analysis of the Fourier Technique

This complex procedure was qualitatively evaluated in several ways. A computer program was designed which calculates the coordinates on orthogonal projections of lines in three-dimensional space. Figure 31 is a print of one of the microfilm sets of the two projections for a series of lines slanting at 45 degrees. It

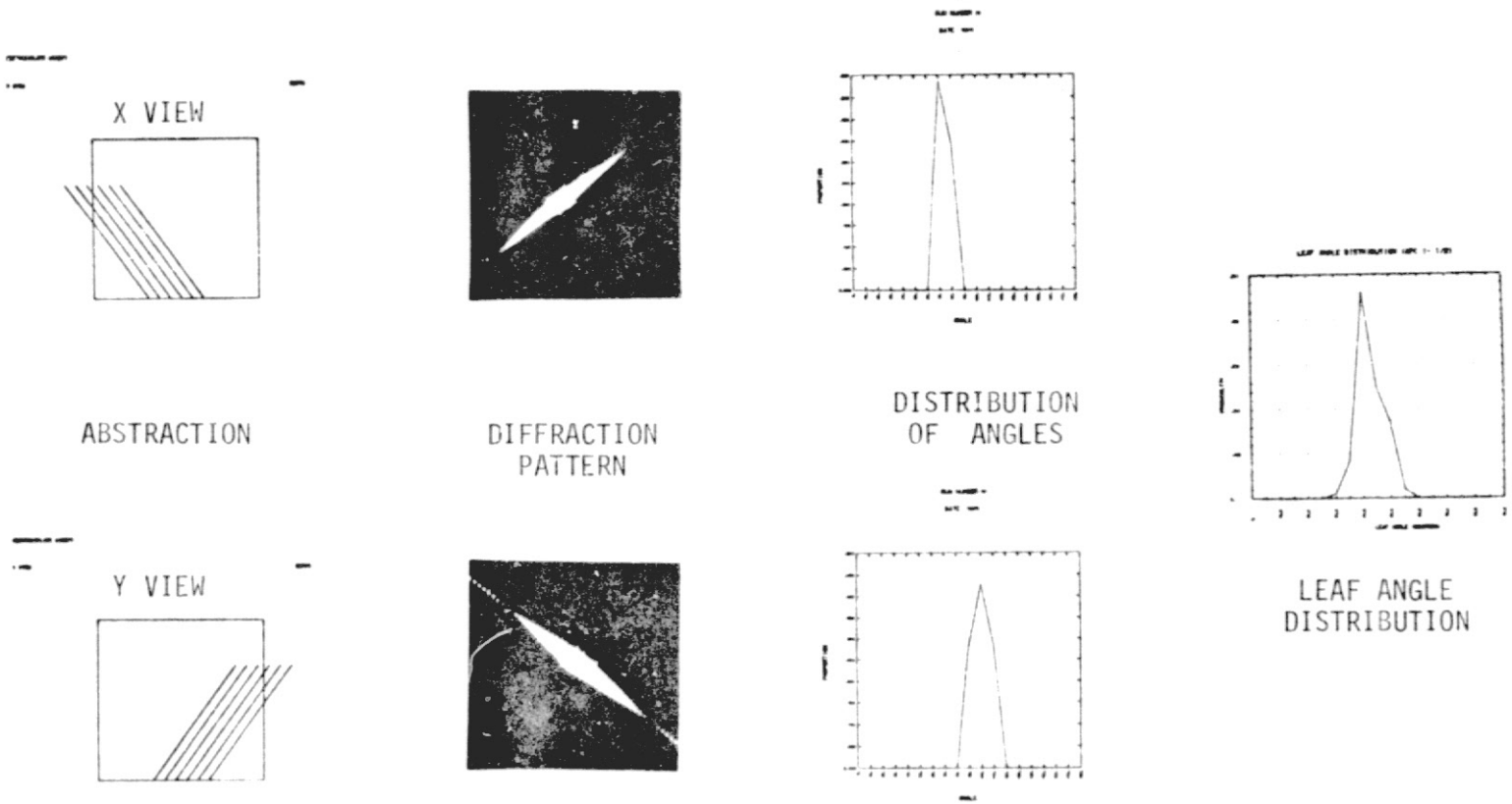

FIGURE 31. UNIFORM ABSTRACT PLANT CANOPY EVALUATION. A computer program was developed which generated microfilm plots of the orthogonal perspectives of a series of lines with a given spatial configuration.

may help the interpretation of these projections by imagining them to be transparent adjacent sides of a cube surrounding a series of sticks. In the X view, the lines form about a 60 degree angle, while in the Y view a 120 degree angle is indicated. The convoluted distribution of angles correctly indicates the true 45 degree three-space angle. Several cases were made for various angles and the procedure tracked them exceptionally well.

Figure 32 shows a typical example of the same program, yet the positioning and angles of the "sticks" were randomly assigned in accordance with a pre-determined distribution of angles. It was anticipated that the convoluted distribution of angles would closely correspond to the defined distribution driving the program. Again promising results were noted. However, as more lines were put into the scene the diffraction patterns became less distinct. This is due to the multiple interactions between lines. In light of these observations it was determined that a conserted effort should be made to reduce the number of silhouetted plant elements in a field photograph.

Figure 33 illustrates another qualitative evaluation method that was utilized. It consisted of taking orthogonal photographs of an abstract plant canopy constructed of tinker toys. All of the branches form 45 degree angles, with stalks perpendicular to the ground. The tracking of these canopy angles was excellent.

An actual field evaluation for both the Fredholm and Fourier techniques was performed and is presented in the next section. The results of this analysis showed the Fourier technique to be an extremely

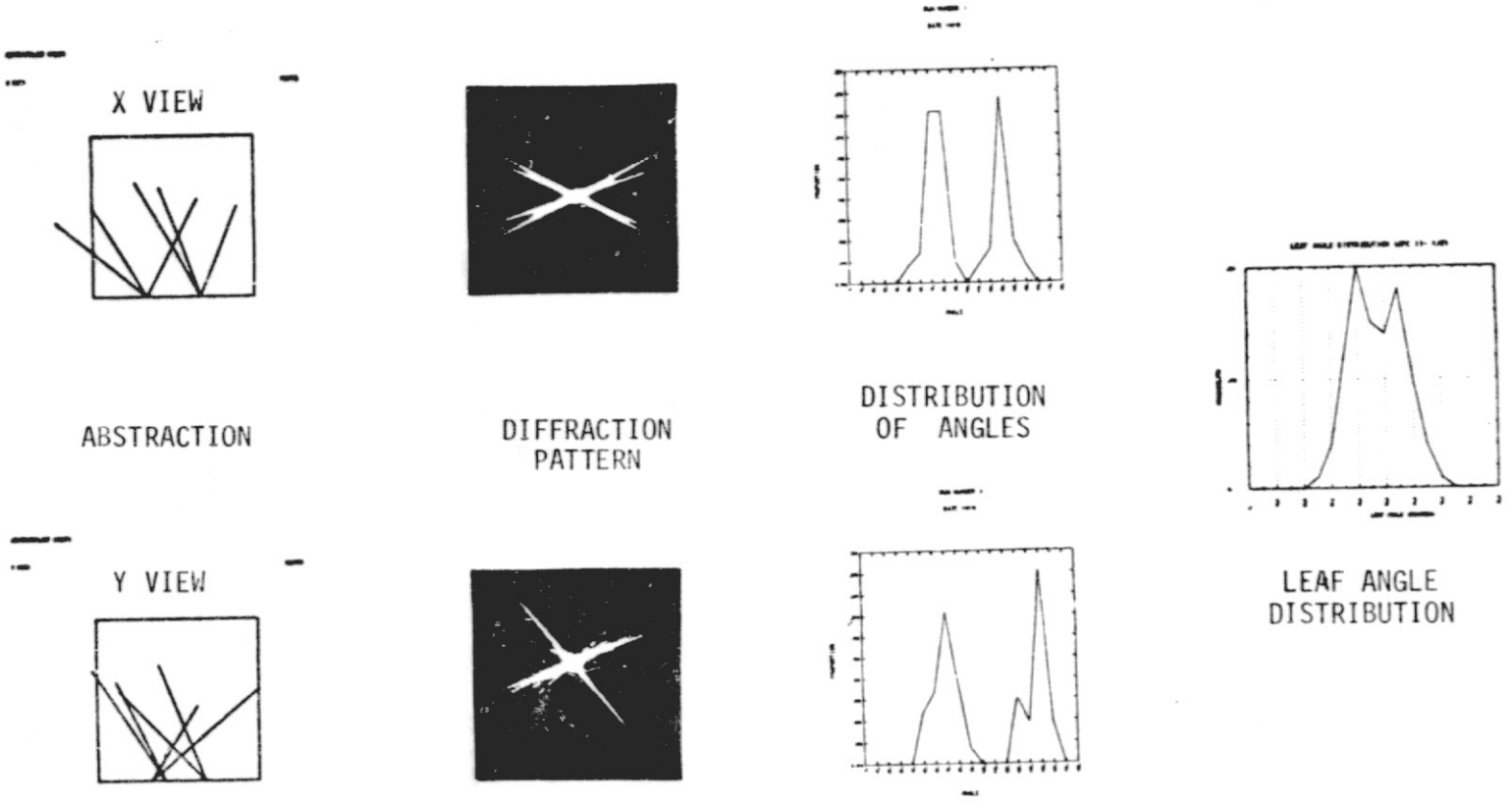

FIGURE 32. RANDOM ABSTRACT PLANT CANOPY EVALUATION. The microfilm plots of orthogonal views analyzed by the Fourier technique were developed by stochastic computing from user defined population statistics of spatial orientation.

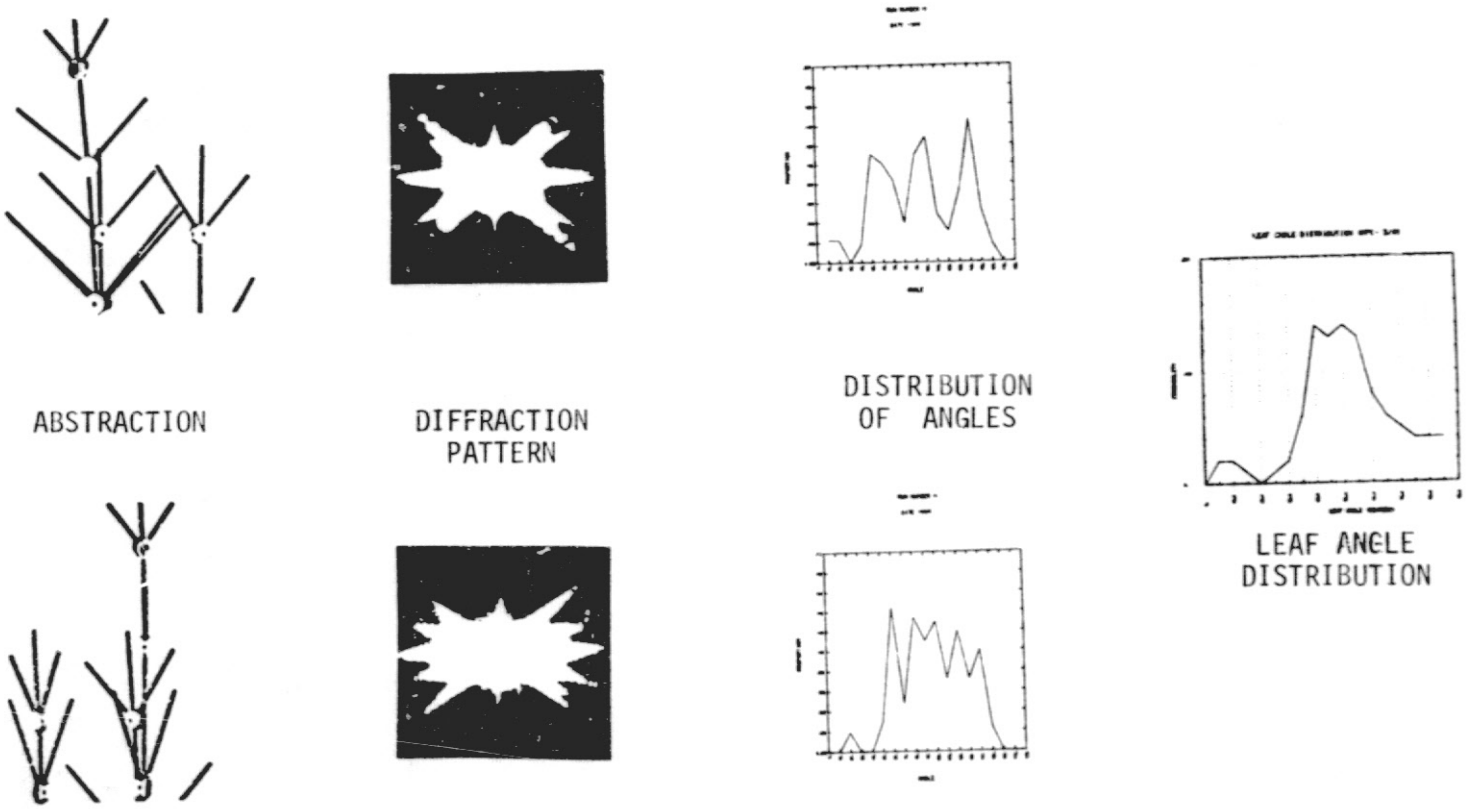

FIGURE 33. TINKER TOY ABSTRACT PLANT CANOPY EVALUATION. Orthogonal photographs of "Tinker Toy" plant canopies, with all branches set at 45 degrees inclination angle, were analyzed.

accurate descriptor of leaf angle distribution. The Fredholm method proved to be less accurate, however, it still offers a rapid technique for first order estimation of leaf angle distributions.

5.0 BENCHMARK COMPARISON OF LAD FIELD TECHNIQUES

A field evaluation was conducted which compared the Fredholm and Fourier methods for measuring leaf angle distributions used in this study. In addition, the Point Quadrat technique, extensively used in the agricultural sciences, and orthogonal tracings of leaves were employed.

An evaluation plot was selected such that it had a low leaf area index (.98) and its plants were uniformly dispersed (Figure 34). The plant type was Western Wheatgrass (Agropyron Smithii), which is characterized as having a conical leaf angle distribution (Oliver and Smith, 1973). The plot dimensions were 16 by 18 inches.

5.1 Description of Techniques

5.1.1 Point Quadrat Technique

It has been shown that the mean foliage angle can be calculated from the number of contacts made by point quadrats passed vertically and horizontally through a plant canopy (Philip, 1965; Wilson, 1959). In practice the error associated with this method rarely exceeds 10%. The technique is in situ, however, appreciable localized trampling is induced around the field plot. The time required for a single angle determination is about 18 man-hours (Knight, 1970). This method is most commonly used to characterize foliage geometry, however, it only estimates the mean inclination angle rather than a distribution of angles.

The field procedure involves the calculation of the average number of contacts a long slender pin makes with the vegetation during a pass through the plant canopy (Figure 35). The length of the pass, for both the horizontal and vertical transects, is dictated by the height of the canopy. Several hundred passes are made from both directions, with the averages for each being multiplied by empirically obtained coefficients to determine the mean foliage angle.

5.1.2 Orthogonal Tracing Technique

The distribution of foliage angles for an individual plant can be accurately determined by analyzing two orthogonal photos of the plant (Oliver and Smith, 1974). The distribution of angles for an entire plot is statistically determined by averaging the distribution of several representative plants. This technique has many of the limiting features associated with the point quadrat method. It is slow, tedious and destructive. However, it is a direct method which makes it useful for comparing the other methods.

With this procedure, individual plants are clipped from a field plot and the silhouetted profiles are photographed from two orthogonal directions (Figure 36). The photographs are then digitized by placing a transparent grid over the photographs and recording the two-dimensional coordinates of straight line segments along the profiles. The profiles are plotted on microfilm (Figure 38) using the digitized data in order to verify the digitization. A computer program was developed for this study which determines the three-dimensional coordinates of the foliage elements from the two sets of orthogonal data, and calculates the average foliage inclination

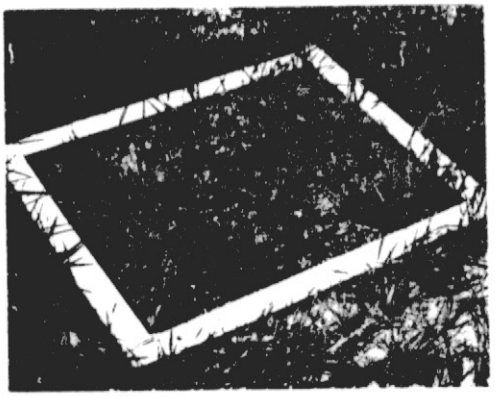

FIGURE 34. EVALUATION PLOT. The evaluation plot was a relatively low density area of western wheatgrass.

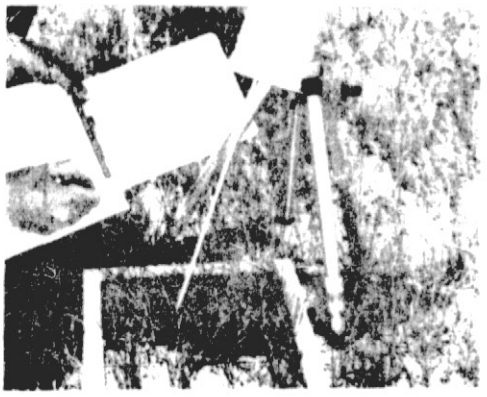

FIGURE 35. POINT QUADRAT FIELD TECHNIQUE. The field procedure consists of noting the number of contacts a long slender pin makes with foliage elements throughout numerous passes through the canopy at specific angles.

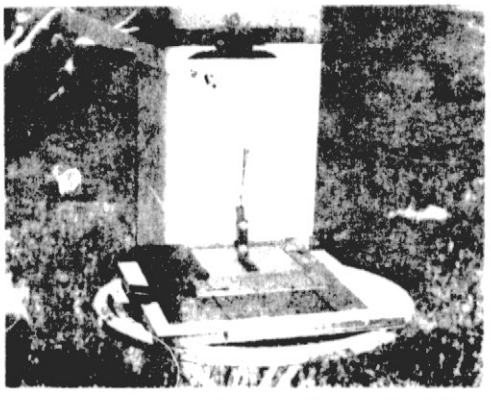

FIGURE 36. ORTHOGONAL TRACING FIELD TECHNIQUE. Orthogonal photographs were made of individual silhoutted plants. These same photographs were used for the Fourier analysis.

FIGURE 37. FREDHOLM FIELD PROCEDURE. Multiple view angle photographs were made of the evaluation plot.

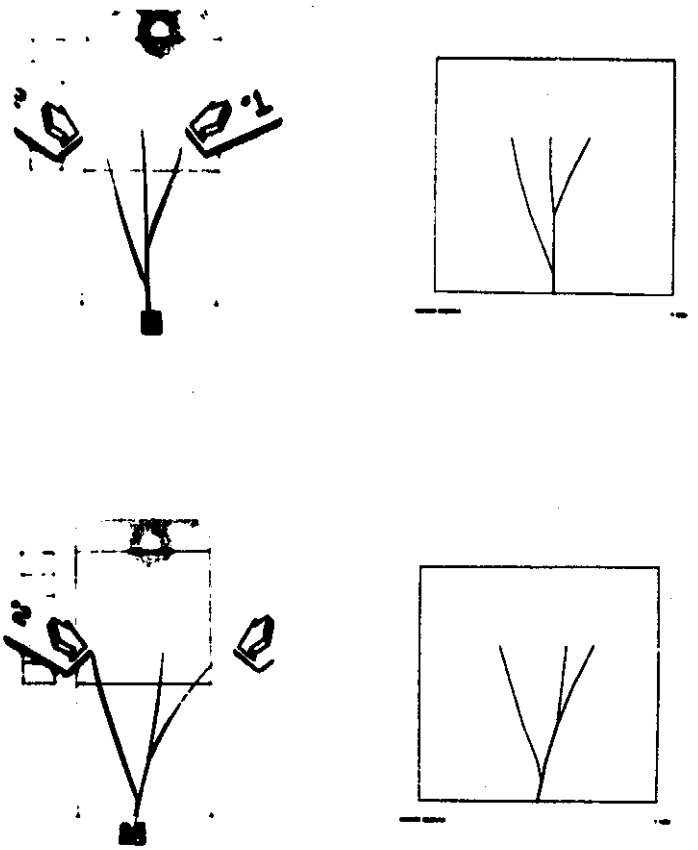

FIGURE 38. ORTHOGONAL TRACING DATA REDUCTION. The orthogonal field photos of individual plants were digitized, with the two-space coordinates serving as input to a computer routine which calculated the three-space distribution of angles.

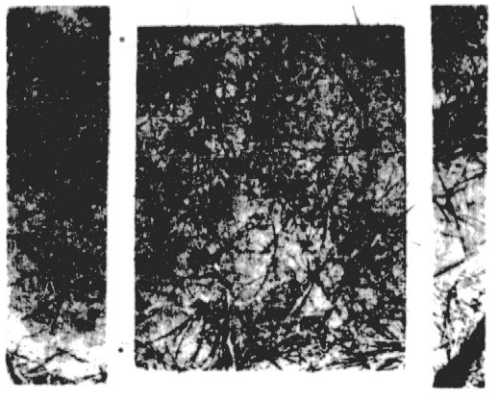

0^{o}

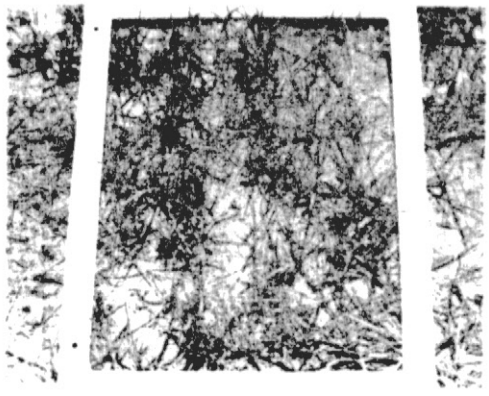

20^{o}

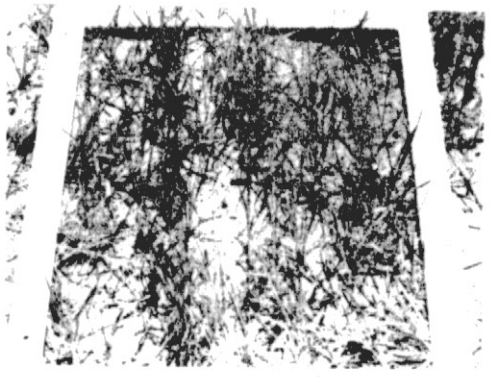

40^{o}

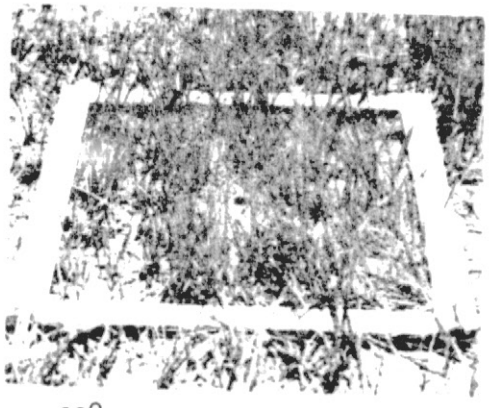

60^{o}

FIGURE 39. FREDHOLM DATA REDUCTION. The percent cover in each of the multiple view angle photographs was determined by dot grid analysis.

angle by direct computation (program, ORTHOG, Appendix C). The distribution for the entire plot is calculated by the weighted averaging of the individual plant distributions based on the size of the plant.

5.1.3 Fredholm and Fourier Techniques

The field procedures and theoretical framework for the Fredholm and Fourier methods are presented in the previous section. Figures 37 and 39 show examples of the field photographs and reduced data. For this evaluation the tracings of the individual plant photographs used in the Orthogonal Tracings technique were used as input in generating the Fourier diffraction patterns (Figure 40).

The relative merit of the Fredholm method is its ease of data collection with a minimum of canopy disturbance. The Fourier technique is much slower and more tedious than the Fredholm method, yet it is still relatively easy and rapid when compared to either the Point Quadrat or Orthogonal Tracing techniques.

5.2 Description of Evaluation Procedure

Two fundamentally different evaluation procedures were used. The first involved the comparison of the four basic techniques' predictions of the leaf angle distribution for a common field plot. The normal steps for the Orthogonal, Fourier, and Fredholm methods are schematically shown in Figure 41. The Point Quadrat technique merely required the simple solution of a linear equation predicated on the field estimation of the number of needle contacts.

The second evaluation approach is more abstract in nature, and addresses the validity of the convoluting algorithm used in the Fourier technique. Figure 42 identifies the major steps in this

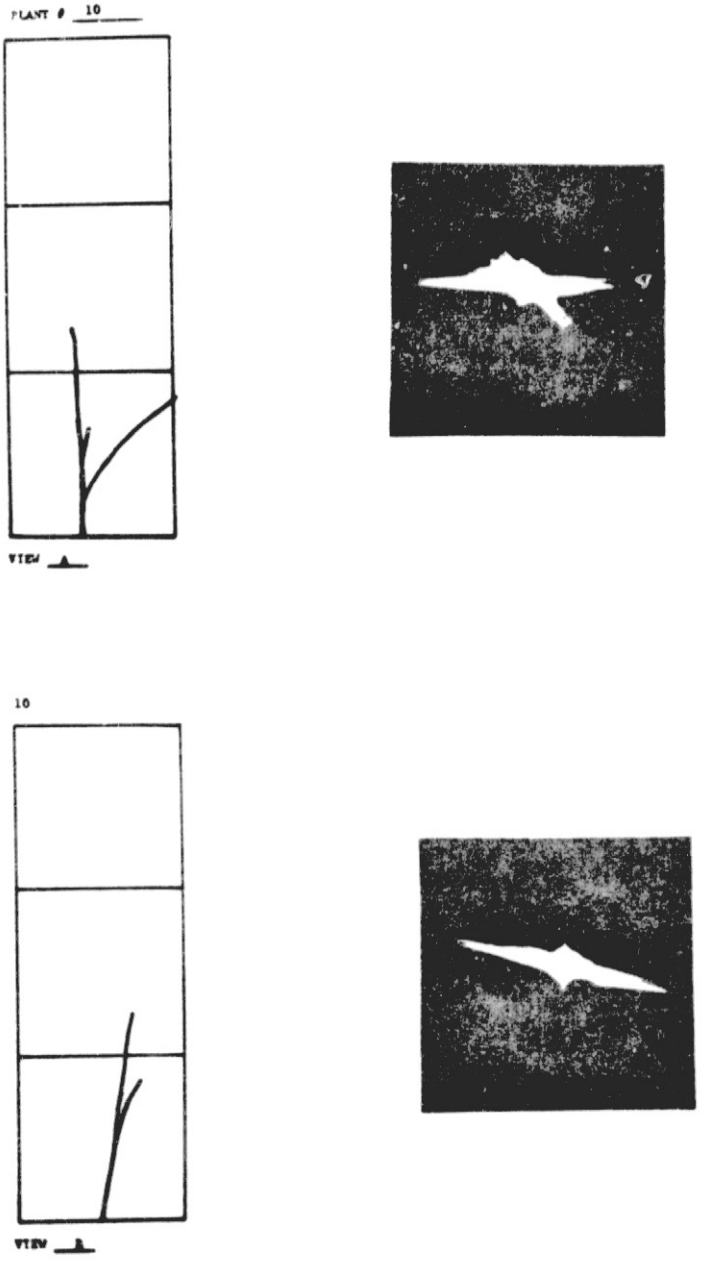

FIGURE 40. FOURIER DATA REDUCTION. Diffraction patterns were generated and analyzed of each of the orthogonal photos of the individual plants.

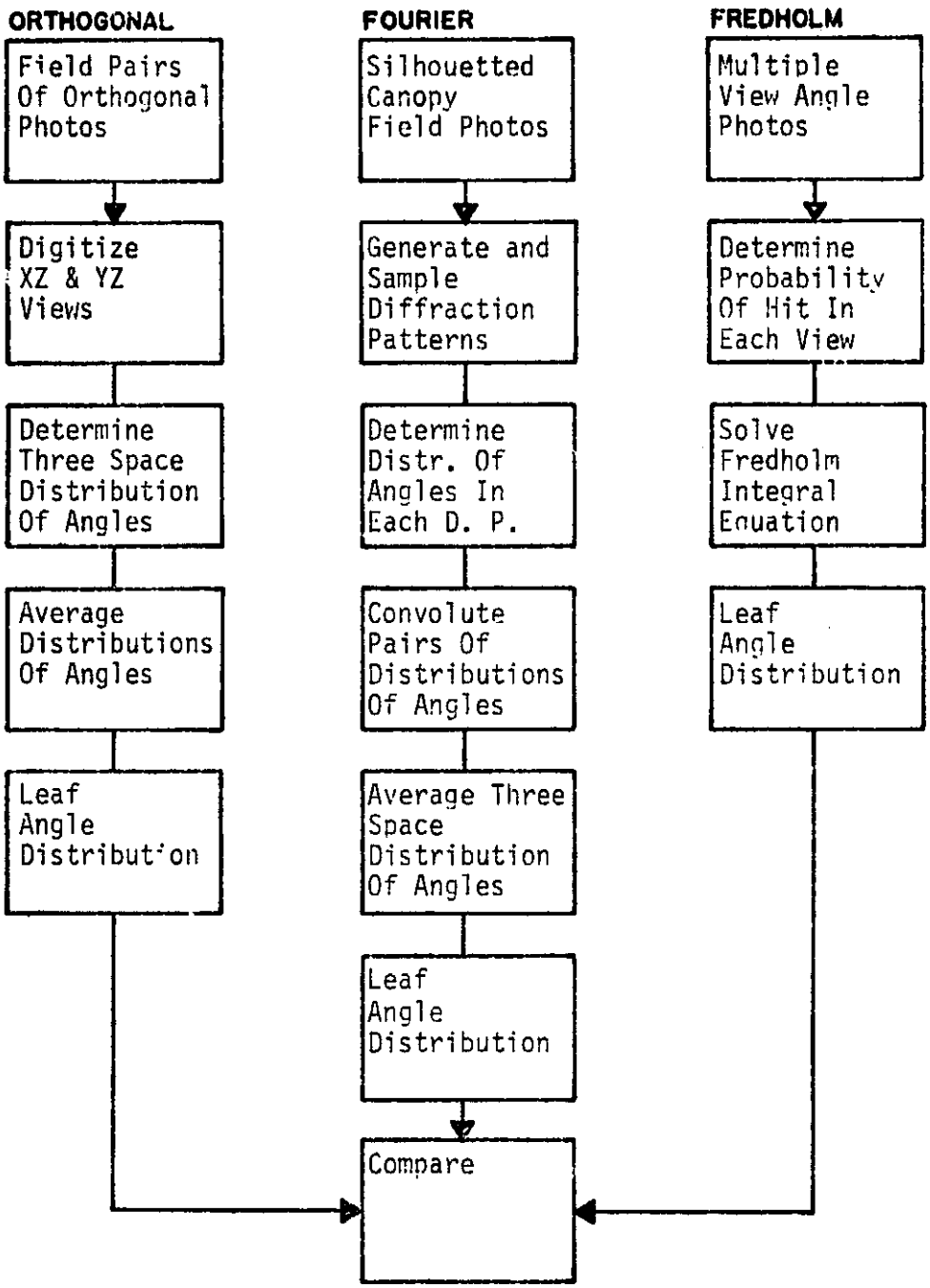

FIGURE 41. TECHNIQUES EVALUATION APPROACH. Each of the three field techniques under study were executed on a common plot, and compared.

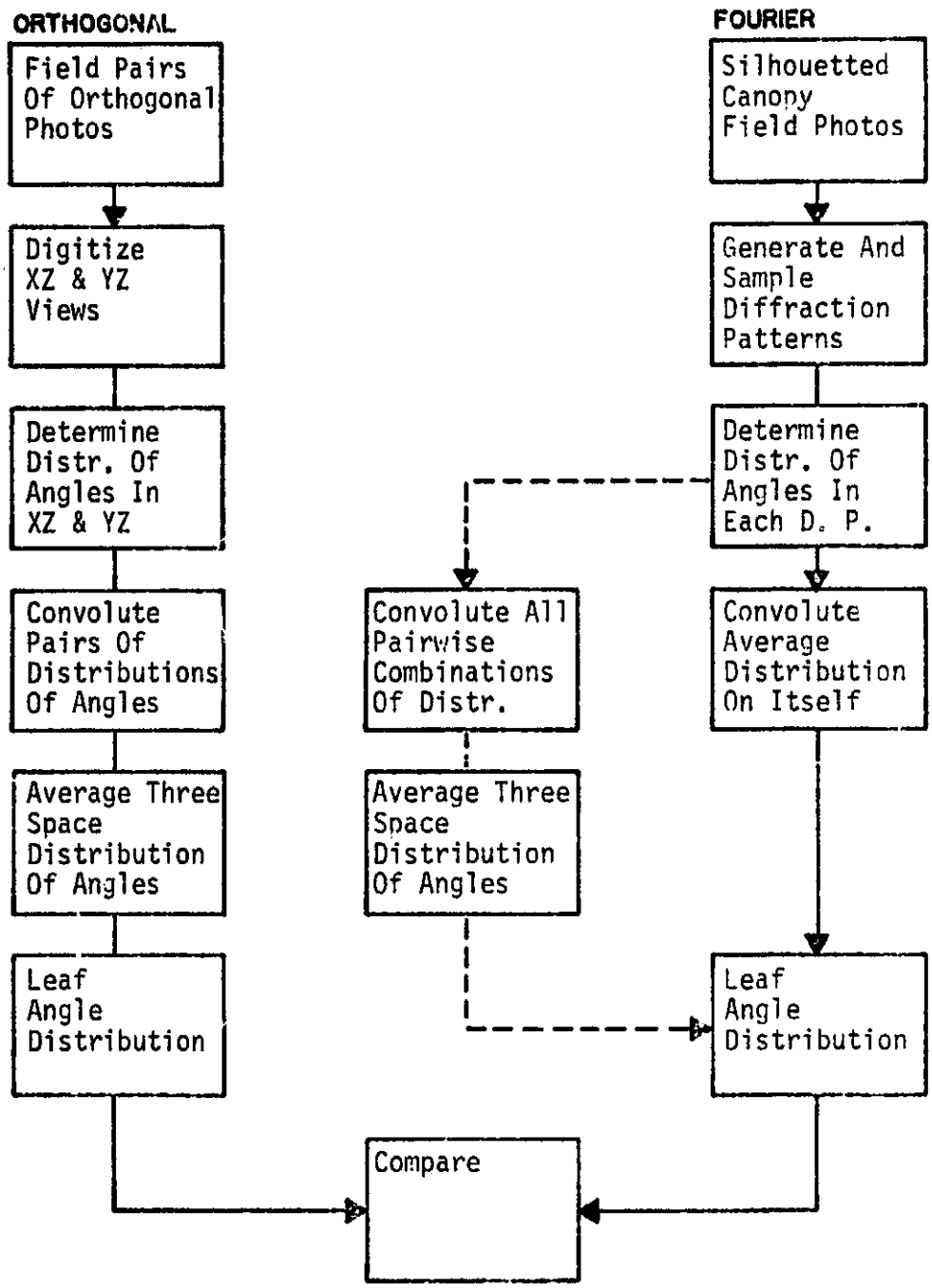

FIGURE 42. FOURIER METHODOLOGY EVALUATION APPROACH. The convoluting algorithm and orthogonal pairing assumption were evaluated.

process. In the left hand flows the digitized photos are used to calculate a relatively exact distribution of angles in each orthogonal view. The orthogonal pairs are then convoluted and finally all three-space distributions are averaged to yield the predicted canopy leaf angle distribution. The ability of this abstract approach to accurately correspond to the normal Orthogonal method is a measure of the validity of the convoluting algorithm.

The right hand flows identify a process designed to evaluate the necessity of having truely orthogonal pairs of silhouetted field photos. If the canopy does not have an azimuthal bias, then there would be no physical reasons for differentiating between photo perspectives, other than statistical sampling requirements. The extreme right hand column incorporates this assumption by determining the average distribution of all the planner projections, and then convoluting this average distribution on itself. A slightly different format (identified by the dotted lines) convolutes all the pairwise combinations of planner distributions, and averages the resulting three-space distributions. The essence of these reviews is to determine whether the Fourier technique is truely dependent on orthogonal field photos.

5.3 Comparison of Results

The results of the separate procedures are summarized in Figures 43 through 49 and Table 1. Figures 43 through 46 correspond to the evaluation of the normal procedures, while Figures 47 through 49 address the convolution assumption of orthogonal views. The results are graphically presented to facilitate a qualitative assessment of each technique's precision.

Table 1. COMPARISON OF FIELD TECHNIQUES FOR ASSESSING LAD.

INCLINATION ANGLE	ORTHOGONAL TRACING	FOURIER	FREDHOLM	ORTHOGONAL CONVOLUTE	FOURIER AVERAGE	FOURIER PAIRWISE
2.5°	0.	0.	0.	0.	0.	0.
7.5	0.	0.	0.	0.	0.	0.
12.5	0.	0.	0.	0.	0.	0.
17.5	0.	0.	0.	0.	0.	0.
22.5	0.	0.	0.002	0.	0.	0.005
27.5	0.	0.001	0.012	0.	0.001	0.005
32.5	0.016	0.005	0.024	0.018	0.006	0.015
37.5	0.026	0.012	0.038	0.025	0.015	0.026
42.5	0.006	0.027	0.051	0.002	0.033	0.055
47.5	0.022	0.046	0.063	0.040	0.050	0.083
52.5	0.114	0.068	0.073	0.058	0.069	0.099
57.5	0.056	0.110	0.083	0.158	0.105	0.132
62.5	0.112	0.121	0.091	0.141	0.111	0.119
67.5	0.139	0.149	0.100	0.132	0.139	0.142
72.5	0.196	0.131	0.106	0.129	0.126	0.117
77.5	0.158	0.111	0.112	0.159	0.112	0.114
82.5	0.088	0.130	0.120	0.080	0.139	0.069
87.5	0.066	0.088	0.126	0.057	0.093	0.023
MEAN FOLIAGE ANGLE	68.0°	68.0°	66.0°	66.7°	67.9°	62.8°

Point Quadrat Mean Inclination Angle = 72.5°

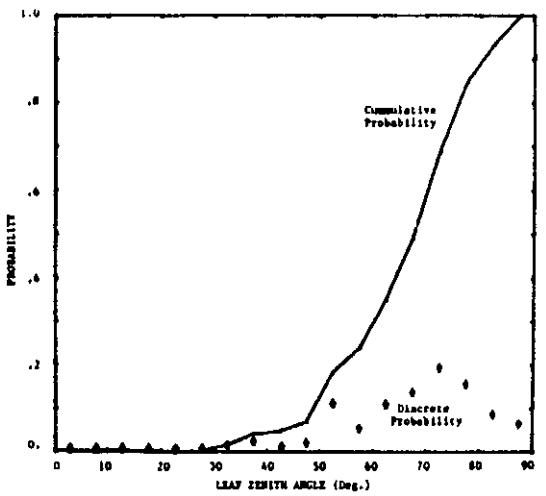

FIGURE 43. ORTHOGONAL TRACING TECHNIQUE RESULTS.

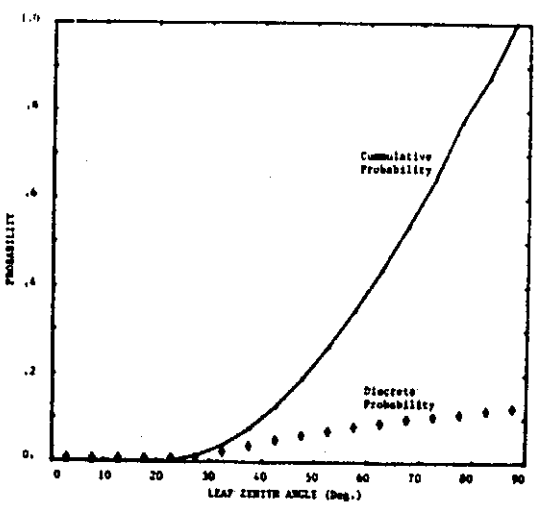

FIGURE 44. FREDHOLM TECHNIQUE RESULTS.

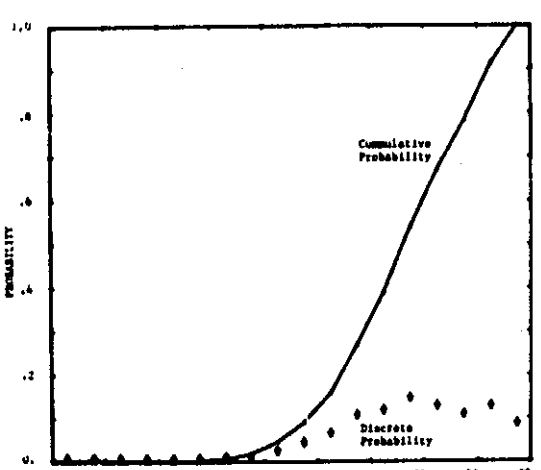

FIGURE 45. FOURIER TECHNIQUE RESULTS.

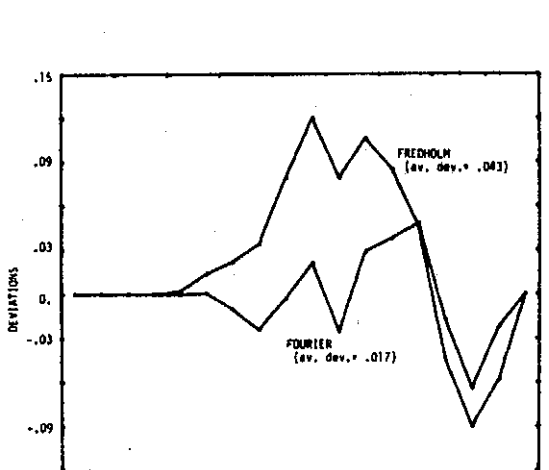

FIGURE 46. FREDHOLM/FOURIER DEVIATIONS.

The mean foliage inclination angle calculated by the Point Quadrat method was 72.5 degrees. In comparing this prediction with those calculated by the other three techniques it appears to be an over-estimate (Table 1). This condition could easily be a result of this author's inexperience with its field procedure. Also contributing to the implied error could be that the empirically derived regression equation employed was developed for general grassland canopies (Knight, 1970) and not specifically for Western Wheatgrass.

Figure 46 compares the effectiveness of the Frednolm and Fourier methods to track the cummulative distribution of angles predicted by the Orthogonal Tracing technique. It is readily apparent that the Fourier procedure compares more favorably. Less obvious is the common pattern of deviations. Both techniques tend to over-estimate the probability of inclination angles less than 80 degrees. This result is most likely due to the averaging approach of both techniques which fail to respond to the sharp fluctuations of the Orthogonal method. This same effect is apparent in the predictions made by convoluting the actual planner distribution of angles calculated by the Orthogonal technique (Figure 47).

The comparison of pairwise and average approaches of convolution (Figures 48 and 49) shows that strict utilization of truely orthogonal pairs is not necessary in these circumstances. In this evaluation, the convolution of the average distribution of angles for all of the planner views did an excellent job in tracking the orthogonal method. However, a rowed crop, such as wheat, may require orthogonal pairing, and further evaluation is warranted.

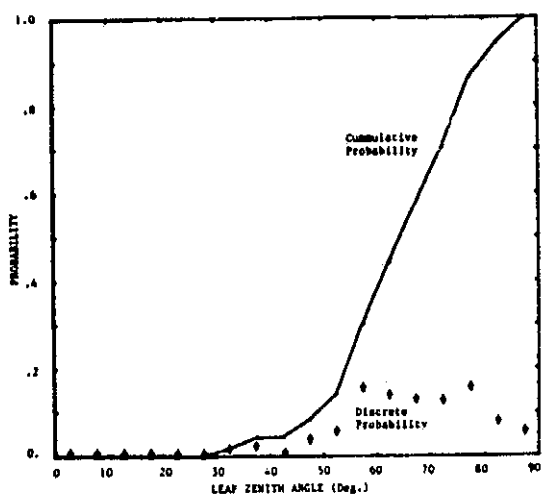

FIGURE 47. CONVOLUTED ORTHOGONAL TRACING RESULTS.

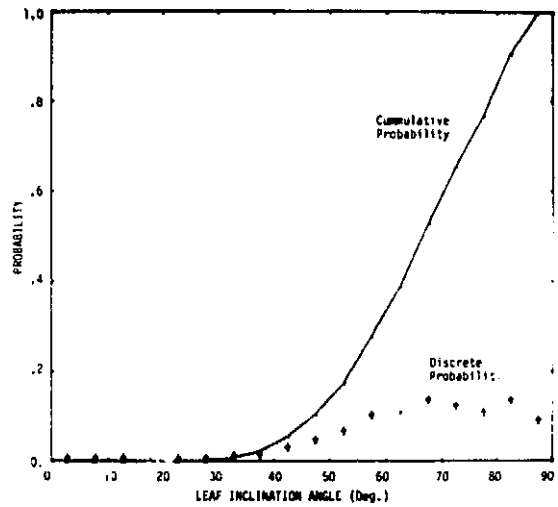

FIGURE 48. CONVOLUTED AVERAGE DISTRIBUTION OF ANGLES

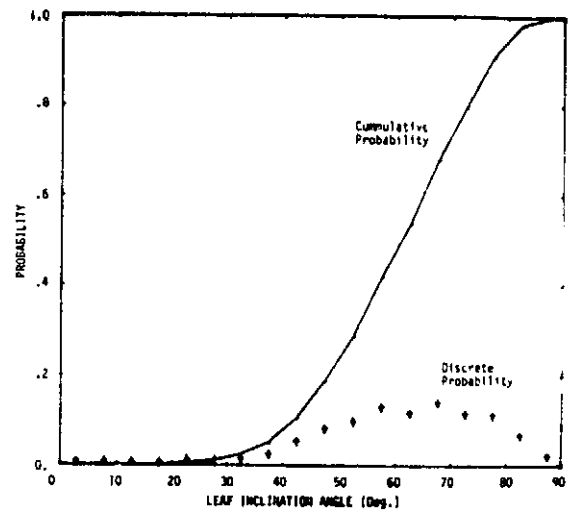

FIGURE 49. CONVOLUTED PAIRWISE COMBINATIONS OF DISTRIBUTIONS OF ANGLES RESULTS.

6.0 MODEL SIMULATION

Fundamental to the hypothesis under investigation is the ability to adequately model the complex system of interactions between solar radiation and a plant canopy. In addition, the interactions between this radiation and the atmosphere must be linked to the canopy model in order to fully describe the physical process. The models adapted to the investigation are briefly discussed in the following subsection. The description of these models is merely intended to familiarize the reader with their basic approaches. The cited literature contains several detailed reports which should be consulted for a more thorough understanding.

The process used in discriminating geometric variables of a plant canopy principally involves the statistical comparison of a sensor measured response to a series of model derived responses. In developing these model responses, the geometric variable of concern is allowed to systematically vary, while all of the other variables remain fixed at their best estimates. The specific procedures used in simulating the surface canopy reflectance and satellite radiance are presented in the last two subsections.

6.1 Canopy Reflectance and Atmospheric Models

The canopy reflectance model used in this study is Colorado State University's Solar Radiation Vegetation Canopy (SRVC) Model (Oliver and Smith, 1973, 1974). This model differs from other plant canopy

models (Suits, 1972; Colwell, 1974; Allen and Richardson, 1968; Kubelka and Munk, 1931) in that the driving variables and canopy structure are based on probability distributions. This orientation results in an estimation of both the mean canopy reflectance and its covariance matrix. The deterministic approach of the other models yields estimates of mean responses, without any direct inference to the central tendency.

The model's input parameters can be divided into two principle classes: 1) environmental factors; and 2) intrinsic scene characteristics. The environmental factors include sun position, diffuse and direct irradiance, and sensor view angle. Leaf area index, leaf angle distribution, and spatial dispersion of foliage elements describe a plant canopy's geometric characteristics. The canopy's radiometric input parameters include soil reflectance and individual leaf reflectance and transmission.

The methodology of the model involves the mathematical tracking of a photon of light as it interacts with a plant canopy. The environmental factors determine the spectral composition and angular dependency of the total scene irradiance. Intrinsic scene parameters are used to develop the probability distributions which stochastically determine the interaction of the solar radiation and the plant canopy, and to calculate the spectral modifications and redirections resulting from the interactions. The model's operation begins with an instantaneous burst of hemispherical irradiance. This pulse is then charted in its multiple interactions with the canopy until all of it has escaped back into the sky or has been absorbed by the canopy and background.

The atmospheric radiative transfer model used in this study is the Environmental Research Institute of Michigan's Model (Turner, 1973). The approach of this model is founded on the solution of a series of explicit mathematical expressions. The basic relationship describes the total spectral radiance at a sensor as,

$$N = (N_{target} * T) + N_{path} \quad (4)$$

where, N = total radiance

N_{target} = target spectral radiance at the surface

T = spectral transmittance between the sensor and the target

N_{path} = spectral path radiance

All three of these quantities depend upon the condition of the atmosphere. The actual state of the atmosphere at any location and at any time is approximated by atmospheric variables and environmental factors. Among the atmospheric variables are the scattering and absorbing properties of gases and particulates that exist in the atmosphere. Environmental factors include sensor attitude and view angle, sun angle, and canopy reflectance.

6.2 Simulation for Surface Canopy Reflectance

The complete procedure for estimating leaf area index from spectral measurements through the use of modeling contains four major activities: 1) the identification of model input parameters through a field measurements program; 2) the construction of a model generated data set which tracts the induced changes in canopy spectral reflectance arising from variations in LAI; 3) the translation of surface

reflectance data into estimated radiance values at an airborne sensor through atmospheric modeling techniques; and 4) the statistical comparison of measured and model derived spectral signatures to yield an estimate of the scene's LAI. The first activity was outlined in Section 3.0, and the fourth is presented in Section 7.0. This section is concerned with the middle two activities.

The canopy model simulation for LAI determination utilized the March and April field measurements, which correspond to the tillering and jointing stages of wheat. These stages were selected as they contain the extremes in LAI and are similar in canopy make-up. Both are characterized by a green canopy prior to seed head development, with their primary difference being a dramatic increase in LAI at the jointing stage.

Figure 50 shows a comparison of field and model estimates of canopy reflectance at the two phenological stages under study. In both cases, the model prediction was made from a nominal input data set representing the best estimates of field conditions. The empirical signature is an average of the direct measurements made from the three intensive field plots. Additional comparisons were made for thirty sun angles obtained from canopy reflectance measurements taken between 1030 and 1630 hours on March 20th, and 1000 and 1800 hours on April 23rd. A complete set of the field and model data from this effort is reported in a paper by Smith, Berry and Heimes (1975). In general, it can be noted that the model was successful in tracking the empirical data during the jointing (April) stage, while it was somewhat less accurate during the tillering stage (March).

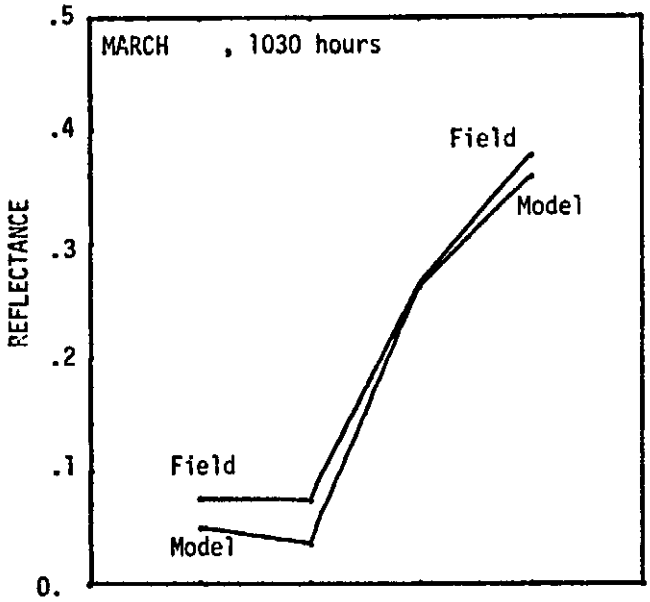

MSS BAND	MODEL	FIELD
4	.050	.076
	±.007	±.004
5	.036	.075
	.005	.005
6	.262	.264
	.004	.031
7	.359	.378
	.058	.075

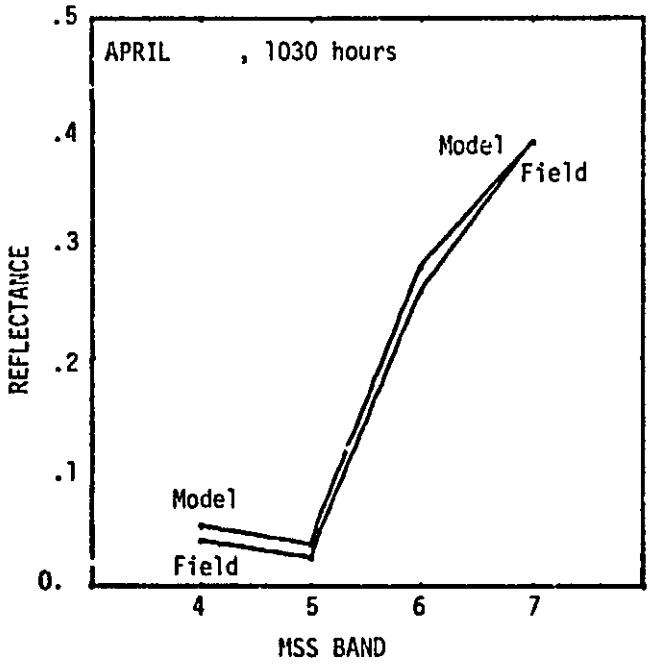

MSS BAND	MODEL	FIELD
4	.053	.040
	±.002	±.005
5	.037	.025
	.001	.005
6	.281	.259
	.030	.031
7	.390	.391
	.014	.041

FIGURE 50. MODEL/FIELD CANOPY REFLECTANCE COMPARISONS.

In both cases, however, the model conformed to the trajectory of the empirical signature. This point is pertinent to the usage of data transformations in the statistical comparison process and will be expanded in Section 5.0.

In simulating LAI effects, all of the variables of the canopy model were fixed in accordance with their field estimates, while the leaf area index was varied from 0.5 to 5.0 for the March simulation, and 3.5 to 8.0 for the April data. A single model execution consisted of ten samples, each comprised of five trials. A .5 step in LAI was used for each execution in simulating both stages. The result of this process was the construction of a Simulated Canopy Reflectance data set containing one hundred row entries, and four column entries corresponding to the four LANDSAT spectral bands. The row entries consist of ten model predicted spectral signatures for each of ten LAI conditions.

Figures 51 and 52 graphically portray the relationship between scene reflectance and LAI for both the field measurements and model predictions in March and April. Table 2 tabularly summarizes the data. The model data for March identifies a positive relationship for MSS bands 4, 6 and 7 which appears to plateau at LAI's above 3.5. Band 5 displays a less prominent negative relationship which also approaches an asymptote at about 3.5 LAI. These general trends favorably agree with published studies of a closely related factor, canopy biomass (Tucker, 1973). The empirical data for these same periods tend to agree with the model data, with the exception of the lowest LAI in March.

Table 2. MODEL/FIELD CANOPY REFLECTANCE AS A FUNCTION OF LAI

	LAI	MSS 4	MSS 5	MSS 6	MSS 7	MSS 7/5
MARCH (MODEL)						
	.5	.043	.045	.149	.200	4.45
	1.0	.052	.045	.239	.326	7.24
	1.5	.047	.037	.233	.320	8.67
	2.0	.053	.042	.264	.361	8.63
	2.5	.049	.035	.257	.353	10.02
	3.0	.053	.038	.279	.380	9.98
	3.5	.050	.035	.269	.373	9.99
	4.0	.051	.035	.272	.378	10.29
	4.5	.052	.036	.277	.385	10.24
	5.0	.0496	.034	.266	.371	10.26
APRIL (MODEL)						
	3.5	.050	.035	.269	.373	10.62
	4.0	.051	.035	.272	.373	10.68
	4.5	.052	.036	.277	.385	10.62
	5.0	.049	.035	.266	.371	10.76
	5.5	.051	.036	.273	.379	10.64
	6.0	.051	.035	.271	.375	10.65
	6.5	.050	.035	.269	.373	10.65
	7.0	.049	.034	.264	.365	10.60
	7.5	.049	.034	.264	.365	10.63
	8.0	.049	.034	.264	.365	10.63
MARCH (EMPIRICAL)						
	1.31	.071	.077	.298	.475	6.17
	2.07	.076	.078	.235	.320	4.10
	4.06	.080	.071	.260	.340	4.79
APRIL (EMPIRICAL)	5.13	.041	.027	.262	.381	14.11
	5.36	.039	.025	.266	.401	16.04
	6.15	.040	.025	.262	.391	15.64

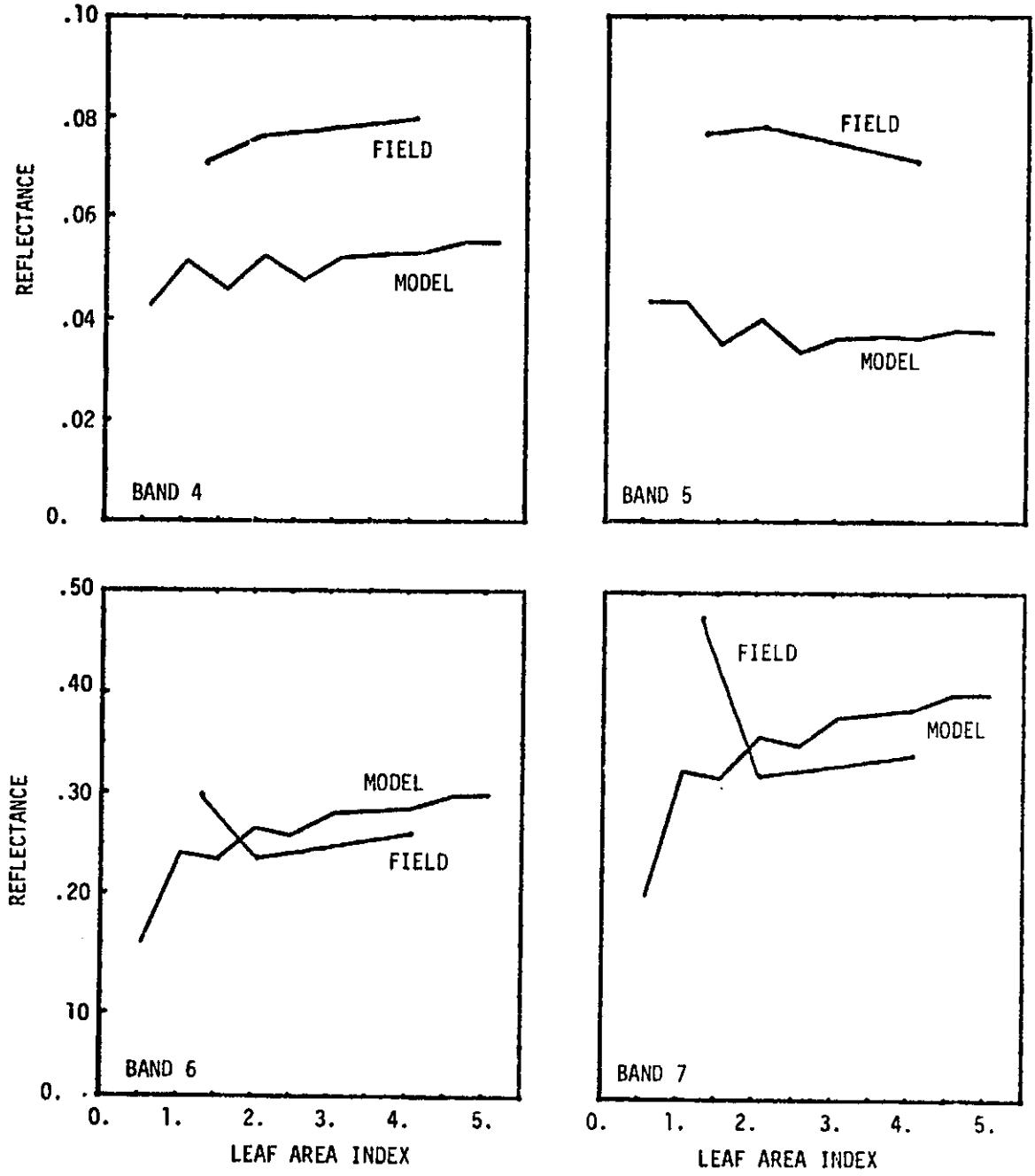

FIGURE 51. REFLECTANCE AS A FUNCTION OF LAI (MARCH).

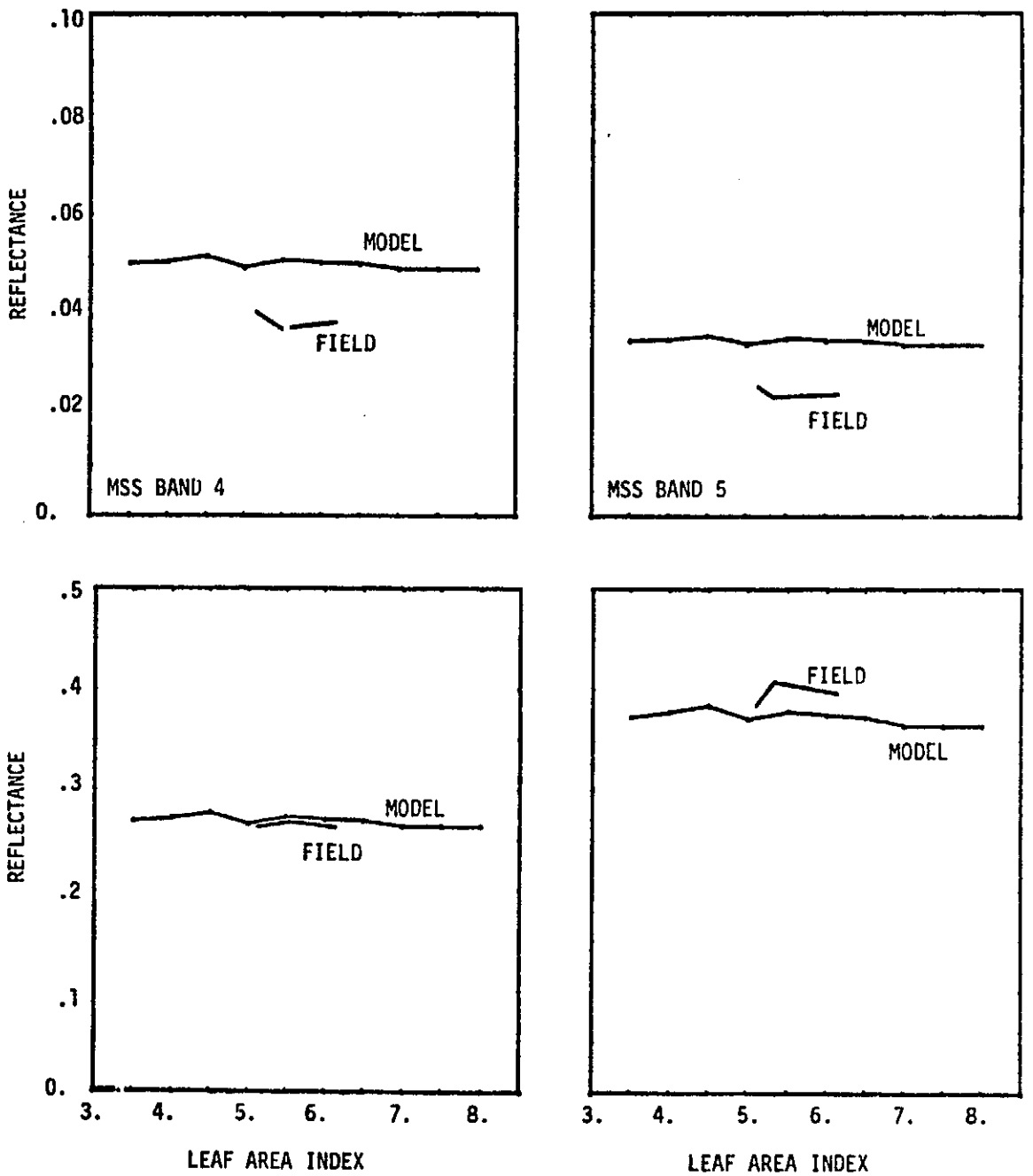

FIGURE 52. REFLECTANCE AS A FUNCTION OF LAI (APRIL).

Figure 53 shows that the reflectance ratio of the extreme infrared band (MSS 7) to the chlorophyll band (MSS 5) increases with plant density. This ratio has been reported as a good data transformation for assessing changes in scene vegetative biomass (Maxwell, 1975), which is closely related to LAI. The characteristic increase in this ratio throughout the lower LAI's, followed by a relatively flat response of the higher indices agrees with the general results of these empirical studies.

6.3 Simulation for Satellite Radiance

The induced atmospheric effects and conversion from canopy reflectance to predicted satellite radiance values was achieved by executing the Turner model with this nominal data set for each canopy reflectance data set. In the case of canopy model generated reflectances, each row of the Simulated Canopy Reflectance table constituted an input. Each individual field measurement acted as input for the empirical case. These basic units were used, rather than average reflectance values, in order to facilitate the calculation of a covariance matrix in terms of radiance units. The mean reflectance values depicted in Table 2 could have been used in establishing the mean radiance values, however, this simple approach ignores the variance associated with each reflectance data point. By translating each reflectance value into radiance units, the variance can be directly calculated.

An additional step is needed in converting the field measurements into estimated signals at a satellite. As the field data was collected throughout a day, considerable sun angle effects are

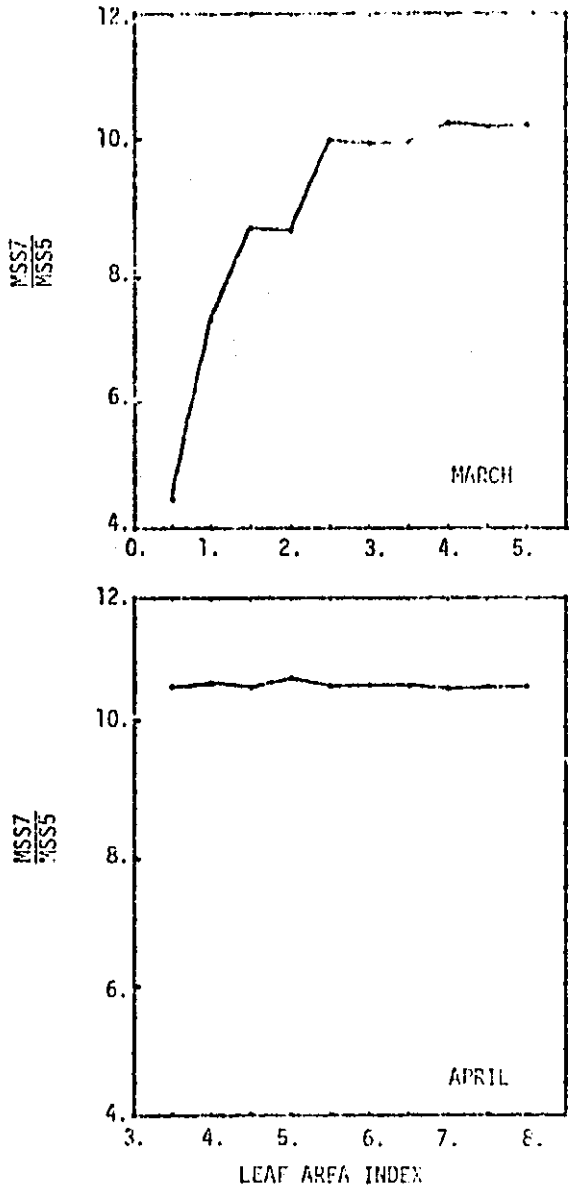

FIGURE 53. RATIO OF BANDS 7/5 AS A FUNCTION OF LAI.

ingrained in the data. This variation is not present in the model data because all of the model runs for each phenological stage were made for a single sun position. In order to make the empirical and model data sets compatable, a sun angle correction factor was applied to each empirical measurement which converted it into terms of the model's sun position.

The procedure for sun angel correction involved the conversion of field measured reflectance into radiance units, while maintaining continuity of sun angle. The result of this operation is an estimated sensor signal keyed to the particular sun angle occuring at the time of measurement. This signal can then be translated into terms of another sun angle by applying a linear correction algorithm (Smith, Berry and Heimes, 1975). For example, the March model predictions were made for a sun angle of 51 degrees zenith. A field data set taken at 1730 hours denotes a 35 degree zenith sun angle. The correction procedure would involve the execution of the Turner model using the measured reflectance values and specifying a 35° degree sun angle. This prediction could then be expressed in terms of the model's sun position by solving the following equation:

$$N_{51^o} = (\alpha_{51^o,35^o} * N_{35^o}) + \beta_{51^o,35^o} \qquad (5)$$

where,

N_{51^o} = corrected radiance for 51^o sun angle

N_{35^o} = radiance for 35^o sun angle

$\alpha_{51^o,35^o}$ = multiplicative correction factor for adjusting 35^o to 51^o sun angle

$\beta_{51^o,35^o}$ = additive correction factor for adjusting 35^o to 51^o sun angle.

This correction procedure was applied to each field measurement, and the mean vector and covariance matrix were calculated for each plot. Table 3 and Figures 54 and 55 present the radiance data for both the model and empirical reflectance data sets. The interpretation of the general trends in the data is similar to those presented for the reflectance data in the previous section. The only differences are subtle changes in the plot values due to the correction for varying sun angles.

6.4 Analysis of Model Data

In general, the ability of the canopy reflectance model to track the empirical measurements is good. In addition to the comparisons outlined in this section, a diurnal reflectance comparison between model predictions and actual field measurements was made and described in a report by Smith, Berry and Heimes (1975). The results of this evaluation were also positive. However, three aspects of the data warrant detailed discussion.

The first aspect is the relative inaccuracy of the March model predictions for MSS bands 4 and 5. The source of error in these predictions is most likely a result of the model's inability to adequately deal with the pronounced rowing effect at low LAI's, and the strong contribution of a highly variable soil reflectance. This problem is addressed in the canopy model in an input parameter denoting spatial dispersion of foliage elements. However, this parameter was not determined in this study.

Table 3. MODEL/FIELD SIMULATED RADIANCE AS A FUNCTION OF LAI.

	LAI	MSS 4	MSS 5	MSS 6	MSS 7	MSS 7/5
MARCH (MODEL)						
	.5	2.700	1.922	3.670	3.217	1.674
	1.0	2.951	1.922	5.642	5.146	2.677
	1.5	2.805	1.714	5.528	5.056	2.950
	2.0	2.981	1.840	6.204	5.683	3.089
	2.5	2.874	1.684	6.148	5.649	3.355
	3.0	2.973	1.746	6.527	5.983	3.427
	3.5	2.987	1.756	6.595	6.050	3.445
	4.0	2.989	1.738	6.666	6.116	3.519
	4.5	3.055	1.781	6.929	6.356	3.569
	5.0	3.055	1.781	6.934	6.364	3.573
APRIL (MODEL)						
	3.5	3.456	1.986	7.598	7.051	3.550
	4.0	3.469	1.995	7.6711	7.151	3.584
	4.5	3.504	2.018	7.808	7.268	3.602
	5.0	3.428	1.966	7.515	7.020	3.571
	5.5	3.479	2.001	7.705	7.157	3.577
	6.0	3.460	1.989	7.633	7.091	3.565
	6.5	3.452	1.983	7.588	7.045	3.553
	7.0	3.422	1.963	7.446	6.899	3.515
	7.5	3.421	1.962	7.442	6.895	3.514
	8.0	3.421	1.962	7.422	6.895	3.514
MARCH (EMPIRICAL)						
	1.31	3.467	2.626	6.888	6.922	2.636
	2.07	3.520	2.750	5.574	5.142	1.870
	4.06	3.655	2.824	6.057	5.434	1.924
APRIL (EMPIRICAL)						
	5.13	3.333	1.891	7.286	7.422	3.925
	5.36	3.218	1.733	7.776	7.753	4.373
	6.15	3.248	1.780	7.898	7.803	4.384

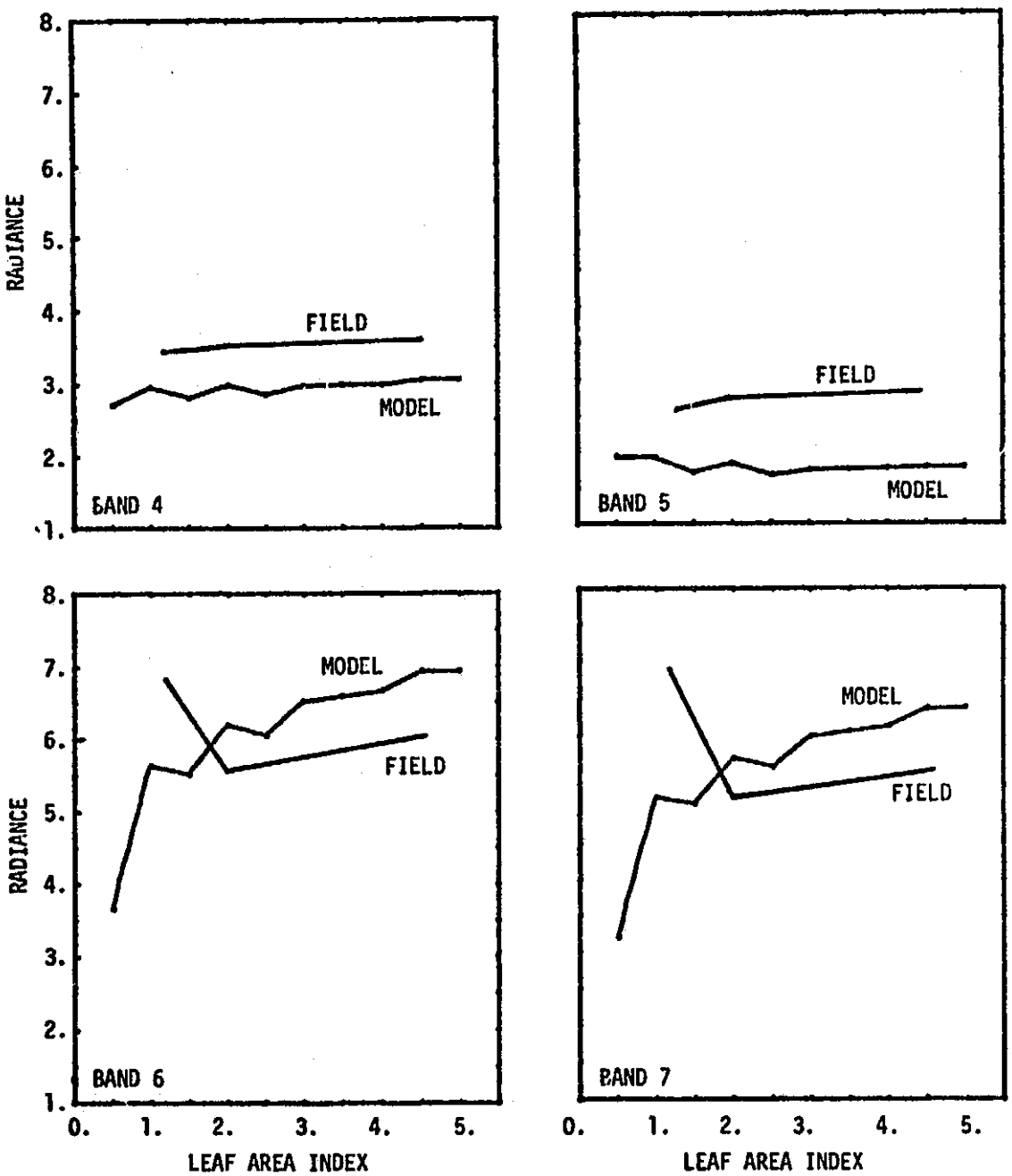

FIGURE 54. RADIANCE AS A FUNCTION OF LAI (MARCH).

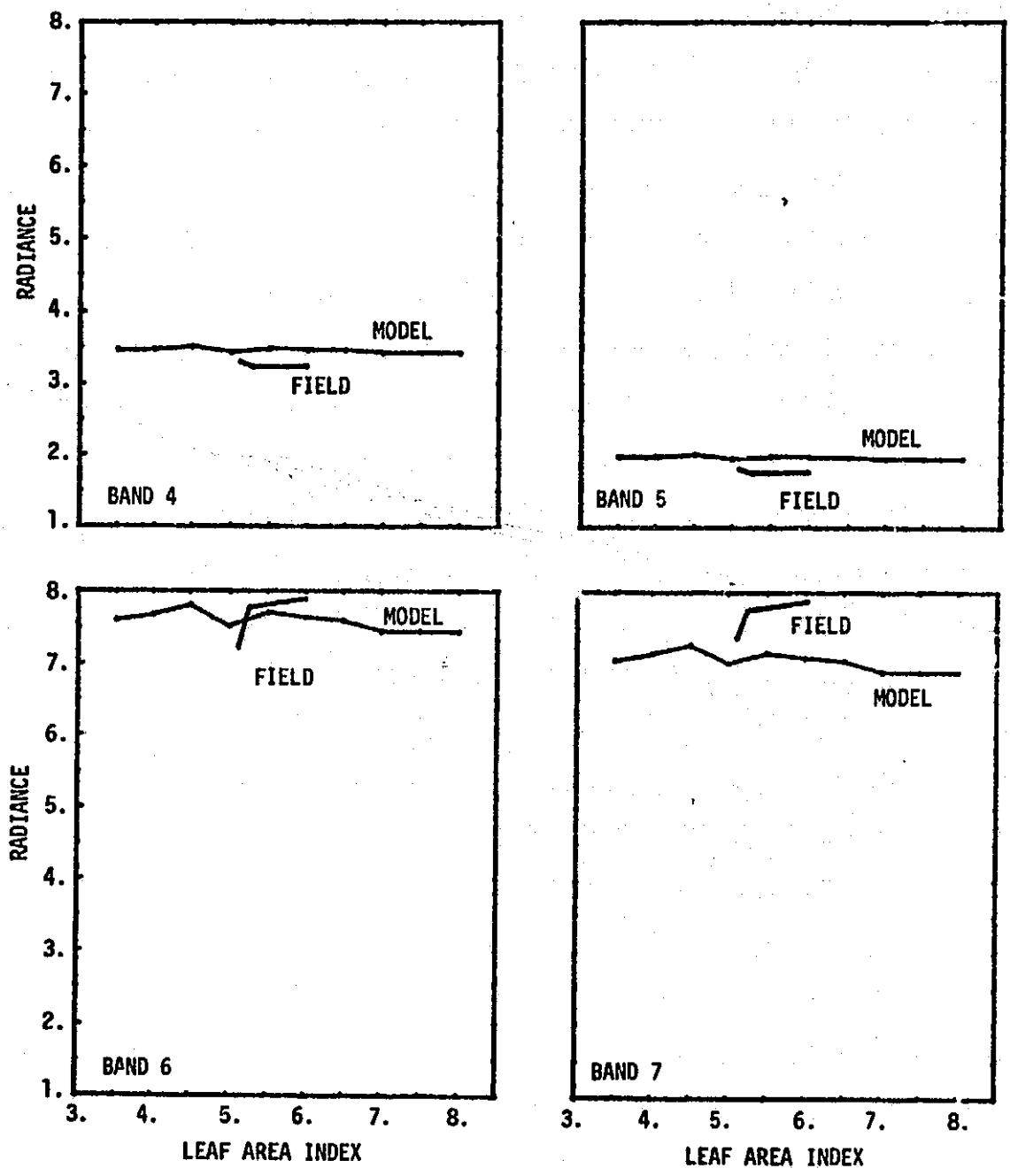

FIGURE 55. RADIANCE AS A FUNCTION OF LAI (APRIL).

The second aspect is the pronounced descrepency in March between model and field determined reflectance as a function of leaf area index. This disparity is particularly apparent in the infrared bands. The empirical data indicates a declining trend in reflectance as LAI is increased, whereas the model trend is the opposite. Previous studies in this area (Johnson, 1975; Pearson and Miller, 1973) tend to support the model derived trend. An atypical field reflectance measurement could result through the highly variable soil reflectance contribution and differing percent ground covers circumscribed by the field of view of the LANDSAT field radiometer.

The final aspect is the degeneracy of some of the model's derived covariance matrices. The covariances between all bands were unusually high, which resulted in unfeasible divergence calculations. The source of this effect is most likely ingrained in the model's treatment of the leaf and soil radiometric parameters. The general form of the SRVC model allows all of the scene component to be stochastic. However, for its application in this study, leaf transmission and reflectance and soil reflectance were represented by constant parameters. This covariance between spectral bands was therefore highly correlated.

7.0 CLASSIFICATION PROCEDURE

The previous sections of this paper have described and developed the data base necessary to infer leaf area index from plant canopy spectral measurements. A field measurements program was designed to establish physical parameters used to calibrate and execute a canopy reflectance model. This model was then used to derive a data base expressing the direct relationship between LAI and canopy reflectance. A second model was employed to simulate atmospheric effects and predict the resultant relationship between LAI and radiance received at a satellite sensor. In a similar manner, the field measured canopy reflectance for several evaluation plots was transcribed into predicted radiance values. This section presents a description of the technique used in classifying plots of unknown leaf area index.

7.1 The Swain-Fu Distance Measure

The data classification procedure used in this research is a hybrid of the two general approaches used in pattern recognition. It is similar to supervised classification in that a priori knowledge is assumed. The descriptive statistics for the various classes of LAI, however, were developed through computer modeling, rather than empirical derivation from ground truth training sets. The actual classification algorithm used, employs distance measures in the same manner as unsupervised clustering techniques. The classification

procedure involves comparing the spectral response of an area with unknown LAI to those responses of known LAI. The divergence between each unknown model response pair is calculated, and the unknown point is assigned an implied LAI equal to that of the "closest" model response. Throughout this discussion "effects" will refer to the model generated responses used to classify the unknown LAI responses of "plots".

The most familiar distance or divergence measure is Euclidean distance. This technique employs only the mean vector to assess the point to point distance between two responses. It principally involves calculating a directionally independent difference between the means of two responses. In mathematical terms, the Euclidean distance for two n-dimensional points ($\underline{X}$, $\underline{Y}$) is:

$$D_{Euclidean} = \left(\sum_{i=1}^{n} (X_i - Y_i)^2 \right)^{\frac{1}{2}} \qquad (6)$$

A variation of Euclidean distance considers the dispersion of data as well as the mean response vector in comparing the separation of points. This dispersion is approximated in terms of the "ellipsoid of concentration", which is calculated from the mean vector and covariance matrix. This geometric configuration can be conceptualized as replacing a "cloud" of individual data points, plotted in three-space, with a football centered about the mean vector. The surface of the football describes the bounds of the ellipsoid of concentration. In contrast, Euclidean distance considers only the epicenters of the footballs, while the more advanced measures judge the shape and orientation as well.

Figure 56 is a two-space portrayal of the Swain-Fu distance measure developed at Purdue University (Swain, 1973). In terms of the distance shown (D_{12},D_1,D_2), the Swain-Fu is given by:

$$D_{Swain\text{-}Fu} = \frac{D_{12}}{D_1 + D_2} \tag{7}$$

In narrative terms, the divergence is calculated by weighting the sample Euclidean distance (D_{12}) by the inverse of the spread of the data along the axis connecting the centers of the clusters (D_1 and D_2). In terms of the mean vectors and covariance matrices associated with the clusters, the distance is expressed as,

$$D_{Swain\text{-}Fu} = \frac{(C_{k,1} * C_{1,k})^{\frac{1}{2}}}{(C_{k,1})^{\frac{1}{2}} + (C_{1,k})^{\frac{1}{2}}} \tag{8}$$

where,

$$C_{1,k} = tr\left(\underline{\Sigma}_1^{-1} (\underline{U}_1 - \underline{U}_k)(\underline{U}_1 - \underline{U}_k)^T \right) \tag{9}$$

$$C_{k,1} = tr\left(\underline{\Sigma}_k^{-1} (\underline{U}_k - \underline{U}_1)(\underline{U}_k - \underline{U}_1)^T \right) \tag{10}$$

$tr(\underline{N})$ = trace of matrix $\underline{N}$

$\underline{\Sigma}_n$ = covariance matrix for cluster n

$\underline{U}_n$ = mean vector for cluster n

7.2 Covariance Matrix Modification

The original intention of this process was to use the actual covariance matrices derived from the field measurement for the "plots", and those developed by the stochastic canopy model for the "effects". However, several of the model generated covariance

matrices proved degenerate, and yielded undefined Swain-Fu distances. An explanation as to the probable cause of the degeneracy is given in Section 6.4.

The covariance matrices were modified by replacing the hyper-ellipsoid clusters with hyper-spheres of equal volume. Figure 57 is a two-dimensional schematic of the important factors in this technique. The equation for the surface area of an ellipse is,

$$A = \pi ab \tag{11}$$

where, a and b = major and minor axes, respectively. The surface of a circle is calculated by,

$$A = \pi r^2 \tag{12}$$

where,

r = radius.

Principal Component theory shows that the axes of any elliptical form are the eigenvalues of the square matrix defining the form (λ_1 and λ_2 in the schematic). Thus, equation (11) can be rewritten as,

$$A = \pi \lambda_1 \lambda_2 \tag{13}$$

Setting equation (11) and (12) equal to each other, and solving for r, results in,

$$\pi r^2 = \pi \lambda_1 \lambda_2$$

$$r = (\lambda_1 \lambda_2)^{\frac{1}{2}} \tag{14}$$

This final equation allows the solution for the radius of a circle having the same surface area of a given ellipse, in terms of its eigenvalues. This same relationship, expressed in terms of

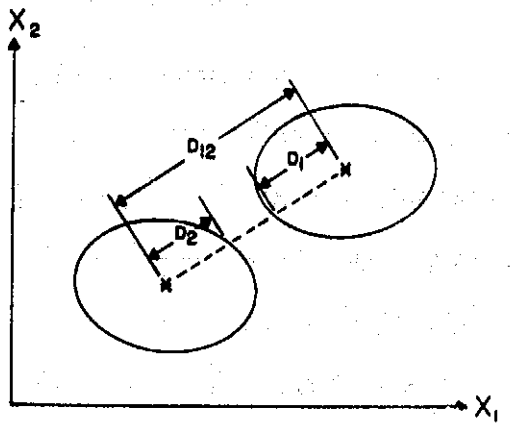

FIGURE 56. SWAIN-FU DISTANCE MEASURE. The Swain-Fu distance measure utilizes simple cluster distance (D_{12}) weighted cluster dispersion (D_1 and D_2).

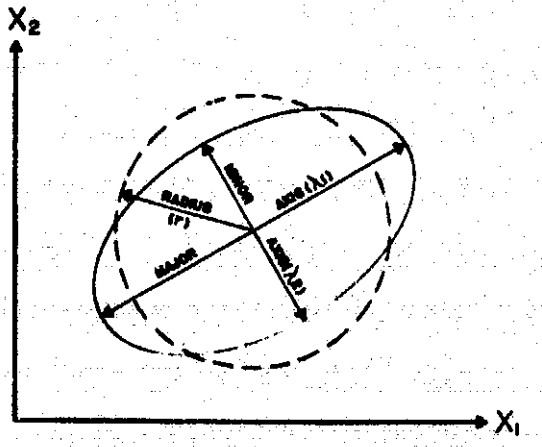

FIGURE 57. ELEMENTS OF ELLIPTICAL SURFACE AREA.

hyper-geometry, is,

$$r_{n\text{-space}} = (\lambda_1 * \lambda_2 * \ldots * \lambda_n)^{1/n} \qquad (15)$$

The derived hyper-sphere can then be substituted for the actual ellipsoid of concentration by replacing the actual covariance matrix with a diagonalized matrix based on the radius of the circle.

This modified Swain-Fu distance measure forms the foundation of the classification procedure used in this research. Program SUFU (Appendix C) is the FORTRAN coded version of the computer algorithm developed. The program consists of four phases: 1) input and data modification; 2) weighted distance calculation; 3) classification; and 4) output. The first phase allows for the input of the scaled "effects", "plots" with unknown leaf area indices, and specific program parameters for control. Data modification can be performed on both the mean vectors and covariance matrices. The divergence calculation phase solves for the Swain-Fu distance measure for each "effect/plot" pair. This procedure first evaluates expressions (4) and (5) for the weighted one-way distances between clusters. These values, termed C-factor distances, are then substituted into equation (3) to develop the overall divergence measures. The third phase of the routine determines the "effect/plot" pair with minimal divergence. Leaf area index classification of the "plot" is achieved by its association with the closest "effect". The final phase outputs the results in the forms of a C-factor matrix, Swain-Fu distances, and a printer plot of divergence. Details of the specific procedures are contained in the SUFU program listing presented in Appendix C.

8.0 CLASSIFICATION RESULTS

The basic classification of the field plots by the SUFU routine involved a 4-dimensional feature space, with the response in each of the LANDSAT bands forming a single feature vector. Classification of the data was made by considering only Euclidean distances between the "effects" and the "plots" data clusters. Two additional approaches were also executed, in which the Swain-Fu distance was used. The first considered two raw data preprocessing transformations: 1) spherical elipsoid of concentration; and 2) correction for sun angle effects. The final approach utilized the preprocessed data to form new feature vectors. These derived feature vectors include: 1) the ratio of bands 7 to 5; 2) the ratio of bands 6 to 4; and 3) the simultaneous consideration of the 7 to 5 and 6 to 4 ratios.

The field measured leaf area index for each of the field "plots" used in this study is identified in Table 4. During the March measurement period, "plot" 2 had an unusually high LAI of 4.60. "Plots" 1 and 3 are more nearly normal, having LAI's of 2.07 and 1.31, respectively. The April measurements show "plot" 3 as having a LAI of 6.15, with "plots" 1 and 2 being nearly equal at 5.13 and 5.36, respectively.

Table 4. FIELD MEASURED LEAF AREA INDEX.

DATE	PLOT	LAI	RANKING
March	1	2.07	2
	2	4.06	1
	3	1.31	3
April	1	5.13	3
	2	5.36	2
	3	6.15	1

8.1 Raw Data Classification

In the raw data classification scheme, the SUFU program was used in a manner which approximated a Euclidean distance measurement of divergence. The mean vectors for the "plots" were developed by averaging the radiometer measurements taken throughout a day. This has the impact of tacitly disregarding any sun-angle effects on the spectral signatures. The mean vectors for the "effects" consisted of the model predicted responses.

In order to force the SUFU routine to act as a Euclidean distance classifier, a common covariance matrix was used for all "plots" and "effects". The matrix was diagonalized, with the diagonal elements set to unity. This operation has the effect of containing the dispersion of the data about each mean vector, which removes any classification information based on differential data dispersion. By default, all of the classification intelligence became embedded in the mean vector positioning.

Figure 58 shows the results of the raw data classification using the measured and modeled reflectance values. The March assignments show very strong classifications. This is indicated by the minimum normalized divergence for each case being less than .5. In descriptive terms, a .5 normalized divergence denotes a cluster which is half the distance between the "plot" and the farthest away "effect". At this level, an appreciable difference between the closest "effect" and the other "effects" appears to exist. Less pronounced classifications occur for the April reflectance data, as shown by the minimal normalized divergences being about .6.

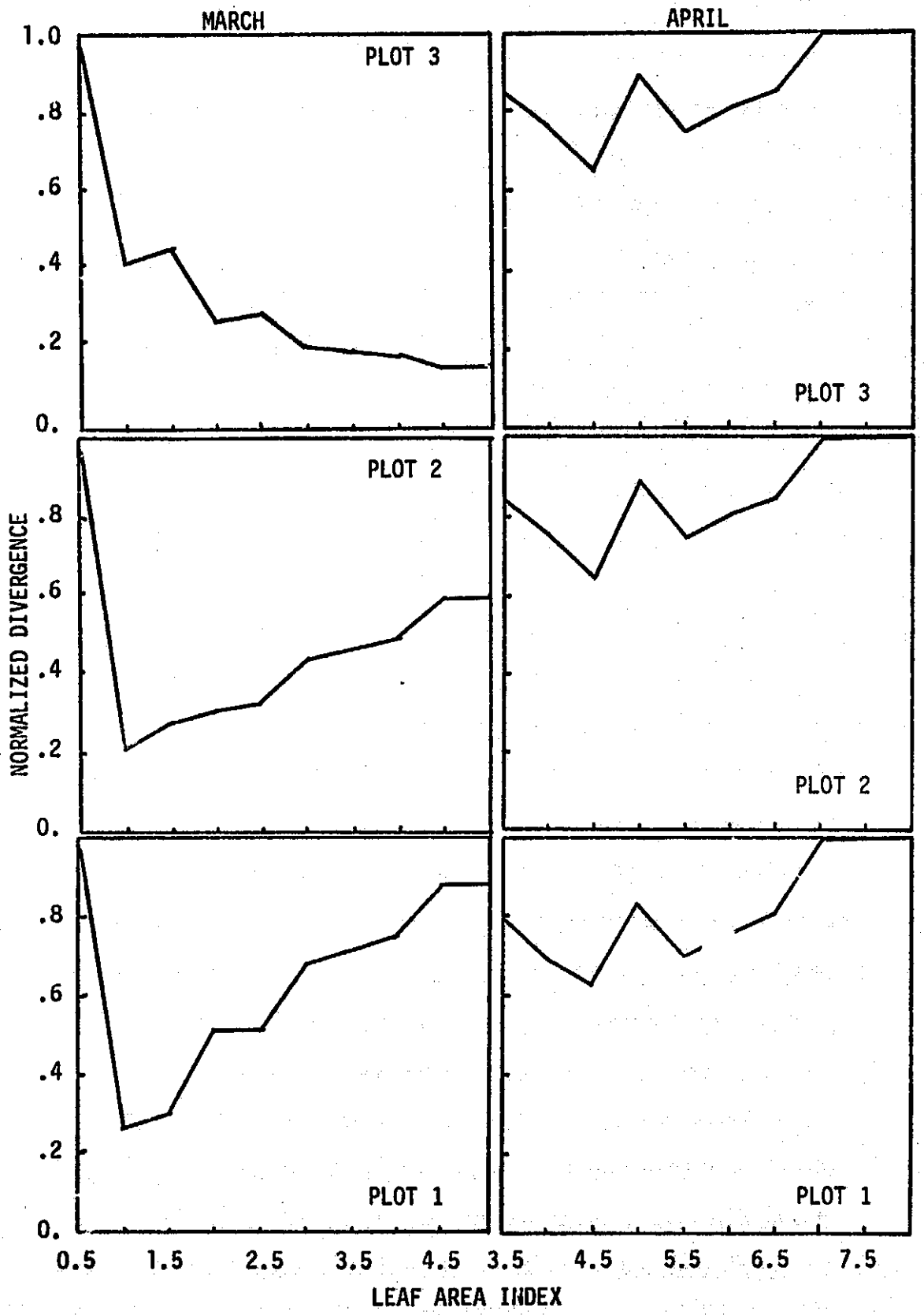

FIGURE 58. RAW REFLECTANCE DATA DIVERGENCE PLOT.

The classification accuracy of the raw reflectance data appears best during the April period. The program predicts a LAI of 4.5 for all three "plots", which is close to their 5.5 average LAI. The March predictions, however, are less accurate and more difficult to interpret. The assigned LAI for both "plots" 1 and 2 is 1.0, with "plot" 3 indicating an LAI of 5.0. The assignment for "plot" 1 is relatively near the measured 2.07 LAI. The classifying of "plots" 2 and 3, on the other hand, are nearly the reverse of the measured 4.60 and 1.31 LAI for the respective plots.

Figure 59 identifies the LAI classification based on the unaltered radiance data predicted by the atmospheric model. The classification results and divergence graphs are nearly the same as those of the previous case. The notable exception occurs for "plot" 1 during the April period. The classification of this "plot" changes slightly from 4.0 to 4.5 LAI. The general similarity of these classifications indicates that the relative positioning of the mean vectors are somewhat insensitive to atmospheric effects.

8.2 Preprocessed Data Classification

Figure 1 of Appendix B portrays the results of the SUFU classification based on the covariance weighted distance measure. It is apparent that the consideration of covariance in the divergence calculation using surface reflectance data had no impact on LAI classification, and only minimal effects on the normalized divergence plots. The result indicates that the covariance matrices for both the "plots" and "effects" tend to be similar, and without any dominating lobes. Subsequent review of the covariance matrices of the data, support this contention.

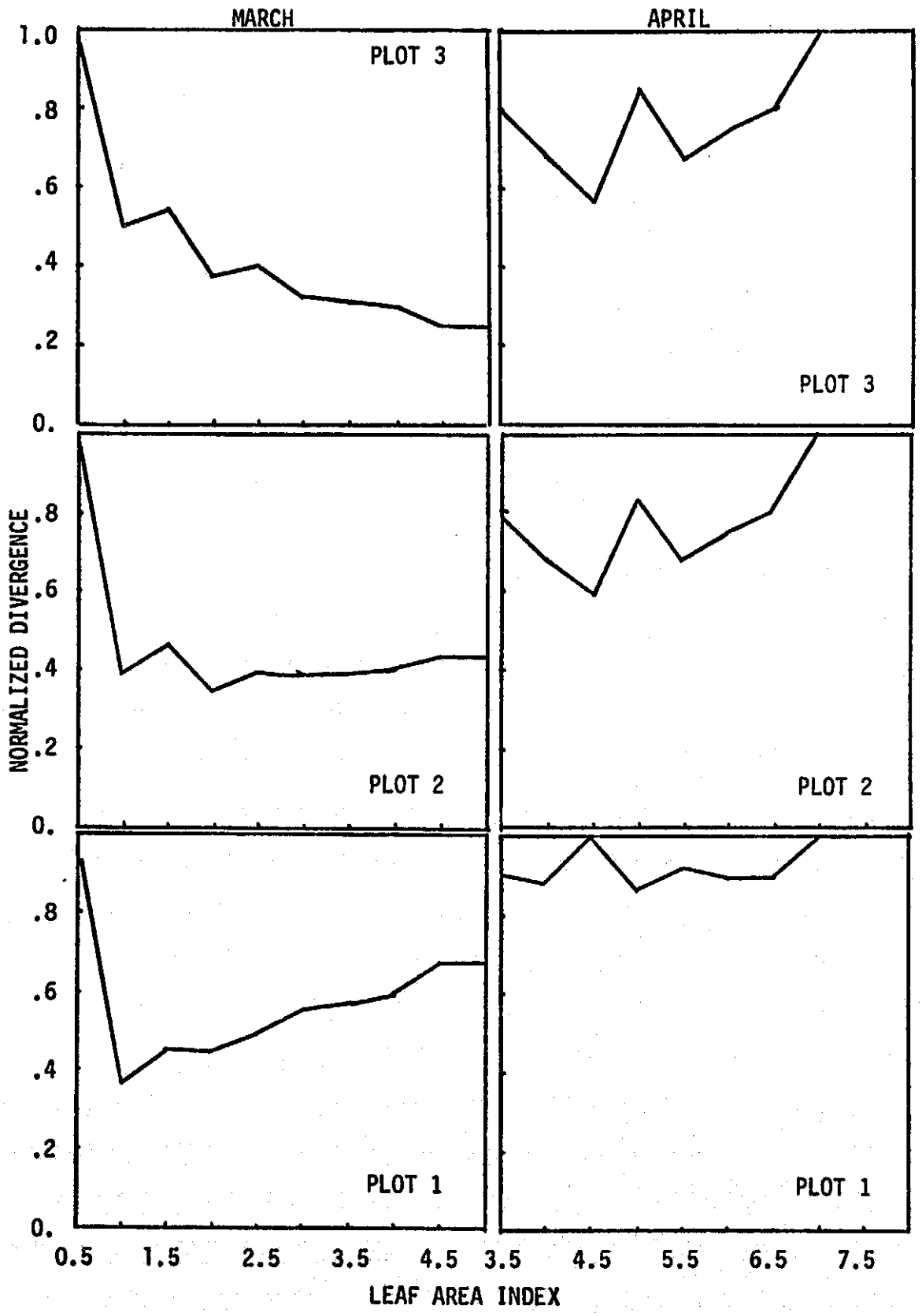

FIGURE 59. RAW RADIANCE DATA DIVERGENCE PLOT.

A sharp contrast is noted for the classification based on radiance data, using the spherical approximation of the actual covariance matrices. Figure 3 of Appendix B summarizes these results. Whereas the Euclidean classifier tagged the March "plot" 2 as having an LAI of 1.0, the covariance weighted procedure identified it as having an LAI of 2.0. In a similar manner, April "plots" 1 and 3 are classified as having LAI's of 5.0 and 4.5, respectively, by Euclidean distance. The data dispersion weighted technique, however, identifies these same plots as both having an LAI of 4.0.

These descrepencies are most likely the result of the incorporation of spherical approximations of the data dispersion. Another possible explanation is that the dispersion of the data is selectively altered by atmospheric effects. As noted earlier, the mean vector positioning, however, is relatively unaltered. The within wavelength band variance has a possible physical explanation in the effects of selective absorption and scattering affecting the path radiance component of the satellite signal.

In addition to the data preprocessing for spherical covariances, a case was executed in which the "plot" data for both periods were corrected for sun angle effects. A linear correction algorithm, specifically developed for this data, was used. The procedure first involved relating the time of day for each canopy reflectance measurement to the appropriate sun angle. Once the sun angle for each field measurement was determined, the corresponding mean radiance prediction could be corrected to the base sun angle used in the model

derivation of the "effect". The theoretical foundation and details of this correction technique are presented in a report by Smith, Berry and Heimes (1975).

The classification results, shown in Figure 3 of Appendix B are nearly the same as those for the uncorrected data. The divergence plots are also very similar. This outcome appears to demonstrate that sun angle effects, over the range of sun angels involved in this study, have a negligible effect on LAI classification.

8.3 Derived Feature Vector Classification

To this point, the preprocessing of data has concentrated on meaningful transformations of the responses themselves. Another technique frequently used in remote sensing is data transformations designed to derive new feature vectors. These include ratioing bands, adding or subtracting them, and applying arithmetic functions to stretch and distort the original data. The purpose of these operations is to identify new feature spaces which enhance particular characteristics of a scene. For example, a relatively low response in band 4, when compared to band 7, might provide the same amount of information as the four band signatures in identifying vegetated areas.

Figures 4 through 6 of Appendix B report the results of using band ratios of 7/5, 6/4, and 7/5 with 6/4. The data used in these feature vector transformations utilized spherical covariance matrices and sun angle corrected mean vectors. The selection of these transformations was based on the work by G. Johnson (1976) in assessing plant biomass from LANDSAT data. The results, for the most

part appear disappointing. Numerous departures from the previous classifications are noted, and the normalized divergence plots often display minimal deflections. This erratic behavior is most likely caused by the severe averaging effect of the ratioing and the minimal number of feature vectors for classification. Of the three transformations, the 6/4 ratio is the closest to the original classifications, but underestimates the March leaf area indices.

8.4 Summary of Classification Results

A summary of the classification results for the radiance data of this study is reported in Table 5. The table is constructed in accordance with the major classification categories. The row entries are organized according to phenology stage and field plot number. The column organization reflects the three classification techniques: 1) raw data using Euclidean distance; 2) corrected data using Swain-Fu divergence; and 3) ratioed data, also using the Swain-Fu measure.

The best overall results were achieved by the simple classification of mean spectral responses using a Euclidean distance classifier. The introduction of data dispersion information in classification, through the consideration of spherical covariance, actually degraded the results. Preprocessing the data for sun angle only slightly improved the classification accuracy. The use of derived feature vectors resulted in the worst classifications, and consistently understated the leaf area indices for the March period.

The ability of the procedure to differentiate between conditions of average high plant density and low density is apparent. During the low density tillering stage in March the average deviation of

Table 5. SUMMARY OF CLASSIFICATION RESULTS.

DATE	PLOT	MEASURED LAI	TECHNIQUE I MEAN RAW DATA LAI	TECHNIQUE I MEAN RAW DATA DEV.	TECHNIQUE II SPHERICAL LAI	TECHNIQUE II SPHERICAL DEV.	TECHNIQUE II SUN ANGLE LAI	TECHNIQUE II SUN ANGLE DEV.
MARCH	1	2.07	1.0	1.07	1.0	1.07	1.0	1.07
	2	4.06	1.0	3.06	2.0	2.06	2.0	2.06
	3	1.31	5.0	-3.69	5.0	-3.69	5.0	-3.69
	average	2.48	2.33	0.15	2.67	-0.19	2.67	-0.19
APRIL	1	5.13	5.0	0.13	4.0	1.13	4.0	1.13
	2	5.36	4.5	0.86	4.5	0.86	4.5	0.86
	3	6.15	4.5	1.65	4.0	2.15	4.5	1.65
	average	5.55	4.67	0.88	4.17	1.38	4.33	1.22

DATE	PLOT	TECHNIQUE III LAI	TECHNIQUE III DEV.	LAI	DEV.	LAI	DEV.
MARCH	1	0.5	1.57	1.0	1.07	0.5	1.57
	2	0.5	3.56	1.0	3.06	0.5	3.56
	3	1.0	0.31	1.5	-0.19	1.5	-0.19
	average	0.67	1.81	1.16	1.32	0.83	1.65
APRIL	1	4.5	0.63	7.0	1.87	4.5	0.63
	2	4.5	0.86	4.5	0.86	4.5	0.86
	3	4.5	1.65	4.5	1.65	4.5	1.65
	average	4.50	1.05	5.33	0.22	4.50	1.05

predictions based on technique I was .15. The worst technique (ratio of bands 7/5) yielded an average deviation of 1.81 for this same period. The average deviations associated with the more dense heading stage in April proved to be more consistent between techniques, resulting in average deviations from .22 to 1.38.

9.0 CONCLUSION

The fundamental purpose of this research was to investigate the feasibility of using abstract computer modeling to infer inherent scene characteristics from remote sensing data. The principle hypothesis of the study was:

- Plant canopy reflectance and atmospheric modeling can be used to infer intrinsic scene geometry variables from spectral measurements.

The specific geometric variable under study was the leaf area index (LAI) of a wheat canopy. A stochastic plant canopy reflectance model was used to develop a simulated reflectance data base which tracked the induced effects of changes in the LAI variable. An atmospheric model was employed to translate the surface reflectance predictions into simulated satellite signals. The results of these operations were two data sets responding to systematic changes in LAI: one in terms of scene reflectance, and the other identifying radiance. Classification of measured field reflectance and corresponding simulated radiance was achieved by determining the minimum divergence between the model spectral signatures of known LAI, and the signatures of the responses to be identified. The leaf area index for an unknown area was assigned the same value as that of its most similar model derived signature.

In partial support of this approach, an intensive field measurement program was conducted. These data were utilized in the

study in two ways. First, the data acted as input to the canopy reflectance model and allowed for the calibration of the model's performance. The second major use was in the evaluation of the hypotheses under investigation.

9.1 Hypotheses Results

In addressing the general hypothesis of using modeling to infer scene geometry from spectral data, two sub-hypotheses were made:

- Wheat canopy reflectance can be predicted by computer modeling, both as a function of low and high plant densities, and as a function of sun angle.
- Low wheat density and high wheat density categories can be inferred from model data sets.

The results of the investigation into the first sub-hypothesis demonstrates that reflectance modeling is applicable to wheat canopies. Section 6.2 describes this investigation. Figure 50 and Tables 2 and 3 summarize the results of this study. It was found that the general agreement between model and field spectral signatures for both the March (low LAI) and the April (high LAI) periods, were excellent. The March period was less accurate, most likely as a result of the pronounced rowing effect of the canopy, and an initial assumption made by the author which constrained the model's operation. The ability of the reflectance model to track sun angle effects was also apparent. A detailed account of this result is reported in a paper by Smith and this author (1975).

The results of the second sub-hypothesis is reported in Section 8.0 and Table 5. During the low density stage in March the average

measured LAI was 2.48 while the average model prediction, using the best technique, inferred a LAI of 2.33. A comparison of April LAI's, noted an actual average of 5.55, and an inferred index of 4.67, using the same classification technique.

The general hypothesis is inconclusive when applied to individual plots. This results primarily from the limited number of field plots measured in this study as discussed in Section 8.4.

9.2 Other Major Contributions of the Study

In addition to the major efforts of applying and validating a reflectance model to wheat canopies, and the development of a methodology for inferring leaf area index, several other contributions of this study should be noted. An extensive field measured data base was collected which incorporates the primary environmental and intrinsic scene variables, with actual canopy reflectance, for the four major phenology stages of wheat. This data base is further extended by the addition of model derived canopy reflectance as functions of both sun angle and leaf area index.

The empirical study was also valuable in that several unique data collection techniques were developed. In particular, were the design and construction of an instrument for field measurement of individual leaf transmission (Section 3.2.1), and two rapid, in situ, field techniques for assessing leaf angle distributions (LAD) Sections 3.2.2, 3.3, 4.0 and 5.0.

Two major mathematical contributions were made. The sensitivity analysis of the Fredholm technique (Section 4.1) describes a procedure for evaluating the magnitude and direction of the sensitivity

of an individual input vector on an indivisible output vector. The Fourier technique required the development of a mathematical procedure for convoluting two orthogonal distributions of angles, in order to estimate the true 3-space leaf angle distribution of a plant canopy (Section 4.2.2).

The final contribution of the study involves an evaluation of several data transformations and classification algorithms, as to their effect in classifying leaf area index from spectral data (Section 8.0). The specific procedures investigated were: 1) Euclidean and covariance weighted classifiers; 2) sun angle corrections; and 3) derived feature vectors. In conjunction with the first procedure a technique was implemented which transforms the ellipsoid of concentration of a data cluster into a hyper-sphere approximating the data dispersion information.

9.3 Future Research

The most apparent area of future research associated with this study, is the evaluation of the procedure under more variable conditions and with actual aircraft or satellite data. In a study of this type, an operational test could be designed in which extensive ground measurements of LAI would serve as evaluation points. The hypotheses of such a study might include the principle hypothesis outlined in this report and a sub-hypothesis concerned with the extent of varietal or physical condition variations.

A second area of potential study is ingrained in the refinement and extension of the procedure. This research might be concerned with the modeling approaches and assumptions. In addition, a more

rigorous investigation into classification techniques is warranted. Finally, the basic technique could be employed to determine the feasibility of inferring other intrinsic scene parameters, e.g., individual leaf reflectance and transmission.

LITERATURE CITED

Allen, W. A. and A. J. Richardson. 1968. Interaction of light with a plant canopy. J. Optical Soc. of Amer. 58:1023-1028.

Colwell, J. E. 1974. Grass canopy bidirectional spectral reflectance. Proc. Ninth Inter. Symp. on Remote Sensing of Envir., Univ. of Michigan, Ann Arbor, Mich. p. 1061-1084.

Dobrin, M. B. 1968. Optical processing in the earth sciences. I.E.E.E. Spectrum, September, 1968. p. 59-66.

Flechner, J. E. and M. E. Robinson. 1956. A capacitance meter for estimating forage weight. J. Range Manage. 9:96-97.

Gausman, H., et al. 1971. The leaf mesophylls of twenty crops, their light spectra, and optical and geometric properties. SW Research Report 423, Weslaco, Texas. 98 p.

Goodall, D. W. 1952. Some considerations in the use of point quadrats for the analysis of vegetation. Aust. J. of Sci. Res. B5-1-41.

Goodman, J. W. 1968. Introduction to fourier optics. McGraw-Hill Book Co., New York. 287 p.

Harlan, J. C. 1976. Analysis of spectral data for wheat. Annual Report, NAS 9-14770, NASA Johnson Spacecraft Center, Houston Texas. In preparation.

Johnson, G. R. 1975. Remote spatial estimation of herbaceous biomass. Rocky Mt. Forest and Range Exper. Sta. Report 2118-F, Fort Collins, Colo. 15 p.

Knight, D. H. 1970. Some measurements of vegetation structure on the Pawnee Grassland. Colorado State Univ., IBP Grassland Biome Tech. Rep. 72. Fort Collins, Colo. 43 p.

Kubelka, P. and F. Munk. 1931. Ein Beitrag Zur Optik der Farbanstriche. A. Techn. Physic. 12:593-601.

Maxwell, E. L. 1975. Multispectral analysis of rangeland conditions. Ph.D. dissertation, Colorado State Univ., Fort Collins, Colo. 144 p.

Miller, L. D. and R. L. Pearson. 1971. Aerial mapping program of the IBP Grassland Biome: remote sensing the productivity of the shortgrass prairie as input into biosystem models. Proc. Seventh Inter. Symp. on Remote Sensing of Envir., Univ. of Michigan, Ann Arbor, Mich. p. 165-205.

Nilson T. 1971. A theoretical analysis of the frequency of gaps in plant stands. Agr. Meterol. 8:25-38.

Oliver, R. E. and J. A. Smith. 1973. Vegetation canopy reflectance models. Final Report, DA-ARO-D-31-124-71-G164, U. S. Army Research Office, Durham, N. C. 65 p.

Oliver, R. E. and J. A. Smith. 1974. A stochastic canopy model of diurnal reflectance. Final Report, DAHC04 74 G0001, U. S. Army Research Office, Durham, N. C. 82 p.

Pearson, R. L. and L. D. Miller, 1972. Remote spectral measurements as a method for determining plant cover. IBP Grassland Biome Tech. Rep. 167. Fort Collins, Colo. 48 p.

Pearson, R. L. and L. D. Miller. 1973. Remote multispectral sensing of biomass. Science Series 10. Dept. of Watershed Science. Colorado State Univ., Fort Collins, Colo. 150 p.

Pechanec, J. F. and G. D. Pickford. 1937. A weight estimation method for determination of range or pasture production. Amer. Soc. Agron. J. 29:894-904.

Philip, J. R. 1965. The distribution of foliage density with foliage angle estimated from inclined point quadrat observations. Aust. J. of Bot. 13:357-366.

Pincus, H. J. and M. G. Dobrin. 1966. Optical processing of geologic data. J. Geophys. Res. 71(20):4861-4870.

Pincus, H. 1969. Analysis of remote sensing displays by optical diffraction. Proc. Sixth Annual Symp. on Remote Sensing of Envir., Univ. of Michigan, Ann Arbor. p. 261-274.

Smith, J. A. and R. E. Oliver. 1972. Plant canopy models for simulating composite scene spectroradiance in the .4 to 1.04 mm region. Proc. Eighth Inter. Symp. on Remote Sensing of Envir., Univ. of Michigan, Ann Arbor, Mich. p. 1333-1353.

Smith, J. A. and R. E. Oliver. 1974. Effects of changing canopy directional reflectance on feature selection. App. Optics, 13(7):1599-1604.

Smith, J. A., J. K. Berry and F. Heimes. 1975. Signature extension for sun angle. Final Report, NAS 9-14467, NASA Johnson Spacecraft Center, Houston, Texas. 146 p.

Suits, G. H. 1972. The calculation of directional reflectance of a vegetative canopy. Remote Sensing of Envir. 2:117-125.

Swain, P. H. 1973. Pattern recognition: a basis for remote sensing data analysis. LARS Info. Note 111572, Lab. for Appl. of Remote Sensing, Purdue, Univ., W. Lafayette, Ind. 41 p.

Tucker, C. J. 1973. The remote estimation of a grassland canopy. Ph.D. dissertation, Colorado State Univ., Fort Collins, Colo. 111 p.

Turner, R. E. and M. M. Spencer. 1973. Atmospheric model for correction of spacecraft data. Proc. Eighth Inter. Symp. on Remote Sensing of Envir., Univ. of Michigan, Ann Arbor, Mich. p. 895-911.

Vanderbilt, V. 1975. Personal communication. Graduate student, Lab. for Appl. of Remote Sensing, Purdue Univ., W. Lafayette, Ind.

Wilson, W. J. 1959. Analysis of the spatial distribution of foliage by two dimensional point quadrats. New Phytol. 58:92-101.

Wilson W. J. 1963. Estimation of foliage denseness and foliage angle by inclined point quadrats. Aust. J. Bot. 11:95-105.

Page intentionally left blank

APPENDIX A

APPENDIX A

Radiometric and Geometric Field Data

The principle field data collected by TAMU/CSU for the canopy modeling effort consists of periodic canopy reflectance, intensive leaf area index (LAI) measures, extensive LAI estimates, individual leaf transmission measurements, and canopy geometry photos. Relatively complete data sets are available for March 20, 1975 (Tillering Stage, TAMU), April 23, 1975 (Jointing Stage, TAMU/CSU), and May 20, 1975 (Heading Stage, TAMU). Less complete data sets were collected on November 24, 1974 (Winter Tillering Stage, TAMU/CSU) and June 26, 1975 (Ripening Stage, TAMU/CSU). The following table summarizes the data set. A more detailed presentation of the March and April data sets is included in the remaining parts of this section.

Table A-1. FINNEY COUNTY DATA SUMMARY. The field measurements of the radiometric and geometric parameters of the canopy were made for four phenological stages. Diurnal canopy reflectance was collected for each stage. The diffuse to direct iradiance ratio and soil reflectance were sampled periodically for each data.

I. March 20, 1975 Tillering Stage Field 416

-Canopy Reflectance:

Time:	Plot 1	Plot 2	Plot 3
	1100 hrs.	1045	1030
	1145	1130	1115
	1300	1245	1230
	1400	1345	1330

-Leaf Area Index: 2.07 4.06 1.31

-Canopy Geometry: Fredholm Field Photos

-Leaf Transmission: Not Taken

-10" LAI Plots:

Field	367	369	370	414	421
Plot 1	2.22	2.15	1.48	8.53	4.54
Plot 2	2.78	2.43	8.45	9.17	3.60

II. April 23, 1975 Jointing Stage Field 416

-Canopy Reflectance:

Time:	Plot 1	Plot 2	Plot 3
	1000 hrs.	1045	1115
	1130	1145	1200
	1315	1345	1400
	1715	1730	1800

-Leaf Area Index: 5.13 5.36 6.15

-Canopy Geometry: Fourier Field Photos

-Leaf Transmission: Not Taken

-10" LAI Plots:

Field	367	369	370	414	421
Plot 1	2.22	2.15	1.48	8.53	4.54
Plot 2	2.78	2.43	8.45	9.17	3.60

Table A-1. (Continued)

III. May 20, 1975 Heading Stage Field 416

-Canopy Reflectance:

	Plot 1	Plot 2	Plot 3
Time:	0945 hrs.	1015	1045
	1100	1115	1130
	1200	1215	1245
	1300	1315	1345

-Leaf Area Index: 4.11 5.32 6.04

-Canopy Geometry: Fourier Field Photos

-Leaf Transmission: Green, Yellowing, Dead

-10" LAI Plots:

Field	367	369	370	414	421
Plot 1	3.82	1.83	3.12	5.65	1.80
Plot 2	3.22	5.68	9.76	7.64	2.16

IV. June 26, 1975 Ripening Stage Field 416

-Canopy Reflectance:

	Plot 1	Plot 2	Plot 3
Time:	--	1115	1000
	--	1200	1115
	--	1245	--
	--	1300	--

-Leaf Area Index: 1.79 2.17 2.04

-Canopy Geometry: Fourier Field Photos

-Leaf Transmission: Dead

-10"LAI Plots:

Field	367	369	370	414	421
Plot 1	.78	1.15	.94	1.79	1.02
Plot 2	.85	2.00	3.14	2.63	1.08

Table A-2. MARCH LEAF AREA INDEX AND DESCRIPTIVE PARAMETERS.

March 20, 1975	Tillering Stage	Field 416
Crop Type :	Santana Wheat (10" drill; EW)	
Height :	8-9 cm.	
Chlorotic :	Green Foliage	
Weeds :	0%	
Soil Condition :	Moist	
Wind :	12-15 mph NW	

	PLOT 1	PLOT 2	PLOT 3
Leaf Area Index	2.07	4.60	1.31
Dry Weight (2' X 2' Plot)	58.10 gm	--	39.90
Number of Tillers (2' X 2' Plot)			
Live	803.00	--	1372.00
Dead	0.00	--	0.00
Total	803.00	--	1372.00
Average Tillers/Plant			
Live	8.64	--	11.00
Dead	0.00	--	0.00
Total	8.64	--	11.00
Average Lead Area/Plant			
Green	39.39 cm^2	--	60.09
Yellow	0.00	--	0.00
Dead	0.00	--	0.00
Total	37.39	--	60.09

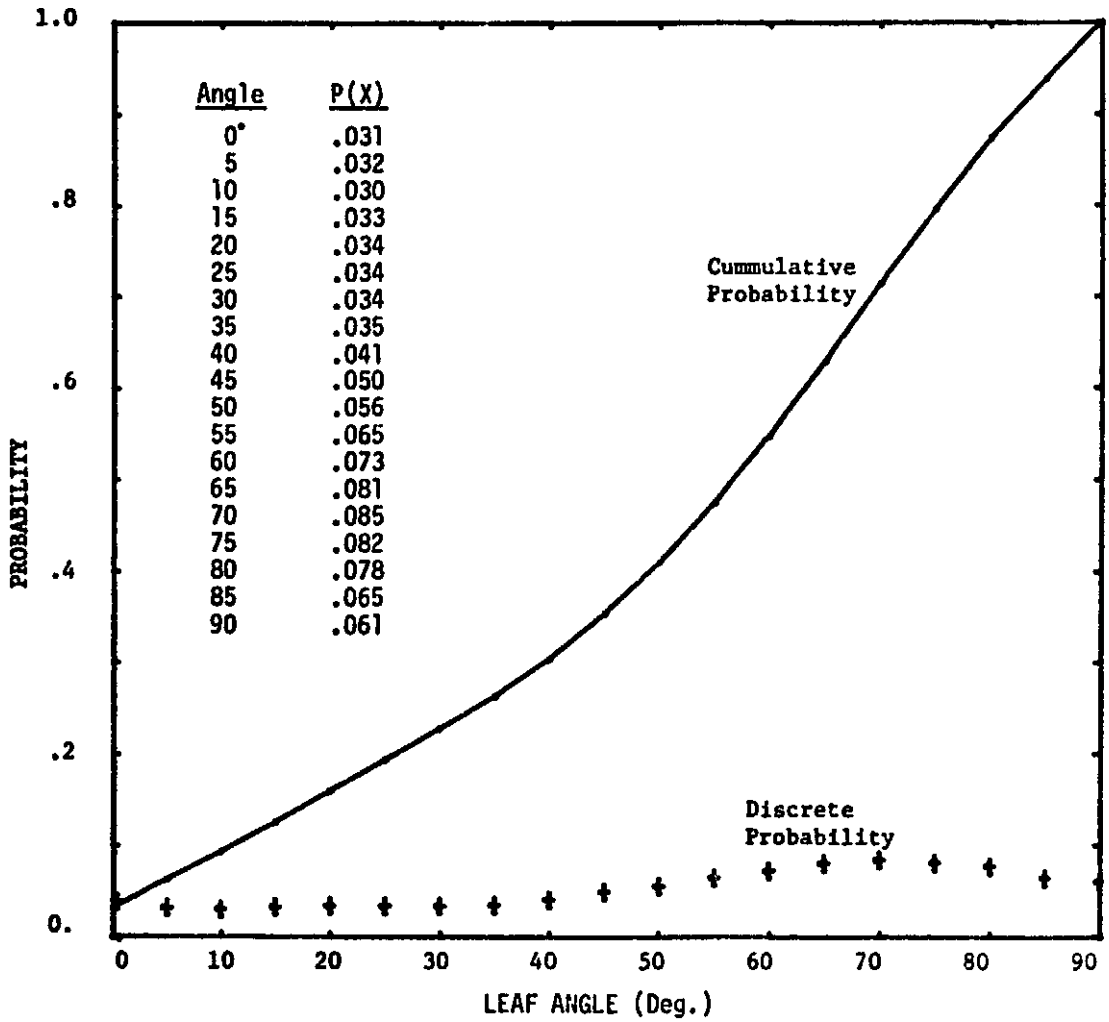

FIGURE A-1. LEAF ANGLE DISTRIBUTION FOR MARCH.

Table A-3. MARCH RADIOMETRIC DATA.

DATE	TIME	CROP AND LOCATION	PLOT NUMBER	ORIENTATION	REFLECTANCE= BAND1	BAND2	BAND3	BAND4
032075	1052	WHEAT KS.	416-1	OFF ROW	.074	.081	.242	.338
032075	1055	WHEAT KS.	416-1	ON ROW	.078	.079	.254	.329
032075	1057	WHEAT KS.	416-1	ON ROW	.077	.078	.224	.297
032075	1058	WHEAT KS.	416-1	OFF ROW	.074	.074	.219	.319
032075	1136	WHEAT KS.	416-1	OFF ROW	.063	.070	.217	.318
032075	1138	WHEAT KS.	416-1	ON ROW	.069	.075	.222	.337
032075	1140	WHEAT KS.	416-1	ON ROW	.063	.069	.227	.301
032075	1142	WHEAT KS.	416-1	OFF ROW	.066	.072	.208	.307
032075	0104	WHEAT KS.	416-1	OFF ROW	.065	.060	.215	.296
032075	0105	WHEAT KS.	416-1	ON ROW	.060	.060	.190	.280
032075	0106	WHEAT KS.	416-1	ON ROW	.060	.050	.214	.314
032075	0107	WHEAT KS.	416-1	OFF ROW	.063	.065	.218	.304
032075	0155	WHEAT KS.	416-1	ON ROW	.052	.070	.205	.294
032075	0156	WHEAT KS.	416-1	OFF ROW	.076	.075	.218	.307
032075	0158	WHEAT KS.	416-1	OFF ROW	.070	.074	.211	.291
032075	0159	WHEAT KS.	416-1	ON ROW	.070	.061	.205	.304
032075	0435	WHEAT KS.	416-1	OFF ROW	.074	.075	.242	.311
032075	0436	WHEAT KS.	416-1	ON ROW	.061	.077	.210	.324
032075	0437	WHEAT KS.	416-1	ON ROW	.059	.073	.246	.343
032075	0441	WHEAT KS.	416-1	OFF ROW	.074	.075	.262	.347
032075	1044	WHEAT KS.	416-2	ON ROW	.080	.066	.246	.333
032075	1045	WHEAT KS.	416-2	OFF ROW	.082	.064	.259	.350
032075	1046	WHEAT KS.	416-2	OFF ROW	.079	.077	.276	.358
032075	1047	WHEAT KS.	416-2	ON ROW	.078	.074	.259	.310
032075	1127	WHEAT KS.	416-2	OFF ROW	.081	.069	.250	.338
032075	1127	WHEAT KS.	416-2	ON ROW	.068	.071	.230	.316
032075	1128	WHEAT KS.	416-2	ON ROW	.068	.069	.235	.338
032075	1129	WHEAT KS.	416-2	OFF ROW	.080	.070	.250	.338
032075	1252	WHEAT KS.	416-2	OFF ROW	.065	.067	.244	.330
032075	1254	WHEAT KS.	416-2	ON ROW	.067	.075	.238	.339
032075	1256	WHEAT KS.	416-2	ON ROW	.068	.068	.225	.309
032075	[illegible]	WHEAT KS.	416-2	OFF ROW	.065	.070	.241	.337
032075	[illegible].2	WHEAT KS.	416-2	ON ROW	.063	.060	.239	.333
032075	0142	WHEAT KS.	416-2	OFF ROW	.068	.071	.230	.328
032075	0143	WHEAT KS.	416-2	ON ROW	.068	.074	.222	.314
032075	0144	WHEAT KS.	416-2	OFF ROW	.069	.071	.225	.311
032075	0315	WHEAT KS.	416-2	ON ROW	.080	.092	.253	.360
032075	0335	WHEAT KS.	416-2	OFF ROW	.073	.082	.244	.333
032075	0339	WHEAT KS.	416-2	ON ROW	.071	.084	.229	.322
032075	0341	WHEAT KS.	416-2	OFF ROW	.071	.082	.241	.326
032075	1033	WHEAT KS.	416-3	ON ROW	.070	.077	.300	.510
032075	1035	WHEAT KS.	416-3	ON ROW	.074	.080	.321	.470
032075	1036	WHEAT KS.	416-3	ON ROW	.070	.070	.270	.480
032075	1037	WHEAT KS.	416-3	OFF ROW	.070	.080	.300	.440

Table A-3- cont.

032075	1114	WHEAT KS.	416-3	OFF ROW	.070	.070	.300	.430
032075	1115	WHEAT KS.	416-3	ON ROW	.070	.070	.300	.450
032075	1116	WHEAT KS.	416-3	ON ROW	.060	.080	.290	.460
032075	1117	WHEAT KS.	416-3	OFF ROW	.080	.080	.310	.430
032075	1236	WHEAT KS.	416-3	ON ROW	.060	.050	.240	.380
032075	1237	WHEAT KS.	416-3	OFF ROW	.060	.050	.260	.380
032075	1238	WHEAT KS.	416-3	OFF ROW	.050	.050	.260	.380
032075	1239	WHEAT KS.	416-3	OFF ROW	.050	.050	.240	.390
032075	0126	WHEAT KS.	416-3	OFF ROW	.060	.060	.270	.390
032075	0128	WHEAT KS.	416-3	ON ROW	.060	.050	.250	.400
032075	0130	WHEAT KS.	416-3	ON ROW	.060	.050	.250	.400
032075	0131	WHEAT KS.	416-3	OFF ROW	.060	.060	.260	.370
032075	0423	WHEAT KS.	416-3	OFF ROW	.073	.080	.300	.440
032075	0424	WHEAT KS.	416-3	ON ROW	.070	.070	.270	.420
032075	0425	WHEAT KS.	416-3	ON ROW	.070	.070	.290	.420
032075	0426	WHEAT KS.	416-3	OFF ROW	.080	.090	.290	.440

Table A-4. APRIL LEAF AREA INDEX AND DESCRIPTIVE PARAMETERS.

April 23, 1975 Jointing Stage Field 416

Crop Type : Satanta Wheat (10" drill; EW)

Height : 28-35 cm

Chlorotic : 2-5% Yellowing

Weeds : 0%

Soil Condition : Dry

Wind : Calm

	PLOT 1	PLOT 2	PLOT 3
Lear Area Index	5.13	5.36	6.15
Dry Weight (2' X 2' Plot)	142.24 gm	148.70	207.63
Number of Tillers (2' X 2' Plot)			
Live	907.00	1179.00	931.00
Dead	52.00	75.00	33.00
Total	959.00	1254.00	964.00
Average Tillers/Plant			
Live	8.80	10.80	8.40
Dead	.60	1.60	.80
Total	9.40	12.40	9.20
Average Leaf Area/Plant			
Green	100.84 cm^2	83.48	89.70
Yellow	33.21	42.50	19.16
Dead	40.99	32.02	31.49
Total	175.04	158.00	140.35

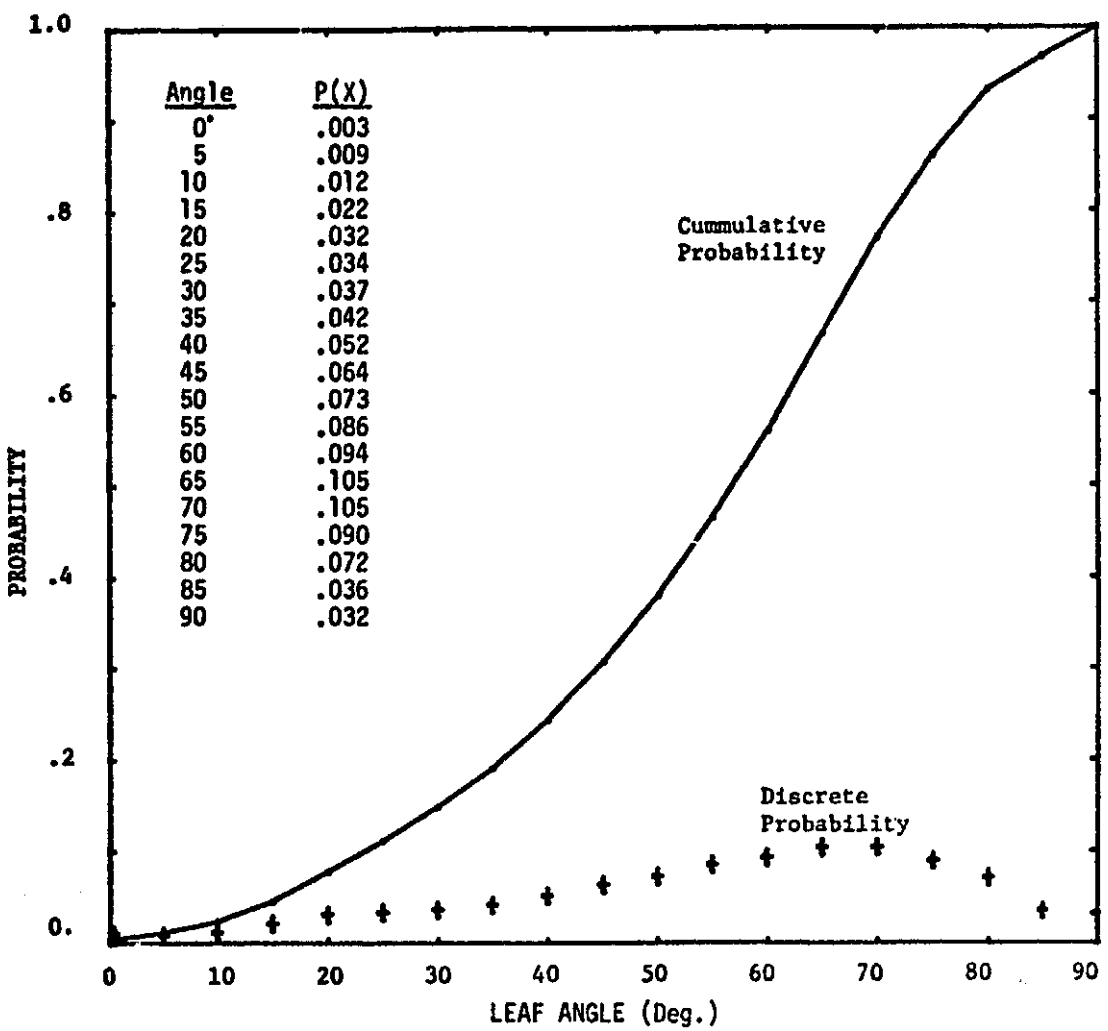

Angle	P(X)
0°	.003
5	.009
10	.012
15	.022
20	.032
25	.034
30	.037
35	.042
40	.052
45	.064
50	.073
55	.086
60	.094
65	.105
70	.105
75	.090
80	.072
85	.036
90	.032

FIGURE A-2. LEAF ANGLE DISTRIBUTION FOR APRIL.

Table A-5. APRIL RADIOMETRIC DATA.

DATE	TIME	CROP AND LOCATION	PLOT NUMBER	ORIENTATION	REFLECTANCE=	BAND1	BAND2	BAND3	BAND4
042375	1009	WHEAT KS.	416-1	ON ROW		.037	.023	.284	.407
042375	1013	WHEAT KS.	416-1	ON ROW		.036	.019	.251	.365
042375	1015	WHEAT KS.	416-1	OFF ROW		.050	.036	.252	.393
042375	1016	WHEAT KS.	416-1	OFF ROW		.041	.028	.262	.357
042375	1128	WHEAT KS.	416-1	ON ROW		.043	.027	.280	.434
042375	1130	WHEAT KS.	416-1	ON ROW		.047	.030	.272	.437
042375	1133	WHEAT KS.	416-1	OFF ROW		.050	.035	.254	.394
042375	1135	WHEAT KS.	416-1	OFF ROW		.049	.038	.224	.369
042375	0120	WHEAT KS.	416-1	OFF ROW		.070	.051	.240	.368
042375	0124	WHEAT KS.	416-1	OFF ROW		.055	.043	.222	.367
042375	0125	WHEAT KS.	416-1	ON ROW		.053	.036	.292	.462
042375	0127	WHEAT KS.	416-1	ON ROW		.052	.036	.277	.443
042375	0521	WHEAT KS.	416-1	OFF ROW		.053	.024	.270	.395
042375	0523	WHEAT KS.	416-1	OFF ROW		.058	.028	.278	.404
042375	0525	WHEAT KS.	416-1	ON ROW		.051	.033	.253	.380
042375	0527	WHEAT KS.	416-1	OFF ROW		.052	.031	.270	.475
042375	1042	WHEAT KS.	416-2	ON ROW		.039	.025	.284	.450
042375	1044	WHEAT KS.	416-2	ON ROW		.039	.025	.283	.434
042375	1046	WHEAT KS.	416-2	OFF ROW		.038	.023	.243	.350
042375	1048	WHEAT KS.	416-2	OFF ROW		.041	.026	.254	.371
042375	1146	WHEAT KS.	416-2	ON ROW		.043	.031	.277	.413
042375	1148	WHEAT KS.	416-2	ON ROW		.042	.029	.298	.423
042375	1150	WHEAT KS.	416-2	OFF ROW		.041	.029	.221	.340
042375	1153	WHEAT KS.	416-2	OFF ROW		.044	.031	.247	.348
042375	0140	WHEAT KS.	416-2	ON ROW		.047	.035	.300	.437
042375	0143	WHEAT KS.	416-2	ON ROW		.051	.037	.294	.441
042375	0146	WHEAT KS.	416-2	OFF ROW		.049	.035	.256	.354
042375	0148	WHEAT KS.	416-2	OFF ROW		.047	.032	.251	.372
042375	0538	WHEAT KS.	416-2	ON ROW		.053	.025	.343	.577
042375	0540	WHEAT KS.	416-2	ON ROW		.057	.029	.352	.571
042375	0541	WHEAT KS.	416-2	OFF ROW		.048	.024	.294	.420
042375	0543	WHEAT KS.	416-2	OFF ROW		.056	.021	.293	.439

Table A-5- cont.

042375	1110	WHEAT KS.	416-3	ON ROW	.047	.029	.305	.453
042375	1113	WHEAT KS.	416-3	ON ROW	.032	.019	.230	.347
042375	1114	WHEAT KS.	416-3	OFF ROW	.036	.023	.218	.344
042375	1115	WHEAT KS.	416-3	OFF ROW	.044	.028	.293	.421
042375	1203	WHEAT KS.	416-3	ON ROW	.042	.027	.263	.401
042375	1207	WHEAT KS.	416-3	ON ROW	.050	.034	.291	.464
042375	1210	WHEAT KS.	416-3	OFF ROW	.045	.032	.280	.393
042375	1212	WHEAT KS.	416-3	OFF ROW	.041	.029	.230	.323
042375	0207	WHEAT KS.	416-3	ON ROW	.050	.036	.301	.450
042375	0209	WHEAT KS.	416-3	ON ROW	.046	.034	.253	.415
042375	0211	WHEAT KS.	416-3	OFF ROW	.049	.037	.264	.366
042375	0212	WHEAT KS.	416-3	OFF ROW	.050	.034	.286	.402
042375	0554	WHEAT KS.	416-3	ON ROW	.050	.026	.327	.521
042375	0555	WHEAT KS.	416-3	OFF ROW	.052	.027	.323	.502
042375	0557	WHEAT KS.	416-3	OFF ROW	.060	.023	.337	.478
042375	0559	WHEAT KS.	416-3	OFF ROW	.056	.023	.364	.508

Table A-6. AVERAGE DIURNAL CANOPY REFLECTANCE. Canopy reflectance is averaged over on-row and off-row set ups.

March 20	Band 4	Band 5	Band 6	Band 7
PLOT 1				
1052 hrs.	.076	.078	.235	.315
1136	.065	.072	.217	.316
1304	.062	.059	.209	.299
1355	.067	.070	.210	.299
1635	.067	.075	.240	.329
PLOT 2				
1044	.075	.071	.260	.230
1127	.074	.070	.244	.333
1252	.066	.070	.237	.326
1342	.067	.069	.231	.322
1515	.074	.086	.242	.335
PLOT 3				
1033	.071	.083	.298	.475
1114	.055	.075	.300	.443
1236	.055	.050	.250	.383
1331	.060	.055	.258	.390
1623	.068	.073	.288	.430

April 23	Band 4	Band 5	Band 6	Band 7
PLOT 1				
1009 hrs.	.023	.027	.249	.381
1128	.047	.033	.258	.409
1302	.058	.058	.258	.405
1738	.054	.029	.270	.416
PLOT 2				
1042	.039	.025	.266	.401
1146	.043	.030	.261	.381
1340	.049	.035	.275	.402
1738	.054	.025	.321	.503
PLOT 3				
1110	.040	.025	.262	.391
1203	.045	.031	.266	.395
1407	.049	.035	.276	.408
1754	.055	.025	.338	.519

APPENDIX B

Normalized Divergence Plots

The divergence between the model derived spectral signatures and the signatures of areas with unknown LAI were calculated using several different techniques. Figures B-1 through B-3 show the normalized divergence plots for transformed data. Figures B-4 through B-6 depict the normalized divergence for derived feature vectors.

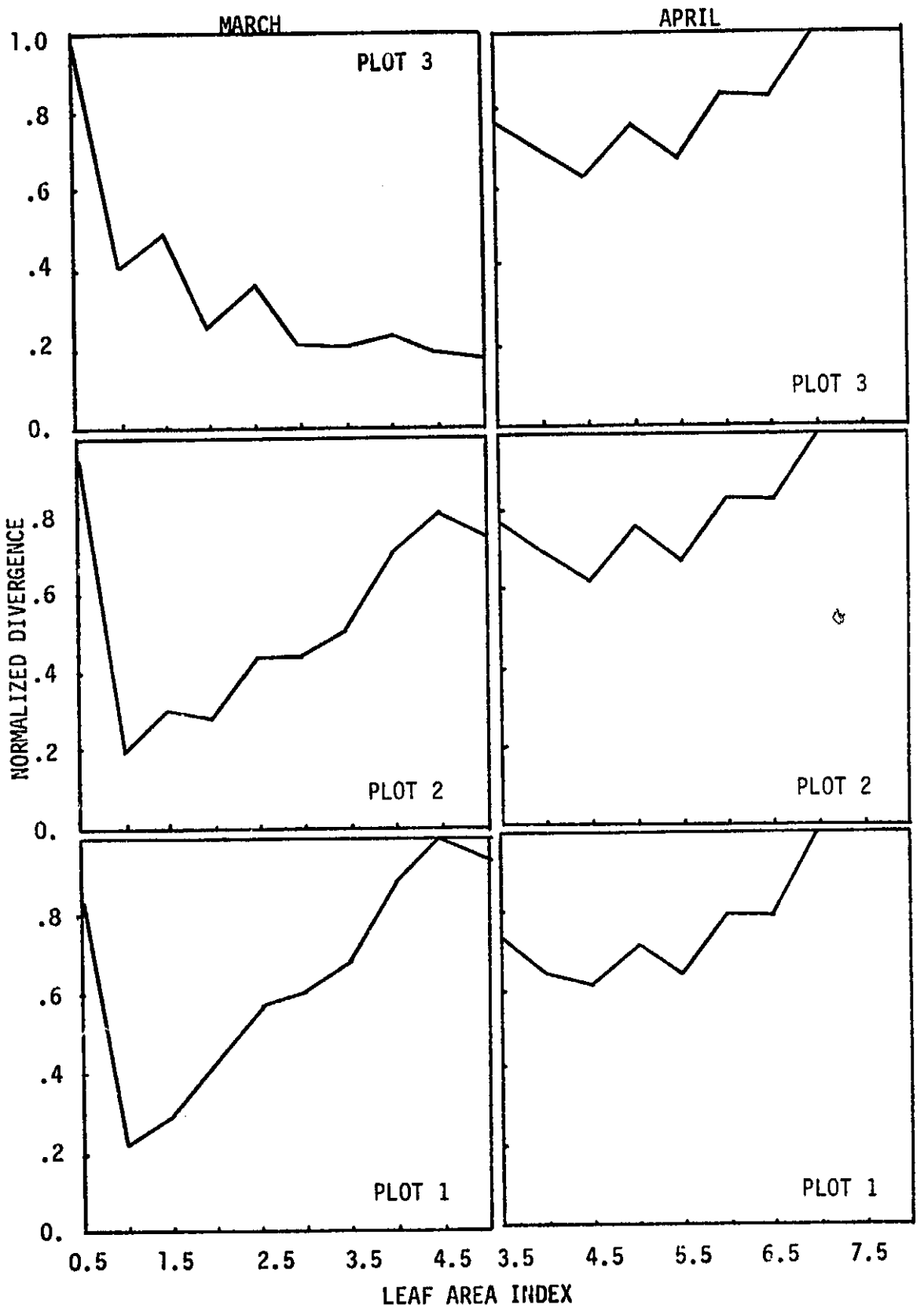

FIGURE B-1. NORMALIZED DIVERGENCE USING SPHERICAL COVARIANCE MATRICES (REFLECTANCE DATA).

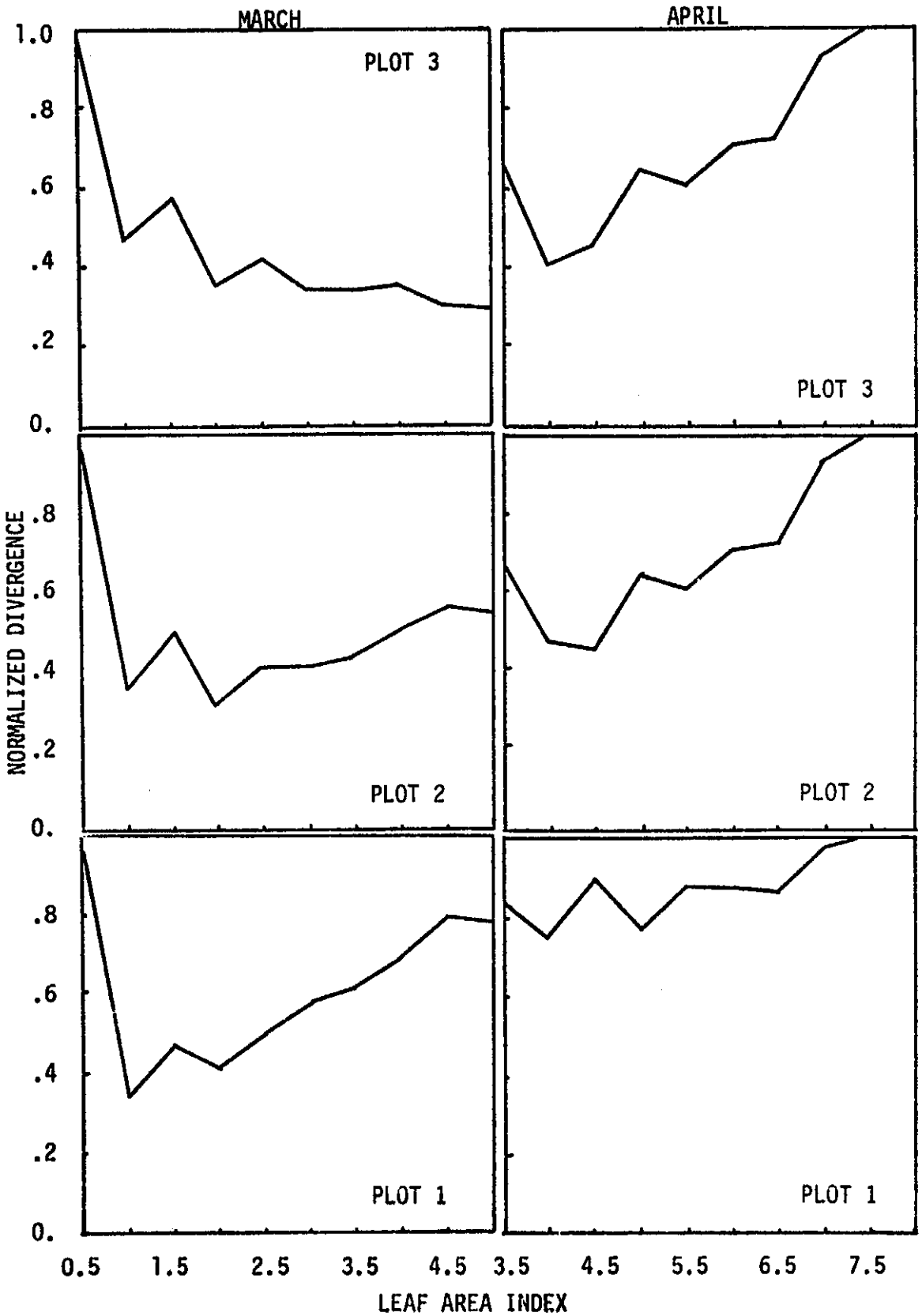

FIGURE B-2. NORMALIZED DIVERGENCE USING SPHERICAL COVARIANCE MATRICES (RADIANCE DATA).

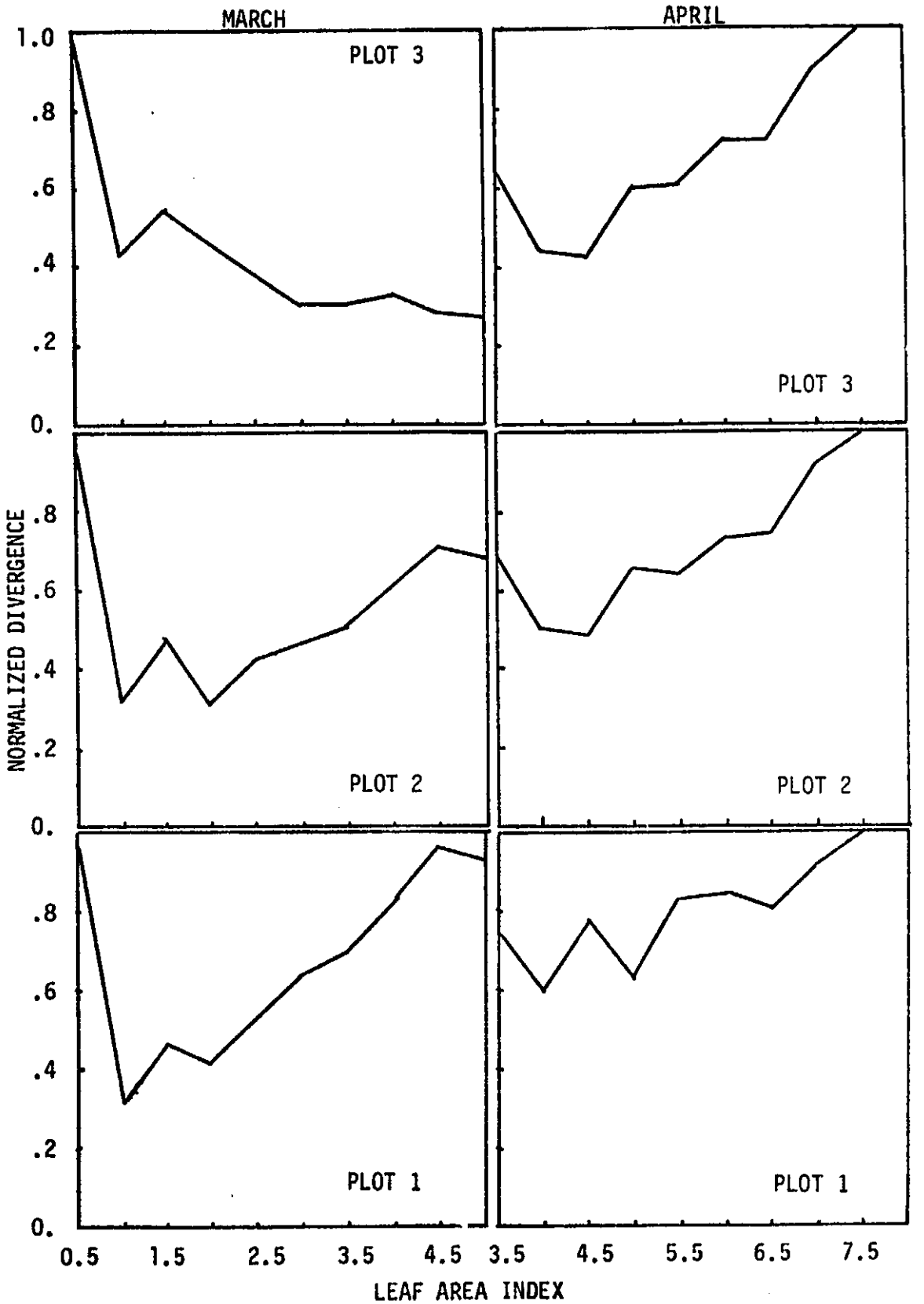

FIGURE B-3. NORMALIZED DIVERGENCE USING SUN ANGLE CORRECTED RADIANCE.

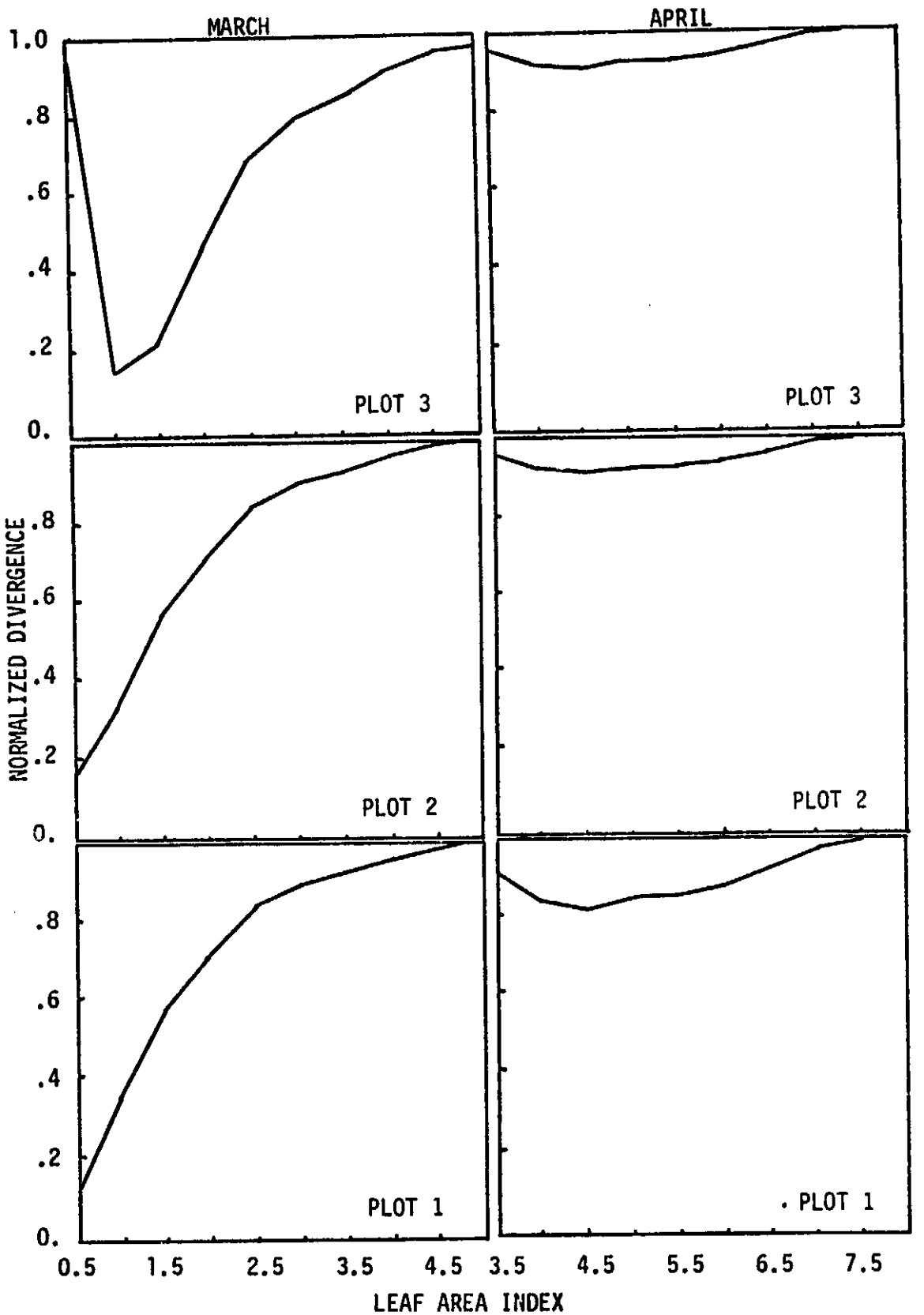

FIGURE B-4. NORMALIZED DIVERGENCE USING RATIO OF BANDS 6/4.

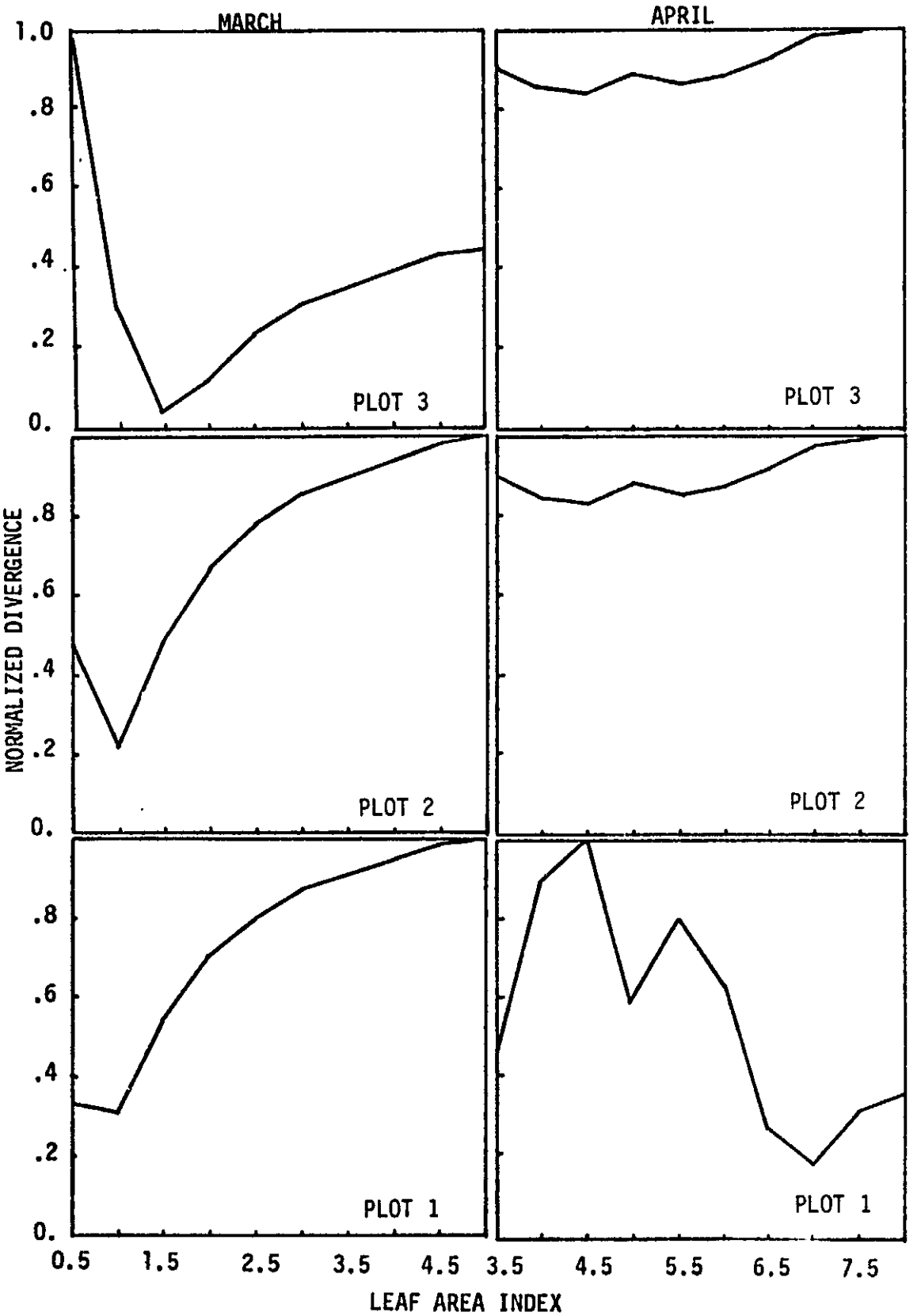

FIGURE B-5. NORMALIZED DIVERGENCE USING RATIO OF BANDS 6/4.

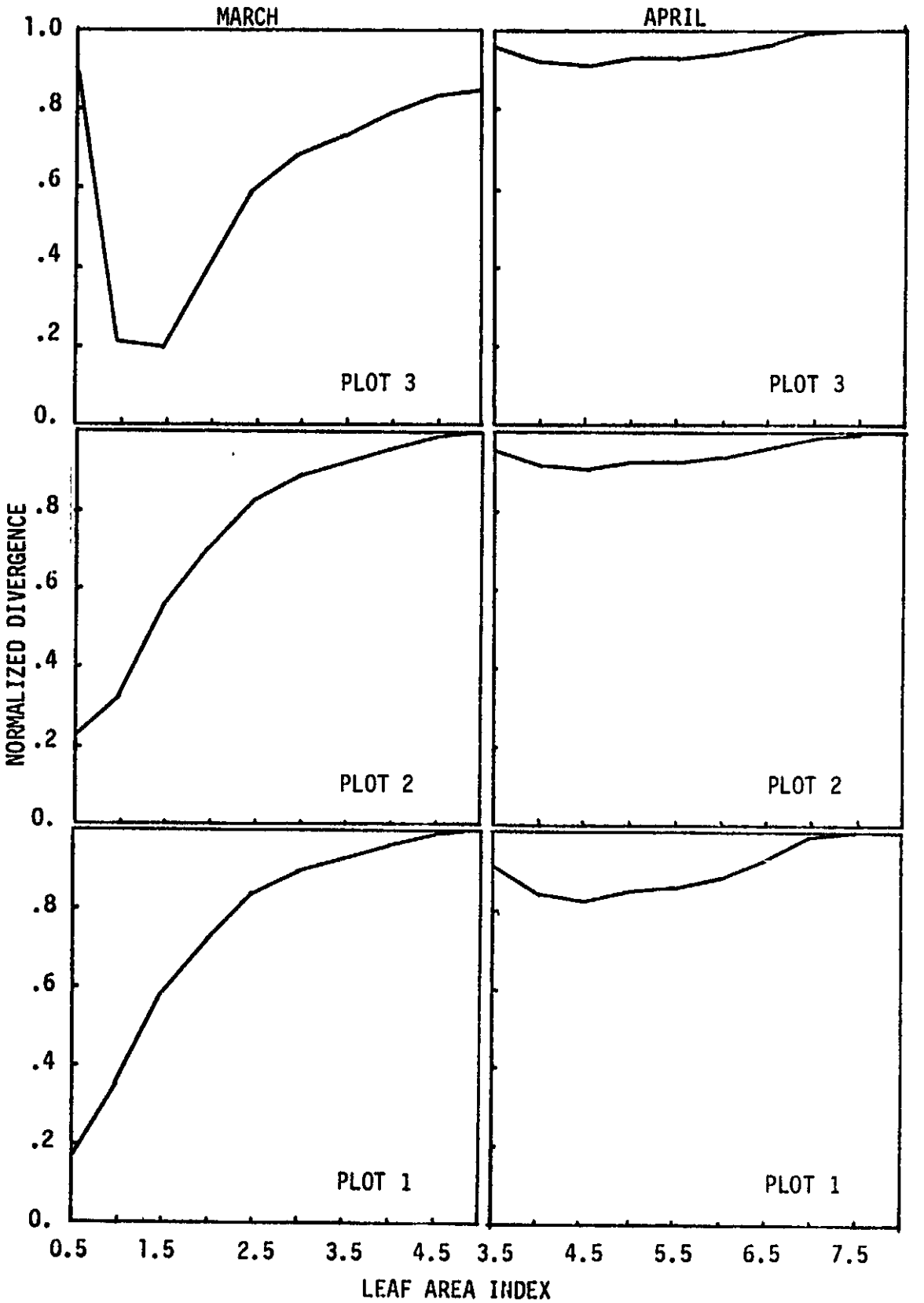

FIGURE B-6. NORMALIZED DIVERGENCE USING RATIO OF BANDS 7/5 and 6/4.

APPENDIX C

Computer Programs

Five FORTRAN programs are presented in this appendix. The first three (PROP, THETA and CONVOL) are used in converting the measured angular bias of Fourier diffraction patterns, generated from field photographs, into estimates of the 3-space leaf angle distribution (LAD) of a plant canopy. Program ORTHOG utilizes digitized silhouettes of individual plants in calculating the distribution of angles for individual plants, and the overall LAD. Program SUFU is the classification routine developed in this study. All other programs used in the study are available through the refererces.

Page intentionally left blank

Exhibit C-1. PROGRAM PROP.

Program Name: PROP

Subroutines Required: GRAPH

Narrative:

PROP accepts as input desitometer readings which wedge sample the diffraction pattern of an orthogonal view of a plant canopy. A plot of the distribution of leaf slopes contained in the original image is then generated.

Control Card Input:

Card 1			
Column 1-4	(I4)	(NRUN)	Number of runs
Column 5-10	(I6)	(NDATE)	Date in 6 INTEGERS
Column 11-20	(F10.5)	(DERCT)	Threshold value
Column 21-30	(F10.5)	(BADJ)	Base adjustment for aperture
Column 31-40	(F10.5)	(DTEST)	Minimum divergence test value
Column 41	(I1)	(MTRAIL)	Test for end of data (other than 0 for end of data)
Cards 2 & 3			
Column 1-80; Card 2	(16F5.1)	DATAE)	Densitometer values
Column 1-15: Card 3	(16F5.1)	(DATAE)	Densitometer values

Repeat Card 1 and Card 2 and 3 formats for each successive group of 3 data cards until all desired data has been entered. End of data is indicated by a single card with some integer value other than 0 for Column 41.

```
      PROGRAM PROP(INPUT,OUTPUT,TAPE5=INPUT,TAPE6=OUTPUT,PUNCH,FILMPL)
C.....PROGRAM PROP IS DESIGNED TO DEVELOP A DENSITY FUNCTION OF THE
C     ANGLES IN THE INPUT SCENE, BASED ON THE INTENSITY IN AN
C     CORRESPONDING DIFFRACTION PATTERN NEGATIVE.  THE PRINCIPAL
C     OUTPUT IS A DISTRIBUTION OF ANGLES INFERRED IN THE INPUT,
C     IN 10 DEGREE INCREMENTS FROM 0 TO 90 DEGREES.
C.....INPUT
C        IDENTIFICATION (NRUN, NDATE)
C        THRESHOLD VALUE (PERCT)
C        BASE ADJUSTMENT FOR APERTURE (BADJ)
C        MINIMUM DIVERGENCE TEST VALUE (DTEST)
C.....OUTPUT
C        ORIGINAL DATA OF INTENSITIES OFF DIFFRACTION PATTERN
C        BASE VALUE
C        MAXIMUM DEVIATION IN THE DATA
C        AVERAGE DEVIATION
C        DEVIATIONS
C        DIFFRACTION PATTERN DENSITY FUNCTION
C        SCENE DENSITY FUNCTION
      DIMENSION DATAE(19),PROPORT(20),DEV(19),TEMP(19),XAXIS(19),LTIT(8)
C
C...SET UP AXISES FOR MAPA ROUTINE
C
      DO 5 J=1,18
      XAXIS(J)=J*10.
    5 CONTINUE
      HT=10HPROPORTION
      VT=10HLEAF ANGLE
      LTIT(1)=10HDENSITY FU
      LTIT(2)=10HNCTION FU
      LTIT(3)=10HR FOURIER
      LTIT(4)=10HTECHNIQUE
      DO 6 J=5,8
    6 LTIT(J)=10H
C
C...ENTER MAJOR LOOP
C
      DO 200 K=1,50
C
C...READ DATA
C
      READ (5,510) NRUN,NDATE,PERCT,BADJ,DTEST,NTRAIL
  510 FORMAT(I4,I6,3F10.5,I1)
      IF(NTRAIL.GT.0) GO TO 300
      READ (5,505) (DATAE(I),I=1,19)
  505 FORMAT(19F5.1)
C
C...DETERMINE BASE VALUE (LARGEST DATA POINT)
C
      DEVIOI=0.
      BASE=DATAE(1)
      DO 10 J=2,19
      IF(BASE.LT.DATAE(J)) BASE=DATAE(J)
   10 CONTINUE
C
C...TEST FOR INCOMPATABILITY BETWEEN 0 AND 180 DEGREE READINGS. IF
C   TEST IS POSITIVE THEN THE DATA MAY BE IN ERROR.
C
      FIRST=ABS(DATAE(1)-DATAE(19))
```

```
      615 FORMAT(///,*      DEVIATIONS*)
      WRITE(6,650) (DEV(I),I=1,19)
      WRITE(6,630)
      630 FORMAT(///,*      DIFFRACTION PATTERN DENSITY FUNCTION VALUES*)
      WRITE(6,650) (TEMP(I),I=1,19)
      WRITE(6,620)
      620 FORMAT(///,*      DENSITY FUNCTION VALUES FOR INPUT*)
      WRITE(6,650) (PROPORT(I),I=1,18)
C     PUNCH 705,NRUN,NDATE
C     PUNCH 710, (PROPORT(I),I=1,18)
      NUMPT=18
      YMAX=0.
      DO 90 J=1,18
      IF(PROPORT(J).GT.YMAX) YMAX=PROPORT(J)
   90 CONTINUE
      MAX=(YMAX+.1)*10.
      YMAX=MAX
      YMAX=YMAX/10.
      CALL GRAPH(XAXIS,PROPORT,YMAX,NUMPT,NRUN,NDATE)
  705 FORMAT(I4,I6)
  710 FORMAT(8F10.4)
      GO TO 200
  250 WRITE(6,625) NRUN
  625 FORMAT(*1*,*      RUN *,I4,* DOES NOT CONTAIN SIGNIFICANT DEVIATION
     1 TO DEVELOP A DENSITY FUNCTION*)
  200 CONTINUE
  300 CONTINUE
      STOP
      END


      SUBROUTINE GRAPH(X,Y,YMAX,NUMPT,NRUN,NDATE)
      DIMENSION X(50),Y(50)
      LTIT1=10HRUN NUMBER
      LTIT2=5HDATE
      LABX=5HANGLE
      LABY=10HPROPORTION
      CALL SET(.1,.8,.1,.8,0.,180.,0.,YMAX,1)
      CALL PWRT(5.400,LABY,10,1,1)
      CALL PWRT(430.5,LABX,5,1,0)
      CALL PWRT(382.1015,LTIT1,10,1,0)
      CALL NUMBR(NRUN,2H13)
      CALL PWRT(395.960,LTIT2,5,1,0)
      CALL NUMBR(NDATE,2H16)
      CALL UNDFMT(5HF10.0,5HF10.3)
      CALL PERIML(18,1,10,1)
      CALL CURVE(X,Y,NUMPT)
      CALL FRAME
      RETURN
      END
```

Exhibit C-2. PROGRAM THETA.

Program Name: THETA

Subroutines Required: None

Narrative:

THETA is entirely self-contained. It derives a matrix of the three-space angles inferred by any pair of orthogonally projected angles from 2.5 to 87.5 degrees. This program outputs a punched deck of the matrix, which is utilized in program CONVOL.

Control Card Input: None

```
      PROGRAM THETA(INPUT,OUTPUT,TAPE5=INPUT,TAPE6=OUTPUT,PUNCH)
C.....PROGRAM THETA IS DESIGNED TO DETERMINE THE THREE SPACE ANGLE FORMED BY
C     ALL PAIRS OF PLANER ANGLES IN FIVE DEGREE INCREMENTS BETWEEN 1 AND 89
C     DEGREES.FOR EXAMPLE IF A LINE FORMS A 10 DEGREE ANGLE IN THE XZ VIEW AND A
C     25 DEGREE ANGLE IN THE YZ VIEW THIS PROGRAM WOULD CALCULATE THE
C     PERSPECTIVE THREE SPACE ANGLE(9.4 DEGREES).
C.....INPUT
C        CDEGTH (INTERNAL ASSIGNMENT OF CONVERSION FACTOR FOR DEGREES TO
C           RADIANS)
C        CRTDEG ( RADIANS TO DEGREES)
C        X (VECTOR REPRESENTING 0-90 DEGREES IN 5 DEGREE INTERVALSIN THE XZ
C           VIEW)
C        Y (VECTOR FOR YZ VIEW)
C.....OUTPUT
C        TD (ARRAY CONTAINING THE THREE SPACE ANGLES OF ALL PAIRS OF ORTHOGONAL
C           VIEW ANGLES)
      DIMENSION X(18),Y(18),TD(18,18),TR(18,18)
C
C...ASSIGN CONVERSION FACTORS
C
      CDEGTH=.0174533
      CRTDEG=57.29578
C
C...SET UP FIVE DEGREE INCREMENYS FOR THE X AND Y VIEWS
C
      R=2.5
      DO 25 I=1,18
      X(I)=R
      Y(I)=R
      R=(R+5.)
   25 CONTINUE
      DO 35 I=1,18
      X(I)=X(I)*CDEGTR
      Y(I)=Y(I)*CDEGTR
   35 CONTINUE
C
C...CALCULATE THE THREE SPACE ANGLE ASSUCIATED WITH WITH ALL PAIRS
C
      DO 50 I=1,18
      DO 50 J=1,18
      ZZ=TAN(X(J))
      YZ=(TAN(X(J)))/(TAN(Y(I)))
      C1=1.+YZ**2
      C=SQRT(C1)
      TR(I,J)=ATAN2(ZZ,C)
      TD(I,J)=(TR(I,J)*CRTDEG)
   50 CONTINUE
C
C...GENERATE OUTPUT
C
      DO 100 I=1,18
      PUNCH 615, (TD(I,J),J=1,18)
  615 FORMAT(8F9.5)
      WRITE(6,610) (TD(I,J),J=1,18)
  610 FORMAT(1H ,18F5.1)
  100 CONTINUE
      STOP
      END
```

Exhibit C-3. PROGRAM CONVOL.

Program Name: CONVOL

Subroutines Required: None

Narrative:

CONVOL uses the joint probabilitie[illegible] orthogonal pairs of planner projected angles to convo[illegible]ogonal distributions of angles. The process involves cycling through a matrix of three-space angles inferred by pairs of orthogonally projected angles. Each element of the matrix is assigned to a three-space angle interval, which in turn, is assigned the value of the joint probability of the orthogonal pairs occurance. These joint probabilities in each class are added, with the final sum indicating the probability of that three-space class's occurrance.

Control Card Input:

Card 1			
Column 1-10	(I10)	(N)	Number of orthogonal pairs
Card 2-55			
Column 1-80	(8F10.5)	(THETA3D)	3-space matrix; THETA output
Card 56			
Column 11-20	(F10.5)	(BASEX)	Base value in D.P.
Column 21-30	(F10.5)	(AVDEVX)	Average deviation in D.P.
Card 57			
Column 11-20	(F10.5)	(BASEY)	Same; Y view
Column 21-30	(F10.5)	(AVDEVY)	Same; Y view

```
      PROGRAM CONVOL (INPUT,OUTPUT,TAPE5=INPUT,TAPE6=OUTPUT,PUNCH)
C.....PROGRAM CONVOL IS DESIGNED TO MERGE TWO ORTHOGONAL PLANER DISTRIBUTIONS
C     OF ANGLES INTO THEIR TRUE THREE SPACE DISTRIBUTION OF ANGLES. THE
C     PROCEDURE INVOLVES DETERMINING THE JOINT PROBABILITY OF ANY PAIR OF
C     ANGLES(EX.- 10 DEGREES IN THE XZ AND 25 DEGREES IN THE YZ PLANES) AND
C     ASSIGNING THE JOINT PROBABILITY TO THE THREE SPACE ANGLE ASSOCIATED WITH
C     THE ORTHOGONAL PAIR (EX.- 10 AND 25 DEGREE PAIR FORMS A 9.4 DEGREE
C     ANGLE IN THREE SPACE). SEVERAL COMBINATIONS OF PLANER PAIRS CAN FORM
C     A SINGLE THREE SPACE ANGLE INTERVAL, THEREFORE THE ACTUAL PROBABILITY
C     OF ANY THREE SPACE ANGLE INTERVAL IS EQUAL TO THE SUM OF ALL THE JOINT
C     PROBABILITIES OF ALL THE ORTHOGONAL PAIRS WHICH FORM THE THREE SPACE
C     ANGLE. PROGRAM THETA DETERMINES THE THREE SPACE ANGLE FORMED BY ALL
C     PAIRS OF ANGLES IN FIVE DEGREE INCREMENTS BETWEEN 1 AND 89 DEGREES. THE
C     OUTPUT FROM PROGRAM THETA (MATRIX OF THREE SPACE ANGLES) ACTS AS INPUT
C     TO THIS PROGRAM.
C.....INPUT
C        N (NUMBER OF ORTHOGONAL PAIRS TO BE MERGED)
C        THETA3D (MATRIX OF THREE SPACE ANGLES)
C        BASEX,BASEY (BASE VALUE OF DIFFRACTION PATTERN-USED BY FOLLOWING
C           PROGRAM)
C        AVDEVX,AVDEVY (AVERAGE DEVIATION IN THE DIFFRACTION PATTERN- USED
C           BY THE FOLLOWING PROGRAM)
C        XZ,YZ (ARRAYS CONTAINING THE PROBABILITY DISTRIBUTIONS OF THE
C           ORTHOGONAL SCENES)
C.....OUTPUT
C        PROB(1-18) (THREE SPACE LEAF ANGLE DISTRIBUTION)
C        PROB(19-22) (BASEX,BASEY,AVDEVX,AVDEVY)
C
C
C
      DIMENSION D(25,19),B(25,2)
      DIMENSION THETA3D(19,19),XZ(19),YZ(19),PROB(22)
C
C...READ PROGRAM PARAMETERS
C
      READ (5,500) N
  500 FORMAT(I10)
      DO 10 I=1,19
   10 READ (5,510) (THETA3D(I,J),J=1,19)
  510 FORMAT(8F10.5)
C
C...SET UP HEADING FOR PRINTER OUTPUT
C
      WRITE(6,610)
  610 FORMAT(*1  5    10    15    20    25    30    35    40    45    50    55    6
     *0    65    70    75    80    85    90          BASEX    AVDEVX   BASEY    AV
     *DEVY*,///)
C
C...READ INPUT (XZ AND YZ DISTRIBUTION OF ANGLES AND THEIR RESPECTIVE BASE
C   AND AVERAGE DEVIATION VALUES)
C
      DO 100 L1=1,N
      READ (5,520) (B(L1,I),I=1,2)
      READ (5,515) (D(L1,I),I=1,19)
  100 CONTINUE
  515 FORMAT(8F10.5)
  520 FORMAT(10X,2F10.5)
      DO 200 L1=1,N
      DO 125 I=1,19
```

```
      XZ(I)=D(L1,I)
      BASEX=B(L1,1)
      AVDEVX=B(L1,2)
  125 CONTINUE
      DO 175 M1=L1,N
      DO 150 I=1,19
      YZ(I)=D(M1,I)
      BASEY=B(M1,1)
      AVDEVY=B(M1,2)
  150 CONTINUE
C
C...CALCULATE JOINT PROBABILITIES OF ALL PAIRS AND ASSIGN EACH PROBABILITY TO
C   A THREE SPACE ANGLE INTERVAL
C
      DO 20 I=1,22
   20 PROB(I)=0.
      DO 30 I=1,19
      DO 30 J=1,19
      INDEX=(I-1)*THETA30(I,J)+5.1/5.)
   30 PROB(INDEX)=PROB(INDEX)+(YZ(I)*XZ(J))
C
C...ASSIGN BASE AND AVERAGE DEVIATION VALUES
C
      PROB(19)=BASEX
      PROB(20)=AVDEVX
      PROB(21)=BASEY
      PROB(22)=AVDEVY
C
C...GENERATE OUTPUT
C
      WRITE(6,620) (PROB(I),I=1,22)
  620 FORMAT(10F5.2,5X,4F8.2,/)
      PUNCH 705,(PROB(I),I=1,22
  705 FORMAT(8F10.5)
C
C...CONTINUE PROCESS UNTIL ALL AIRS HAVE BEEN CONVOLUTED
C
  175 CONTINUE
  200 CONTINUE
      STOP
      END
```

Exhibit C-4. PROGRAM ORTHOG.

Program Name: ORTHOG

Subroutines Required: PLOT

Narrative:

ORTHOG determines the three-space distribution of angles from pairs of digitized orthogonal photos. In addition, it outputs a microfilm plot of each view.

Control Card Input:

Card 1			
Column 1-40	(4A10)	(LTIT)	Title for plot
Card 2			
Column 1-10	(I10)	(NPLANT)	Plant numbering sequence
Column 11-20	(I10)	(NLEAF)	Leaf numbering sequence
Column 21-30	(I10)	(NPTS)	Number of digitized points/leaf
Card 3-n			
Column 1-10	(F10.5)	(Z)	Z coordinate of a digitized point
Column 11-20	(F10.5)	(X)	X coordinate
Column 21-30	(F10.5)	(Y)	Y coordinate

.
.
.

continued for as many columns and cards needed to describe a leaf

Cards n-+
Repeat cards number 3 and 3-n format for remaining leaves and plants.

```
      PROGRAM ORTHOG(INPUT,OUTPUT,TAPE5=INPUT,TAPE6=OUTPUT,PUNCH,FILMPL)
C.....PROGRAM ORTHOG IS DESIGNED TO TAKE THE DIGITIZED DATA FROM ORTHOGONAL
C     VIEWS (XZ AND YZ) AND CONSTRUCT AN ABSTRACT THREE SPACE REPRESENTATION
C     OF THE ORIGINAL PLANT. THE PROGRAM SAMPLES THE THREE SPACE LINEAR
C     SEGMENTS COMPRISING THE PLANT TO DEVELOP A DISTRIBUTION OF ANGLES
C     FORMED BY THE LEAVES OF THE PLANT.
C.....INPUT
C        NPLANT (BOOKKEEPING NUMBER OF THE PLANT)
C        NLEAF (BOOKKEEPING NUMBER ASSIGNED TO EACH LEAF OF THE PLANT)
C        NPTS (NUMBER OF POINTS DEFINING EACH LEAF)
C        LTIT (ARRAY CONTAINING THE TITLE FOR THE MICROFILM PLOT)
C        Z (VECTOR CONTAINING THE Z COORDINATES)
C        X((VECTOR CONTAINING THE X COURDINATES)
C        X((VECTOR CONTAINING THE Y COURDINATES)
C        L1 (INTERNALLY ASSIGNED VARIABLE INDICATING THE NUMBER OF LEAVES)
C        MTEST (AN INTERNAL VARIABLE USED TO FLAG A NEW MICROFILM PLOT)
C        PLTX,PLTY (ARRAYS USED TO HOUSE THE VALUES TO BE PLOTTED)
C        PROB (ARRAY OF THE PROBABILITIES FOR ANGLES 0-90 DEGREES)
C          COSTH (THREE SPACE ANGLE FORMED BY A LINE SEGMENT)
C.....OUTPUT
C        PROB (DISTRIBUTION OF THREE SPACE ANGLES, PRINTER, PUNCH)
C        FILM PLOT OF THE XZ AND YZ VIEWS OF THE PLANT
C
C
C
      DIMENSION Z(5,15),Y(5,15),X(5,15),PROB(18),KK(5),LTIT(4)
      DIMENSION PLTX(18),PLTY(18),PXZ(18),PYZ(18)
C
C...INITIALIZE PARAMETERS
C
      MTEST=1 $ NLINES=0 $ L1=0 $ RSUM=0. $ RASUM=0. $ RYSUM=0.
      DO 3 I=1,18
      PLTX(I)=0.
      PLTY(I)=0.
      PXZ(I)=0.
      PXZ(I)=0.
    3 PROB(I)=0.
C
C...READ PLOT TITLE
C
      READ (5,500) (LTIT(I),I=1,4)
  500 FORMAT(4A10)
C
C...READ VARIABLES DESCRIBING A LEAF
C
   10 READ (5,520) NPLANT,NLEAF,NPTS
  520 FORMAT(3I10)
C
C...TEST FOR A NEW PLANT
C
   11 IF(NPLANT.GT.MTEST) GO TO 200
C
C...TEST FOR END OF DATA SET
C
   12 IF(NLEAF.EQ.0) GO TO 1000
C
C...ASSIGN INTERNAL PARAMETERS
C
      L1=L1+1
```

```
60                KK(L1)=NPTS
                  C
                  C...READ COORDINATES OF A LEAF
                  C
                       READ (5,525) (Z(L1,I),X(L1,I),Y(L1,I),I=1,NPTS)
65                525 FORMAT(8F10.5)
                  C
                  C...CALCULATE THE THREE SPACE ANGLES FOR ALL LINE SEGMENTS DESCRIBING A LEAF
                  C
                       DO 100 L2=2,NPTS
70                     DX=X(L1,L2)-X(L1,L2-1)
                       DY=Y(L1,L2)-Y(L1,L2-1)
                       DZ=Z(L1,L2)-Z(L1,L2-1)
                       R=SQRT(DX**2+DY**2+DZ**2)
                       COSTH=ABS(DZ)/R
75                     COSTH=90.-(ACOS(COSTH)*57.2957795131)
                       RXZ=SQRT(DX**2+DZ**2)
                       THXZ=ABS(DZ)/RXZ
                       THXZ=ACOS(THXZ)*57.2957795131
                       THXZ=90.-THXZ
80                     RYZ=SQRT(DY**2+DZ**2)
                       THYZ=ABS(DZ)/RYZ
                       THYZ=ACOS(THYZ)*57.2957795131
                       THYZ=90.-THYZ
                  C
85                C...ASSIGN EACH THREE SPACE ANGLE TO ONE OF THE 5 DEGREE INTERVALS BETWEEN
                  C    0 AND 90 DEGREES. THE LENGTH OF THE LINE SEGMENT INDICATES THE RELATIVE
                  C    WEIGHTING OF THE ANGLE
                  C
                       INDEX=(COSTH+5.)/5.
90                     PROB(INDEX)=PROB(INDEX)+R
                       RSUM=RSUM + R
                       INDEX=(THXZ+5.)/5.
                       PXZ(INDEX)=PXZ(INDEX)+RXZ
                       RXSUM=RXSUM+RXZ
95                     INDEX=(THYZ+5.)/5.
                       PYZ(INDEX)=PYZ(INDEX)+RYZ
                       RYSUM=RYSUM+RYZ
                  C
                  C...GENERATE INCREMENTAL OUTPUT
100               C
                       IF(NLINES.EQ.0) GO TO 15
                       IF(NLINES.LT.55) GO TO 16
                    15 NLINES=0
                       WRITE(6,600)
105                 600 FORMAT('1PLANT     LEAF        Z1      X1      Y1        Z2      X2
                      1  Y2          DZ      DX      DY      THETA     THXZ      THYZ')
                    16 NLINES=NLINES+1
                       WRITE(6,605) NPLANT,NLEAF,Z(L1,L2-1),X(L1,L2-1),Y(L1,L2-1),Z(L1,L2
                      1),X(L1,L2),Y(L1,L2),DZ,DX,DY,COSTH,THXZ,THYZ
110                 605 FORMAT(2X,I2,8X,I2,1X,3(3X,3F7.1),3X,3F8.3)
                    100 CONTINUE
                  C
                  C...CONTINUE READING NEW LEAVES UNTIL A NEW PLANT IS ENCOUNTERED
                  C
115                    GO TO 10
                  C
                  C...CALCULATE PROBABILITY DISTRIBUTION FOR THE ENTIRE PLANT
                  C
```

```
  200 CONTINUE
      MTEST=NPLANT
      SUM=0.
      XSUM=0.
      YSUM=0.
      DO 210 I=1,18
      XSUM=XSUM+PXZ(I)
      YSUM=YSUM+PYZ(I)
  210 SUM=SUM+PROB(I)
      DO 220 I=1,18
      PXZ(I)=PXZ(I)/XSUM
      PYZ(I)=PYZ(I)/YSUM
  220 PROB(I)=PROB(I)/SUM
C
C...GENERAT PRINTER OUTPUT
C
      NP=NPLANT-1
      WRITE(6,625) NP
  625 FORMAT(///,' PROBABILITY',/,' OF ANGLE',3X,'  5   10   15   20   2
     15   30   35   40   45   50   55   60   65   70   75   80   85   90
     2  FOR PLANT',I3,/)
      WRITE(6,630) (PROB(I),I=1,18)
  630 FORMAT(' 3 SPACE ',18F5.2)
      WRITE(6,655) (PXZ(I),I=1,18)
  655 FORMAT('    XZ    ',18F5.2)
      WRITE(6,665) (PYZ(I),I=1,18)
  665 FORMAT('    YZ    ',18F5.2)
      WRITE(6,635) RSUM
  635 FORMAT(//,'   TOTAL PLANT LENGTH=',F6.3)
C
C...GENERATE PUNCHED OUTPUT
C
      BASE=1.
      PUNCH 705,NP,RSUM
  705 FORMAT(I10,F10.5)
      PUNCH 710,(PROB(I),I=1,18)
  710 FORMAT(8F10.5)
C     PUNCH 707,RXSUM
  707 FORMAT(10X,2F10.5)
C     PUNCH 710, (PXZ(I),I=1,18)
C     PUNCH 707,RYSUM
C     PUNCH 710, (PYZ(I),I=1,18)
C
C...GENERATE FILMPLOT OUTPUT
C
      DO 165 I=1,L1
      KTEST=I
      M1=KK(I)
      DO 160 J=1,M1
      PLTX(J)=X(I,J)
      PLTY(J)=Z(I,J)
  160 CONTINUE
C     CALL PLOT(PLTX,PLTY,1,KTEST,M1,LTIT)
  165 CONTINUE
      DO 175 I=1,L1
      KTEST=I
      M1=KK(I)
      DO 170 J=1,M1
      PLTX(J)=Y(I,J)
```

```
                PLTY(J)=Z(I,J)
  170         CONTINUE
C             CALL PLOT(PLTX,PLTY,2,KTEST,MI,LTIT)
  175         CONTINUE
C
C...REINITIALIZE PARAMETERS
C
  180         NLINES=0 $ L1=0 $ RSUM=0.$ RXSUM=0. $ RYSUM=0.
              DO 250 I=1,18
              PYZ(I)=0.
              PYZ(I)=0.
  250         PROB(I)=0.
              GO TO 12
 1000         CONTINUE
              STOP
              END


              SUBROUTINE PLOT(X,Y,MVIEW,KTEST,KK,LTIT)
              DIMENSION X(20),Y(20),LTIT(4)
              IF(KTEST.GT.1) GO TO 40
              CALL FRAME
              CALL SET(0.,1.,0.,1.,-4.,4.,-1.,7.,1)
              CALL SETLINE(1)
              CALL FRSTPT(-3.5,-.5)
              CALL STRING(LTIT)
              IF(MVIEW.EQ.2) GO TO 20
              LVIEW=10HSUX VIEWS.
              GO TO 30
           20 LVIEW=10HSUY VIEWS.
           30 CALL FRSTPT(3.,-.5)
              CALL STRING(LVIEW)
              CALL LINE(-3.,0.,-1.,6.)
              CALL LINE(-3.,6.,3.,6.)
              CALL LINE(3.,6.,3.,0.)
              CALL LINE(3.,0.,-3.,0.)
           40 M2=KK-1
              DO 100 I=1,M2
              XPT1=X(I)
              YPT1=Y(I)
              XPT2=X(I+1)
              YPT2=Y(I+1)
              CALL LINE(XPT1,YPT1,XPT2,YPT2)
          100 CONTINUE
              RETURN
              END
```

Exhibit C-5. PROGRAM SUFU.

Program Name: SUFU

Subroutines Required:

MODIFY	ADDSUB
FEATURE	TRNSPO
SMEANS	MATMPY
INVERT	

Narrative:

SUFU is a classification routine for comparing a spectral signature of an area with unknown LAI with the spectral signatures of several areas of known LAI, in order to infer the LAI of the unknown area. Subroutines MODIFY, SMEANS and FEATURE are user defined and allow for the modification of the input data. Output consists of a C-factor matrix, calculated divergence, and a printer plot of divergence.

Control Card Input:

Card 1			
Column 1-10	(I10)	(NSIG)	No. of "effects"
Column 11-20	(I10)	(NPLT)	No. of "plots"
Column 21-30	(I10)	(NWAVE)	No. of wavelengths
Column 31-40	(I10)	(MODVAR)	Flag to modify covariance matrix
Column 41-50	(I10)	(MODM)	Flag to modify mean vector
Column 51-60	(I10)	(IFEATV)	Flag to derive feature vectors
Card 2			
Column 1-10	(A10)	(IDENT)	Identification of "plot"/"effect"
Card 3			
Column 1-10	(F10.5)	(MEANS)	Mean vector of "plot"/"effect"
Card 4-n			
Column 1-80	(8F10.5)	(COVAR)	Covariance matrix of "plot"/"effect"

Exhibit C-5. Continued

Cards n-+

Repeat cards number 2, through 4-n for remaining mean vectors and covariance matrices of all of the "effects" and "plots". The order of entry is all of the "effects" data first, followed by all of the "plot" data.

```
      PROGRAM SUFU (INPUT,OUTPUT,TAPE5=INPUT,TAPE6=OUTPUT)
      DIMENSION B(4,4),CMAT(4,4)
      DIMENSION COVAR(4,4,13),IDENT(13),SIG1(4,4),SIG2(4,4)
      DIMENSION XAV1(4,1),XAV2(4,1),C(1,4),Y(4,1),D(1,4),Z(4,1)
 5    DIMENSION CFACT1(3,10),CFACT2(10,3),TEMP(4,4),SUFUD(10)
      DIMENSION W1(4,4),W2(4,4),XAXIS(15)
      DIMENSION E(4,1),F(4,1),FAC1(4,4),FAC2(4,4)
      REAL MEANS(13,4)
C
10    C...READ PROGRAM PARAMETERS AND DATA
C
      READ (5,505) NSIG, NPLT, NWAVE, MODVAR, MODM, IFEATV
  505 FORMAT(8I10)
      KSTP=NSIG + NPLT
15    DO 200 L=1,KSTP
      READ (5,510) IDENT(L)
  510 FORMAT(A10)
      READ (5,515) (MEANS(L,J),J=1,NWAVE)
      DO 200 I=1,NWAVE
20    READ (5,515) (COVAR(I,J,L),J=1,NWAVE)
  515 FORMAT(8F10.5)
  200 CONTINUE
C
C...PRINT INPUT
25    C
      WRITE (6,690)
      WRITE(6,801) NSIG, NPLT, NWAVE, MODVAR, MODM, IFEATV
  801 FORMAT(*   NSIG=*,I4,/,*   NPLT=*,I4,/,*   NWAVE=*,I4,/,
     1*   MODVAR=*,I4,/,*   MODM=*,I4,/,*   IFEATV=*,I4,/////)
30    DO 215 I=1,KSTP
      WRITE(6,632) IDENT(I)
  632 FORMAT(/////,*   RUN.....*,A10)
      WRITE(6,637) (MEANS(I,J),J=1,NWAVE)
  637 FORMAT(//,36X,*    CH1        CH2        CH3        CH4        CH5
     1   CH6        CH7        CH8*,//,*    MEANS BY CHANNEL*,15X,8F10.5)
35    WRITE(6,647)
  647 FORMAT(//,*    COVARIANCE MATRIX*)
      DO 255 K=1,NWAVE
  255 WRITE(6,642) (COVAR(K,J,I),J=1,NWAVE)
40    642 FORMAT(35X,8F10.5)
      215 CONTINUE
      WRITE(6,690)
      KST=NSIG + 1
      IF(MODM.EQ.1) GO TO 216
45    GO TO 217
C
C...SMOUTH MEANS
C
  216 CONTINUE
50    CALL SMEANS (NSIG,NWAVE,MEANS)
      WRITE(6,618)
  618 FORMAT(*1*,5X,* SMOOTHED MEANS USED IN CALCULATIONS....*,//)
      DO 218 I=1,NSIG
  218 WRITE(6,617) I,(MEANS(I,J),J=1,NWAVE)
55    617 FORMAT(10X,I2,5X,8F10.5)
      217 IF(IFEATV.EQ.1) GO TO 703
      GO TO 219
C
C...DETERMINE NEW FEATURE VECTORS
```

```
      C
  703 CALL FEATURE(NUM  ,MEANS,M1,L1,M2,L2,M3,L3,M4,L4)
          WRITE(6,802) NUM, M1,L1,M2,L2,M3,L3,M4,L4
  802 FORMAT(/////,I2,' NEW FEATURE VECTORS WERE DEVELOPED. THEY ARE....
         1',4(/,'     BAND',I2,' /  BAND',I2))
      C
      C...ENTER PLOT LOOP
      C
          DO 400 L=KST,KSTP
      C
      C...IDENTIFY APPROPRIATE MEAN VECTOR AND COVARIANCE MATRIX FOR PLOT
      C
              DO 220 I=1,NWAVE
              DO 220 J=1,NWAVE
              TEMP(I,J)=0.
  220     CONTINUE
              IF(MODVAR.EQ.1) GO TO 230
              DO 225 I=1,NWAVE
              XAVI(I,1)=MEANS(L,I)
              DO 225 J=1,NWAVE
              TEMP(I,J)=COVAR(I,J,L)
  225     CONTINUE
              GO TO 245
      C
      C...MODIFY MEAN VECTOR AND/OR COVARIANCE MATRIX
      C
          DO 230 CONTINUE
              DO 232 I=1,NWAVE
  232     XAVI(I,1)=MEANS(L,I)
              DO 231 I=1,NWAVE
              DO 231 J=1,NWAVE
  231     CMAT(I,J)=COVAR(I,J,L)
              CALL MODIFY(CMAT,B)
              DO 240 I=1,NWAVE
              DO 240 J=1,NWAVE
              TEMP(I,J)=B(I,J)
  240     CONTINUE
              WRITE(6,681) IDENT(L)
  681     FORMAT(///,'      MODIFIED MEAN VECTOR AND/OR COVARIANCE MATRIX FOR
         1 RUN....',A10)
      C
      C...PRINT MEAN VECTOR AND COVARIANCE MATRIX OF PLOT USED IN CALCULATIONS
      C
  245     WRITE(6,715)  (XAVI(J,1),J=1,4)
  715     FORMAT(8F10.5)
              DO 10 I=1,4
              WRITE(6,715)  (TEMP(I,J),J=1,4)
   10     CONTINUE
      C
      C...ENTER EFFECT LOOP
      C
              DO 400 M=1,NSIG
      C
      C...IDENTIFY APPROPRIATE MEAN VECTOR AND COVARIANCE MATRIX FOR EFFECT
      C
              DO 247 I=1,NWAVE
              DO 247 J=1,NWAVE
              SIG2(I,J)=0.
  247     CONTINUE
```

```
                IF(MODVAR.EQ.1) GO TO 260
120             DO 250 I=1,NWAVE
                XAV2(I,1)=MEANS(M,I)
                DO 250 J=1,NWAVE
                SIG2(I,J)=COVAR(I,J,M)
             250 CONTINUE
125             GO TO 270
              C
              C...MODIFY MEAN VECTOR AND/OR COVARIANCE MATRIX
              C
             260 CONTINUE
130             DO 262 I=1,NWAVE
             262 XAV2(I,1)=MEANS(M,I)
                DO 261 I=1,NWAVE
                DO 261 J=1,NWAVE
             261 CMAT(I,J)=COVAR(I,J,M)
135             CALL MODIFY(CMAT,B)
                DO 265 I=1,NWAVE
                DO 265 J=1,NWAVE
                SIG2(I,J)=B(I,J)
             265 CONTINUE
140             WRITE(6,681) IDENT(M)
              C
              C...PRINT MEAN VECTOR AND COVARIANCE MATRIX OF EFFECT USED IN CALCULATIONS
              C
             270 WRITE(6,715) (XAV2(J,1),J=1,4)
145             DO 20 I=1,4
                WRITE(6,715) (SIG2(I,J),J=1,4)
              20 CONTINUE
              C
              C...CALCULATIONS FOR C-FACTORS
150           C
                WRITE(6,656) L,M
             656 FORMAT(///,*    C-FACTORS FOR PLOT*,I3,* AND LAI EFFECT*,I3,/,*  C
               1ALCULATION STEPS COMPLETED...*)
              C
155           C...DETERMINE INVERSE OF COVARIANCE MATRICES
              C
                IWHERE=1
                WRITE(6,651) IWHERE
             651 FORMAT(//,I10)
160           C
              C...ASSIGN COVARIANCE MATRIX OF PLOT TO WORKING MATRIX
              C
                DO 27 I=1,4
                DO 27 J=1,4
165             SIG1(I,J)=TEMP(I,J)
              27 CONTINUE
              C     CALL INVERT (SIG1,NWAVE)
                CALL MATRIX(10,4,4,0,SIG1,4,DETRM)
                DO 1000 I=1,4
170          1000 WRITE(6,691) (SIG1(I,J),J=1,4)
              691 FORMAT(4F20.5)
                IWHERE=2
                WRITE(6,651) IWHERE
              C     CALL INVERT(SIG2,NWAVE)
175             CALL MATRIX(10,4,4,0,SIG2,4,DETRM)
                DO 1001 I=1,4
             1001 WRITE(6,691) (SIG2(I,J),J=1,4)
```

```
C
C...SUBTRACT APPROPRIATE MEAN VECTORS
C
      IWHERE=3
      WRITE(6,651) IWHERE
      CALL ADDSUB (XAV1,XAV2,E,NWAVE,1,Y)
      WRITE(6,692) (Y(I,1),I=1,4)
  692 FORMAT(F20.5,3(/,F20.5))
      IWHERE=4
      WRITE(6,651) IWHERE
      CALL ADDSUB (XAV2,XAV1,F,NWAVE,1,Z)
      WRITE(6,692) (Z(I,1),I=1,4)
C
C...TAKE TRANSPOSE OF SUBTRACTED MEAN VECTORS
C
      IWHERE=5
      WRITE(6,651) IWHERE
      CALL TRNSPO (Y,C,NWAVE,1)
      WRITE(6,691) (C(1,J),J=1,4)
      IWHERE=6
      WRITE(6,651) IWHERE
      CALL TRNSPO (Z,D,NWAVE,1)
      WRITE(6,691) (D(1,J),J=1,4)
C
C...MULTIPY DERIVED VECTORS
C
      IWHERE=7
      WRITE(6,651) IWHERE
      CALL MATMPY (Y,C,W1,4,1,4)
      DO 1002 I=1,4
 1002 WRITE(6,691) (W1(I,J),J=1,4)
      IWHERE=8
      WRITE(6,651) IWHERE
      CALL MATMPY (Z,D,W2,4,1,4)
      DO 1003 I=1,4
 1003 WRITE(6,691) (W2(I,J),J=1,4)
C
C...MULTIPLY INVERSE OF COVARIANCE MATRICES BY THE DERIVED MATRICES
C
      IWHERE=9
      WRITE(6,651) IWHERE
      CALL MATMPY (SIG1,W1,FAC1,4,4,4)
      DO 1004 I=1,4
 1004 WRITE(6,691) (FAC1(I,J),J=1,4)
      IWHERE=10
      WRITE(6,651) IWHERE
      CALL MATMPY (SIG2,W2,FAC2,4,4,4)
      DO 1005 I=1,4
 1005 WRITE(6,691) (FAC2(I,J),J=1,4)
C
C...TAKE THE TRACE OF THE FINAL CALCULATED MATRICES
C
      CU1=0.
      CU2=0.
      DO 325 J=1,NWAVE
      CU1= CU1 + FAC1(J,J)
      CU2= CU2 + FAC2(J,J)
  325 CONTINUE
      IWHERE=11
```

```
      WRITE(6,651) IWHERE
      LSHFT=L - NSIG
      CFACT1(LSHFT,M)=CD1
240   CFACT2(M,LSHFT)=CD2
      WRITE(6,666) L,M,CD1,M,L,CD2
  666 FORMAT(/,*    C-FACTOR FROM PLOT*,I3,* TO LAI EFFECT*,I3,* IS*,F20
     1.5,/,13X,*FROM LAI EFFECT*,I3,* TO PLOT*,I3,* IS*,F20.5,//////////)
  400 CONTINUE
245   C
      C...PRINT C-FACTOR MATRICES
      C
      WRITE(5,690)
      WRITE(6,652)
250   652 FORMAT(/////,*    C-FACTOR MATRICES...*,//)
      WRITE(6,682)
  682 FORMAT(///,*      FROM PLOTS TO EFFECTS*)
      DO 420 I=1,NPLT
      WRITE(6,671) (CFACT1(I,J),J=1,NSIG)
255   671 FORMAT(10F12.3)
  420 CONTINUE
      WRITE(6,683)
  683 FORMAT(///,*      FROM EFFECTS TO PLOTS*)
      DO 425 I=1,NSIG
260   WRITE(6,671)(CFACT2(I,J),J=1,NPLT)
  425 CONTINUE
      DO 601 I=1,NSIG
  601 XAXIS(I)=I
      DO 600 L=1,NPLT
265   C
      C...CALCULATE SU-FU DISTANCES FROM C-FACTOR MATRICES
      C
      WRITE(6,690)
  690 FORMAT(*1*)
270   DIST=1000000.
      MIN=1
      DO 500 M=1,NSIG
      SUFUD(M)=(SQRT(CFACT2(M,L)*CFACT1(L,M)))/(SQRT(CFACT2(M,L))
     1+SQRT(CFACT1(L,M)))
275   IF(SUFUD(M).LE.DIST) GO TO 40
      GO TO 50
   40 DIST=SUFUD(M)
      MIN=M
   50 CONTINUE
280   C
      C...OUTPUT RESULTS
      C
      WRITE(6,662) L,M,SUFUD(M)
  662 FORMAT(*    THE SEPARABILITY BETWEEN PLOT*,I3,* AND SIMULATED LAI
285  1EFFECT*,I3,* IS*,F10.5)
  500 CONTINUE
      WRITE(6,667) DIST,IDENT(MIN)
  667 FORMAT(///,*     THE MINIMUM SWAIN-FU CLUSTER SEPARABILITY DISTANCE
     1 IS*,F10.5,* ASSOCIATED WITH LAI EFFECT*,A10)
290   CALL MAPA (5,XAXIS,SUFUD,,,NSIG,HL,HH,VL,VH,10H EFFECT    *
     110H DIVERG.  ,10HDIVG. PLOT,1)
  600 CONTINUE
      STOP
      END
```

```
      SUBROUTINE FEATURE (NUM,XAVG,   M1,L1,M2,L2,M3,L3,M4,L4)
      DIMENSION XAVG(13,4),XWORK(13,4)
      M1=4 $ L1=2
      M2=0 $ L2=0
5     M3=0 $ L3=0
      M4=0 $ L4=0
      DO 10 J=1,4
      DO 10 I=1,13
      XWORK(I,J)=1.
10    10 CONTINUE
      DO 20 I=1,13
      XWORK(I,1)= XAVG(I,M1) / XAVG(I,L1)
   20 CONTINUE
      NUM=1
15    DO 30 J=1,4
      DO 30 I=1,13
      XAVG(I,J)=XWORK(I,J)
   30 CONTINUE
      RETURN
20    END


      SUBROUTINE SMEANS (NSIG,NWAVE,MEANS)
      REAL MEANS(13,4)
      ISTOP= NSIG - 1
      DO 217 J=1,NWAVE
5     DO 217 I=2,ISTOP
      MEANS(I,J)=(MEANS(I-1,J)/4.)+(MEANS(I,J)/2.)+(MEANS(I+1,J)/4.)
  217 CONTINUE
      RETURN
      END


      SUBROUTINE MODIFY (C,B)
      DIMENSION B(4,4), C(4,4)
      DO 10 I=1,4
      DO 10 J=1,4
5     B(I,J)=0.
      IF(I.EQ.J) B(I,J)=.00001
   10 CONTINUE
      RETURN
      END
```

```
      SUBROUTINE INVERT (A,N)
C
C.....SUBROUTINE INVERT USES THE GAUSS-JORDAN ELIMINATION METHOD TO
C     REPLACE THE MATRIX, A, WITH ITS INVERSE. THE DIMENSION STATEMENT IN THE
C     MAIN PROGRAM MUST HAVE A LISTED MATRIX, 60X60Z HOWEVER, THE ACTUAL NUMBER
C     MAIN PROGRAM MUST HAVE A MATRIX DIMENSIONED WHICH IS EQUAL OR LARGER
C     THAN THE WORKING MATRIX IN THIS PROGRAM. THE ACTUAL NUMBER OF ROWS
C     AND COLUMNS OF .A. THAT ARE USED IS SPECIFIED BY N.
C
      DIMENSION A(4,4),B(4),C(4),LZ(4)
      DO 10 J=1,N
   10 LZ(J)=J
      DO 20 I=1,N
      K=I
      Y=A(I,I)
      L=I-1
      LP=I+1
      IF(N-LP)14,11,11
   11 DO 13 J=LP,N
      W=A(I,J)
      IF(ABS(W)-ABS(Y)) 13,13,12
   12 K=J
      Y=W
   13 CONTINUE
      WRITE(6,615) Y
  615 FORMAT(8F10.5)
   14 DO 15 J=1,N
      C(J)=A(J,K)
      A(J,K)=A(J,I)
      A(J,I)=-C(J)/Y
      A(I,J)=A(I,J)/Y
   15 B(J)=A(I,J)
      A(I,I)=1.0/Y
      J=LZ(I)
      LZ(I)=LZ(K)
      LZ(K)=J
      DO 19 K=1,N
      IF(I-K) 16,19,16
   16 DO 18 J=1,N
      IF(I-J) 17,18,17
   17 A(K,J)=A(K,J)-B(J)*C(K)
   18 CONTINUE
   19 CONTINUE
   20 CONTINUE
      DO 200 I=1,N
      IF(I-LZ(I)) 100,200,100
  100 K=I+1
      DO 500 J=K,N
      IF(I-LZ(J)) 500,600,500
  600 M=LZ(I)
      LZ(I)=LZ(J)
      LZ(J)=M
      DO 700 L=1,N
      C(L)=A(I,L)
      A(I,L)=A(J,L)
  700 A(J,L)=C(L)
  500 CONTINUE
  200 CONTINUE
      RETURN
```

```
      SUBROUTINE ADDSUB (A,B,C,M,N,Y)
C
C.....SUBROUTINE ADDSUB STORES THE RESULT OF A+B IN C AND THE
C     RESULT OF A-B IN Y. MATRICES A,B,C,AND Y MUST ALL BE DIMENSIONED AS
C     MXN MATRICES IN THE CALLING PROGRAM.
C
      DIMENSION A(M,N),B(M,N),C(M,N),Y(M,N)
      DO 1 I=1,M
      DO 1 J=1,N
      C(I,J)=A(I,J)+B(I,J)
    1 Y(I,J)=A(I,J)-B(I,J)
      RETURN
      END
```

```
      SUBROUTINE MATMPY (A,B,C,M,N,L)
C
C.....SUBROUTINE MATMPY MULTIPLIES TWO MATRICES (A*B) TOGETHER
C     AND STORES THE RESULT IN C. THE DIMENSION STATEMENT IN THE
C     MAIN PROGRAM MUST HAVE A DIMENSIONED AS AN MXN MATRIX.
C     B MUST BE DIMENSIONED NXL AND C MUST BE DIMENSIONED MXL.
C
      DIMENSION A(M,N),B(N,L),C(M,L)
      DO 102 I=1,M
      DO 102 J=1,L
      S=0.
      DO 101 K=1,N
  101 S=S+A(I,K)*B(K,J)
  102 C(I,J)=S
      RETURN
      END
```

```
      SUBROUTINE TRNSPO (A,B,M,N)
C
C.....THIS SUBROUTINE CALCULATES THE TRANSPOSE OF THE MXN MATRIX A
C     AND STORES THE RESULT IN B. A MUST BE DIMENSIONED MXN IN THE
C     MAIN PROGRAM AND MUST BE NXM.
C
      DIMENSION A(M,N),B(N,M)
      DO 10 I=1,M
      DO 10 J=1,N
   10 B(J,I)=A(I,J)
      RETURN
      END
```